Cloning and characterization of *Xenopus laevis* proprotein convertases and identification of endogenous convertases of bone morphogenetic protein 4

by

Sylvia Marie Nelsen

A DISSERTATION

Presented to the Department of Molecular & Medical Genetics

and the Oregon Health & Science University

School of Medicine

in partial fulfillment of the requirements

for the degree of Doctor of Philosophy

July 2009

School of Medicine

Oregon Health & Science University

CERTIFICATE OF APPROVAL

This is to certify that the Ph.D. dissertation of

Sylvia Marie Nelsen

has been approved

Dr. Melissa Wong, Chairman of Thesis Committee

Dr. Jan Christian, Thesis Advisor

Dr. David Farrell, Member

Dr. William Skach, Member

Dr. Scott Stadler, Member

TABLE OF CONTENTS

LIST OF TABLES

LIST OF FIGURES

Chapter 1

Chapter 2

LIST OF ABBREVIATIONS

α_1-AT	α_1-antitrypsin
α_1-EK1	α_1-antitrypsin variant EK1
α_1-EK4	α_1-antitrypsin variant EK4
α_1-PDX	α_1-antitrypsin Portland
α_1-PIT	α_1-antitrypsin Pittsburg
ALK	Activin Receptor-Like Kinase
AM	Anopthalmia/Micropthalmia
BAMBI	BMP and Activin Membrane-Bound Inhibitor
BMP	Bone Morphogenetic Protein
BMPR	Bone Morphogenetic Protein Receptor
CMK	Chloromethyl Ketone
Co-Smad	Common Smad
CRD	Cysteine-Rich Domain
C-terminal	Carboxy-terminal
CV	Crossveinless
D	Dextrorotatory
D6R	Hexa-D-Arginine
DAN	Differentially Screening-Selected Gene Aberrative in Neuroblastoma
Dec-	Decanoyl
DPP	Decapentaplegic
ER	Endoplasmic Reticulum

EST	Expressed Sequence Tag
FGF	Fibroblast Growth Factor
FGFR	Fibroblast Growth Factor Receptor
GDF	Growth and Differentiation Factor
GSK3	Glycogen Synthase Kinase 3
HA	Hemaglutinin
HSPG	Heparin Sulfate Proteoglycan
IGF	Insulin-Like Growth Factor
IMAGE	Integrated Molecular Analysis of Genomes and their Expression
I-Smad	Inhibitory Smad
L	Levorotatory
L6R	Hexa-L-Arginine
LPC	Lymphoma Proprotein Convertase
MAPK	Mitogen Activated Protein Kinase
MH	Mad Homology Domain
NOG	Noggin (human gene designation)
N-terminal	Amino-terminal
ODC	Ornithine Decarboxylase
ONT1	Olfactomedin-Noelin-Tiarin Protein 1
PA	Protective Antigen
PACE	Paired basic Amino acid Converting Enzyme
PACS-1	Phosphofurin Acidic Cluster Sorting protein 1
PC	Proprotein Convertase

PCSK	Proprotein Convertase Subtilisin/Kexin Type
PEA	*Pseudomonas aeruginosa* Exotoxin A
PI8	Protease Inhibitor 8
PM	Plasma Membrane
RSL	Reactive Site Loop
R-Smad	Receptor-Regulated Smad
RT	Room temperature
S1	Cleavage Site 1
S2	Cleavage Site 2
SCW	Screw
Serpin	Serine Protease Inhibitor
SI	Stoichiometry of Inhibition
Smurf	Smad Ubiquitination Regulatory Factor
SOG	Short Gastrulation
SPC	Subtilisin-like Proprotein Convertase
SZL	Sizzled
TGFβ	Transforming Growth Factor-β
TGN	*Trans*-Golgi Network
TLD	Tolloid
TSG	Twisted Gastrulation
vWF	von Willebrand Factor
XLD	Xolloid

ACKNOWLEDGEMENTS

First of all, I must thank my advisor, Jan Christian, whose kind guidance, constant encouragement, and occasional firm shove kept me going through the tough times. She is an excellent and very patient teacher and mentor, and I will always be grateful for the absolutely essential role she has played in my education.

I would also like to thank my friends, who traveled with me, and often carried me, through this incredible journey.

And my parents, who always gave me the freedom to pursue my own path, even when they didn't agree with or understand my chosen course.

Finally, I especially would like to express my gratitude to my husband, Paul, without whose infinite patience and quiet support this would not have been possible.

ABSTRACT

Bone morphogenetic protein 4 (BMP4) is a member of the transforming growth factor-β (TGFβ) family of signaling molecules. It has been highly conserved throughout evolution and is essential for many aspects of development and for tissue homeostasis in adults. BMP4 activity is tightly regulated at many levels, including via proteolytic activation of the precursor protein; cleavage of proBMP4 by members of the proprotein convertase (PC) family is required to generate an active ligand. ProBMP4 is initially cleaved at a site adjacent to the mature ligand domain (S1), and then at an upstream site (S2) within the prodomain. Interestingly, cleavage at the S2 site appears to regulate the activity and signaling range of mature BMP4 in a tissue-specific manner. Based upon this intriguing observation, I hypothesized that cleavage of the S2 site might depend on tissue-specific expression of an S2 site-specific enzyme. To test my hypothesis, we cloned and characterized the expression of PC orthologs in *Xenopus* and identified which PCs cleave each site of proBMP4 *in vivo*. Loss of function and protein-based inhibitor techniques revealed that furin and PC6 cleave both the S1 and S2 sites of proBMP4, and that a third S1-specific enzyme, likely PC7, functions redundantly to cleave the S1 site in embryos but not oocytes. These results suggest that PC7, or a convertase with similar substrate specificity, functions to selectively cleave the S1 site of proBMP4 in a developmentally regulated fashion. Constitutive cleavage of proBMP4 at S1 by PC7, which is ubiquitously expressed, combined with S1 + S2 cleavage of proBMP4 by Furin and/or PC6, which display tissue-restricted expression, may be a mechanism by which BMP4 activity could be regulated in a tissue-specific manner.

Chapter 1

Introduction: An overview of the activity and regulation of Bone Morphogenetic Protein 4 and its cleaving enzymes, the proprotein convertases

I. BONE MORPHOGENETIC PROTEIN 4

Bone morphogenetic proteins (BMPs) are members of the transforming growth factor-β (TGFβ) superfamily of signaling molecules, which is characterized by multiple conserved cysteine residues that form a particular fold called a cysteine knot (Sun and Davies, 1995). This family consists of two main branches: the TGFβ/Activin/Nodal branch and the BMP/Growth and Differentiation Factor (GDF)/Müllerian Inhibiting Substance branch (Shi and Massague, 2003). Within this second branch is the group of BMP ligands, the BMP2/BMP4/DPP (Decapentaplegic) group outlined in red in Figure 1-1, that will be the focus of this thesis.

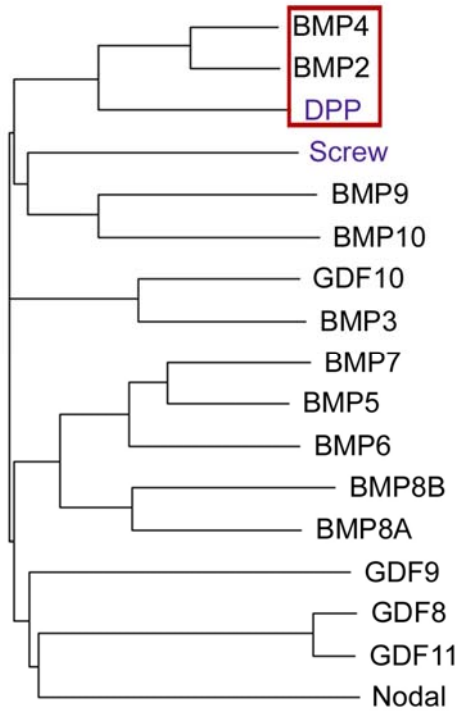

Figure 1-1. Phylogenetic tree of mammalian and *Drosophila* BMPs. Tree was constructed based on mature domain sequences using the T-Coffee alignment and the TREECON phylogenetic tree construction freeware programs (http://www.tcoffee.org/; Van de Peer and De Wachter, 1994). Sequences are from mouse (black text) or *Drosophila melanogaster* (purple text). Nodal is included for reference. Boxed in red is the group of proteins that will be the focus of this work. Sequences are from genbank accession numbers: BMP2 NP_031579, BMP3 NP_775580, BMP4 NP_031580, BMP5 NP_031581, BMP6 NP_031582, BMP7 NP_031583, BMP8A NP_031584, BMP8B NP_031585, BMP9 NP_062379, BMP10 NP_033886, GDF8 NP_034964, GDF9 NP_032136, GDF10 NP_665684, GDF11 NP_034402, DPP NP_477311, Screw NP_524863.

I.A. BMP signaling pathway

BMPs are secreted cell signaling molecules that transmit their signal by binding to a heterotetramer of Type I and Type II serine-threonine kinase receptors (Figure 1-2) (reviewed in Wu and Hill, 2009). Upon binding of the ligand, the Type II receptor

transphosphorylates the Type I receptor, which in turn phosphorylates a receptor-regulated Smad (R-Smad) effector molecule. The R-Smad then binds a common Smad (Co-Smad), and this complex translocates to the nucleus to interact with sequence-specific DNA binding elements. Binding may or may not involve cofactors and can result in activation or repression of the target.

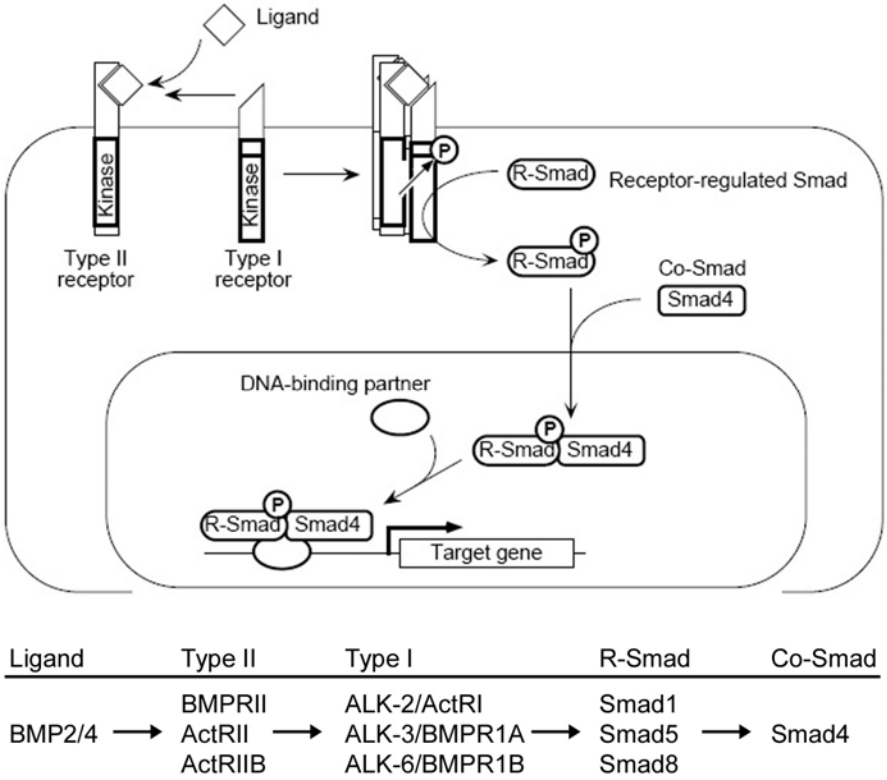

Figure 1-2. BMP signaling pathway. BMP binds its receptors and initiates a signaling cascade through Smad proteins that results in modulation of target genes. See text for details. Reprinted with permission (Massague, 1998).

I.A.1. BMP4 receptors

Several Type I and Type II receptors that bind BMP4 have been identified (Figure 1-2) (Armes and Smith, 1997; Koenig et al., 1994; Nohno et al., 1995; Rosenzweig et al., 1995; ten Dijke et al., 1994). They share a common structure consisting of an amino (N)-terminal extracellular ligand binding domain, a transmembrane domain, and an

intracellular serine-threonine kinase domain. In addition, Type I receptors contain a juxtamembrane GS domain, a TTSGSGSG motif just N-terminal to the kinase domain that is phosphorylated by the Type II receptor. BMP4 can interact with multiple combinations of these receptors. It is unknown, however, which receptor combinations are actually present *in vivo* or if different combinations result in different downstream effects. The BMP4 dimer is thought to bind a dimer of Type I receptors, and this complex has higher affinity for and recruits a dimer of two Type II receptors (Liu et al., 1995). The Type II receptors are autophosphorylated in a ligand independent fashion and are thought to be constitutively active (Mathews and Vale, 1993). Upon ligand binding and complex formation, the Type II receptors phosphorylate the Type I receptors within the GS domain, and the activated Type I receptor can then phosphorylate downstream effector molecules, R-Smads (Chen et al., 1997; Kretzschmar et al., 1997b).

I.A.2. Smads

There are three types of Smad proteins – receptor-regulated Smads (R-Smads), common Smads (Co-Smad), and inhibitory Smads (I-Smads, discussed below) (Massague et al., 2005 and references therein). One group of R-Smads transmits signals from BMP ligands (Smad1, Smad5, Smad8), while another group transmits signals from TGFβ/Activin-like ligands (Smad2, Smad3) (Baker and Harland, 1996; Graff et al., 1996; Liu et al., 1996; Suzuki et al., 1997). Both groups interact with the same Co-Smad (Smad4) (Lagna et al., 1996). The Smad proteins have three main domains – an N-terminal Mad Homology 1 (MH1) domain, a C-terminal MH2 domain, and a less conserved flexible linker region that separates them (Savage et al., 1996). Homology with I-Smads is primarily through the MH2 domain, which is important for multiple

functions including hetero-oligomerization and transcriptional activation (Lagna et al., 1996; Liu et al., 1996; Whitman, 1998). In R-Smads, this is also the site of interaction with, and phosphorylation by, type I receptors (Kretzschmar et al., 1997b; Macias-Silva et al., 1996; Zhang et al., 1996). Unphosphorylated R-Smads form an intramolecular complex between their MH1 and MH2 domains that helps to maintain an inactive state (Baker and Harland, 1996; Hata et al., 1997). Phosphorylation disrupts this interaction and allows the R-Smad to interact with Smad4. The R-Smad/Smad4 complex can then translocate to the nucleus and interact directly with DNA via their MH1 domains (Kim et al., 1997; Liu et al., 1996).

Depending on the context, Smads are able to activate or repress target genes, and the same Smad signal can elicit a different response depending on the cell type in which it is acting (reviewed in Ross and Hill, 2008). Smad3 and Smad4 bind to the minimal Smad binding element, which consists of only four base pairs (5′-AGAC- 3′), while Smad1 binds to GC-rich sequences (5′-GCCGNC- 3′ or 5′-GRCGNC- 3′) (Brugger et al., 2004; Dennler et al., 1998; Ishida et al., 2000; Zawel et al., 1998). Because Smad proteins have relatively low DNA binding specificity, they rely on interactions with each other or with other DNA binding proteins to modulate specific targets (Ross and Hill, 2008 and references therein; Zawel et al., 1998). Members of multiple protein families have been implicated as Smad binding partners, including Ski and Evi-1 transcriptional co-repressors, p300 and CBP histone acetyltransferases, and the zinc finger scaffolding protein Schnurri (Alliston et al., 2005; Pearson et al., 1999; Pouponnot et al., 1998; Wang et al., 2000; Yao et al., 2006). Partners may be ubiquitously expressed, such that the

same response is elicited from multiple cell types, or partners may be cell-type specific in order to elicit varied responses.

I.B. Biological functions of BMP4

BMPs elicit varied responses during development and adult tissue homeostasis. They have been implicated in processes as diverse as cell proliferation, differentiation, apoptosis, adhesion, migration, and morphogenesis (reviewed in Hogan, 1996). Below is an overview of the roles that BMP4 plays in various developmental processes, from early embryonic patterning to formation of specific organs and maintenance of adult tissues.

I.B.1. Role of BMP4 in development

The essential and diverse roles of BMP4 in embryonic patterning have been studied in a variety of organisms, from flies to humans, and the signaling molecules as well as their mechanisms of action have been highly conserved throughout evolution. In flies, the initial dorsal-ventral axis is determined by expression of the *Bmp4* and *Bmp7* orthologs, *decapentaplegic* (*Dpp*) and *screw* (*Scw*), respectively (Arora et al., 1994; Ferguson and Anderson, 1992). Ubiquitous expression of *Scw* combined with high levels of *Dpp* in the dorsal-most region, and high levels of the DPP antagonist Short gastrulation (SOG) on the ventral side, generates a gradient of decreasing activity that spreads toward the ventral side, with the absence of DPP in the ventral-most position resulting in formation of neural ectoderm (Figure 1-3A, C). *Dpp* null mutants are embryonic lethal, whereas those that lack expression in specific imaginal discs show patterning defects in structures derived from the imaginal discs, such as malformed legs or reduced eye, wing, or haltere structures (Spencer et al., 1982).

The dorsal-ventral axis is inverted in vertebrates relative to flies, but BMP4 plays a similar role in specifying this axis in higher organisms. In *Xenopus*, for example, *Bmp4* is initially expressed ubiquitously in the embryo, but then it becomes excluded from the dorsal side (Dale et al., 1992; Fainsod et al., 1994). Higher levels of expression of *Bmp4* on the ventral side, combined with expression of secreted BMP antagonists, such as *Chordin*, in dorsal mesodermal cells, results in an activity gradient with the highest levels of BMP4 signaling on the ventral side (Figure1-3, B, C) (Fainsod et al., 1997; Piccolo et al., 1996; Zimmerman et al., 1996). This activity gradient allows BMP4 to act as a morphogen, specifying different fates in a concentration-dependent manner. For example, Dosch and colleagues showed that injection of increasing amounts of *Bmp4* mRNA results in progressive loss of dorsal mesoderm derivatives. Specifically, embryos first lose notochord, then muscle, and at the highest doses of *Bmp4* they become completely ventralized (Dosch et al., 1997). This gradient is also important for specifying ectodermal tissues: higher BMP4 activity in ventral ectoderm results in epidermis, and inhibition of BMP4 signaling in the dorsal ectoderm is necessary for neural development (Wilson and Hemmati-Brivanlou, 1995). Though knockout strategies are not feasible in *Xenopus* due to its tetraploid genome and long maturation time, protein function can be reduced using several alternative methods, including injection of antisense RNA to degrade a specific mRNA or morpholino oligonucleotides to inhibit translation of a target mRNA (Sive et al., 2000). Also, there are often dominant negative proteins that can be ectopically expressed. Researchers have shown, using these various strategies, that inhibition of BMP4 signaling results in dorsalization of the embryos (Dale and Jones, 1999 and references therein; Graff et al., 1994; Reversade et

al., 2005; Suzuki et al., 1994). Specifically, posterior structures and ventral mesoderm derivatives (ie. blood) are drastically reduced, and dorsal tissues such as notochord and neural ectoderm are expanded.

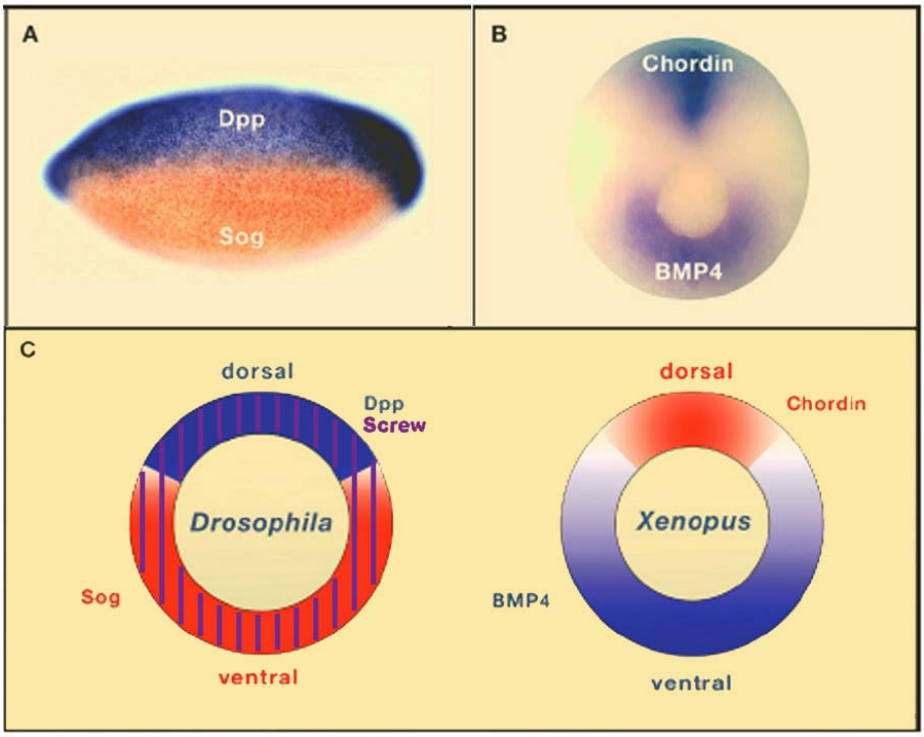

Figure 1-3. BMP activity gradients in early *Drosophila* and *Xenopus* development. A, C. In *Drosophila*, dorsal expression of *Dpp* combined with ubiquitous expression of *Scw* and localized expression of various regulators (discussed below) results in an activity gradient of DPP/SCW in which high levels specify dorsal structures and low levels result in ventral tissues. B, C. In Xenopus, the axis is reversed compared to Drosophila, but a conserved set of molecules generates an activity gradient of BMP signaling with the highest levels specifying ventral tissues. Reprinted with permission (De Robertis, 2008).

Bmp4 is necessary for formation of posterior/ventral mesoderm in mice, as it is in *Xenopus* (Lowe et al., 2001; Varlet et al., 1997; Winnier et al., 1995). Loss of function of *Bmp4* results in embryonic lethality, with most animals dying around the time of gastrulation [~embryonic day (E)7.5] due to a lack of mesodermal structures (Winnier et al., 1995). Those that do develop beyond gastrulation present with disorganized posterior structures and a reduction in extraembryonic mesoderm. Further studies demonstrated that in the absence of BMP4 there are no primordial germ cells, lens induction does not

occur, and hepatogenesis is defective (Furuta et al., 1997; Lawson et al., 1999; Rossi et al., 2001). *Bmp4* heterozygous mutant mice display phenotypes with variable penetrance in several tissues, including the skeleton (polydactlyly, defects in craniofacial bones, ribs and vertebrae), kidney (polycystic kidneys), heart (ventricular septal defects), and eye (micropthalmia) (Dunn et al., 1997; Goldman et al., 2006). In addition, fewer primordial germ cells are specified in these mice (Lawson et al., 1999). Tissue specific inactivation of *Bmp4* and analysis of *Bmp4* hypomorphs has revealed additional roles for this signaling molecule in later stages of heart development, ventral body wall closure, and development of the vestibular apparatus and lung (Chang et al., 2008; Eblaghie et al., 2006; Goldman et al., 2006; Jiao et al., 2003; Liu et al., 2004).

I.B.2. Role of BMP in adult tissue homeostasis and disease

Very few cases have been reported in which a copy of the *BMP4* gene is thought to be non-functional in humans. Patients present with various anomalies, including anopthalmia/micropthalmia (AM), hypothyroidism, poly/syndactyly, and developmental delay (Ahmad et al., 2003; Bakrania et al., 2008; Bennett et al., 1991; Elliott et al., 1993; Hayashi et al., 2008; Lemyre et al., 1998; Nolen et al., 2006; Phadke et al., 1994). Of these patients, some harbor deletions of a portion of chromosome 14 that includes *BMP4* as well as multiple other genes, making it difficult to assign causality to loss of function of any single gene. However, two mutations were recently reported in which the *BMP4* gene itself is affected – one is a frame shift mutation resulting in a premature stop codon identified in a family with AM, retinal dystrophy, myopia, poly/syndactyly, and brain anomalies, and the other is a missense mutation identified in an individual with AM, hand, and brain anomalies (Bakrania et al., 2008). The phenotypes associated with

predicted *BMP4* heterozygosity reinforce the importance of BMP4 signaling in eye and skeletal development, and suggest a role in brain development as well.

Disruption of BMP signaling in humans has additionally been implicated in multiple congenital disorders, especially involving abnormal bone formation. Although nothing is known about the specific role BMP4 plays in these processes, mutations in regulatory molecules and downstream components of the signaling pathway show that BMP function is important. For example, brachydactyly – shortening of the digits – has been associated with multiple mutations in the BMP receptor gene, *BMPR1B*, as well as in the gene encoding the BMP antagonist Noggin (*NOG*; Lehmann et al., 2006; Lehmann et al., 2007; Lehmann et al., 2003). Mutations in *NOG* are also responsible for multiple synostoses syndrome, a genetic disease characterized by fusion of the joints (Gong et al., 1999). Further, a mutation in *ALK2* that causes the encoded receptor to be constitutively active is associated with fibrodysplasia ossificans progressiva, a crippling hereditary disorder in which ectopic bone forms throughout the body (Billings et al., 2008; Shore et al., 2006).

Proper BMP signaling is also important for the maintenance of adult tissues such as the pulmonary arteries and gut (Wu and Hill, 2009). For example, germline mutations in the gene encoding the BMP receptor, BMPPRII, have been identified in patients with familial primary pulmonary hypertension. In this disease, faulty remodeling of the pulmonary arteries leads to constriction of the vessels and therefore increased blood pressure and eventual heart failure (Deng et al., 2000; Lane et al., 2000). Another disease associated with mutations in genes encoding a BMP receptor (BMPRIA) or downstream signal transducer (SMAD4) is juvenile polyposis, a condition diagnosed by the presence

of five or more hamartomatous (benign) gastrointestinal polyps that is associated with a high risk of developing malignant gastrointestinal tumors (Howe et al., 2001; Howe et al., 1998; Jarvinen and Franssila, 1984; Veale et al., 1966).

I.C. Regulation of BMP4 signaling activity

Based on the various cellular behaviors that BMP4 signaling is able to elicit, and the deleterious outcomes of BMP4 loss or gain of function, it is clear that activity must be tightly regulated. This occurs at multiple levels using a variety of mechanisms (Figure 1-4).

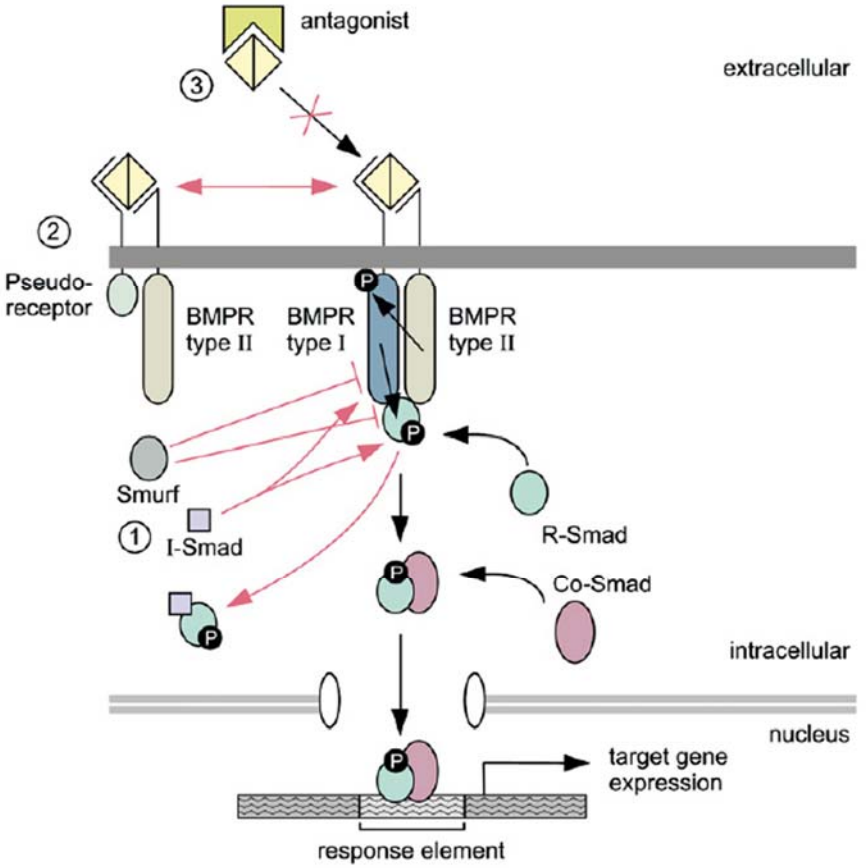

Figure 1-4. Summary of BMP signal regulation. Transmission of a BMP signal to the nucleus is regulated at three main levels: (1) I-Smads and Smurfs work together to inhibit/terminate the intracellular cascade, (2) the pseudoreceptor BAMBI forms a heteromeric complex with receptors to prevent their activation, and (3) a complex network of extracellular antagonists and their inhibitors regulate access of ligands to their receptors. Reprinted with permission (Balemans and Van Hul, 2002).

I.C.1. Regulation downstream of receptors – Smads

Since both the Smad2/3 and the Smad1/5/8 pathways require Smad4 as a downstream effector, competition can exist such that only one pathway is able to propogate its signal (Candia et al., 1997; Lagna et al., 1996). Also, post-translational modifications of R-Smads that result in inactivation or degradation are important for regulating the duration of a signal, and a distinct class of inhibitory Smads (I-Smads) exist that use multiple mechanisms to antagonize signals as discussed below.

R-Smads and Smad4 continuously cycle between the cytoplasm and the nucleus (Schmierer and Hill, 2005). Upon phosphorylation of R-Smads by their Type I receptors, these proteins hetero-oligomerize and accumulate in the nucleus to modulate transcription (Hoodless et al., 1996; Liu et al., 1996). Multiple nuclear phosphatases are present, such as Pyruvate Dehydrogenase Phosphatase (PDP) and Small C-terminal Phosphatases (SCP1, 2, and 3), that remove the activating phosphate group to promote nuclear export (Chen et al., 2006; Knockaert et al., 2006). If the Type I receptor is still active, it can rephosphorylate its R-Smad and begin the cycle again (Inman et al., 2002). In this way, the R-Smads are constantly sampling the activation status of their receptors, and the duration of the signal can be tightly controlled.

Other sites of phosphorylation on R-Smads are important for integration of signals from multiple sources (reviewed in Ross and Hill, 2008). For example, Smad1 is phosphorylated on four serines within its linker region by MAPK in response to stress-inducing MAPK signals or fibroblast growth factor (FGF) and insulin-like growth factor (IGF) (Kretzschmar et al., 1997a; Pera et al., 2003; Sapkota et al., 2007). In addition, GSK3 phosphorylates Smad1 after it has been phosphorylated by the MAPK pathway

(Fuentealba et al., 2007). These phosphate modifications inhibit BMP-induced signaling by preventing nuclear import of Smad1 and/or promoting its degradation, and they provide a means to integrate BMP, MAPK, and Wnt signals.

One group of proteins that mediate Smad degradation is the HECT-domain Smad Ubiquitination Regulatory Factor (Smurf) E3 ubiquitin ligases. Smurf1 and Smurf2 target Smad1 and Smad5 for proteosomal degradation, and this is thought to be important for maintaining a lack of signal in the absence of ligand as well as for terminating a signal (Lo and Massague, 1999; Zhu et al., 1999). In addition, Smurf1 and Smurf2 can mediate degradation of activated receptors to further ensure the termination of signal, and this is mediated by Smad7 (Ebisawa et al., 2001; Kavsak et al., 2000).

Smad6 and Smad7 are I-Smads that negatively regulate TGFβ signaling through several potential mechanisms (reviewed in Shi and Massague, 2003). Both I-Smads bind to the intracellular domain of TGFβ family Type I receptors and prevent phosphorylation of R-Smads (Hayashi et al., 1997; Imamura et al., 1997; Nakao et al., 1997). In addition, Smad7 can form a complex with Smurfs, and this complex targets to the plasma membrane where Smad7 interacts with activated TGFβ Type I receptors, inhibiting their interaction with R-Smads and resulting in their degradation (Ebisawa et al., 2001; Kavsak et al., 2000). Smad6 has also been suggested to inhibit BMP signal transduction by competing with activated Smad1 for binding to Smad4 (Hata et al., 1998).

I.C.2. Regulation at the level of receptors - pseudoreceptors

In addition to the variety of intracellular molecules that positively and negatively regulate BMP signaling, at least one cell-surface protein inhibits signaling by interacting with the receptor itself. The pseudoreceptor, BMP and Activin Membrane-Bound

Inhibitor (BAMBI), is homologous to TGFβ family Type I receptors except that it lacks the intracellular kinase domains necessary for signaling (Onichtchouk et al., 1999). BAMBI binds to multiple TGFβ family Type I receptors, including TβR1, ActR-IB, BMPR-IA, ALK1, and BMPR-IB, and can inhibit BMP signaling when ectopically expressed in *Xenopus* embryos. BAMBI is proposed to inhibit signal propagation by binding to Type I receptors. In the presence of ligand, the BAMBI containing Type I heterodimer is then incorporated into Type I/Type II heterotetramers that cannot be activated.

I.C.3. Regulaton upstream of receptors – extracellular binding proteins

The ability of BMP to activate its receptors is highly regulated by a diverse group of soluble binding proteins. There are four distinct types of these ligand binding traps including Follistatin, members of the DAN family, Noggin, and Chordin (Balemans and Van Hul, 2002).

Follistatin was first described as an inhibitor of Activin, but it was subsequently found to bind and inhibit BMPs as well (Fainsod et al., 1997; Hemmati-Brivanlou et al., 1994). Unlike the other soluble BMP antagonists described below, Follistatin does not prevent BMPs from binding to their receptors. Instead, it forms a stable, ternary complex with the ligand and the Type I receptor, somehow preventing its activation (Iemura et al., 1998). It is possible that follistatin prevents the Type II receptor from binding to this complex and activating the Type I receptor, thereby inhibiting BMP signaling, but this has not been tested.

The DAN family of TGFβ inhibitors, like BMPs, all contain a characteristic cysteine knot domain (Hsu et al., 1998). Three members of this family have been shown

to inhibit BMPs – DAN, Cerberus, and Gremlin – and they are thought to physically block ligand/receptor interaction by directly binding to BMPs.

Noggin is a small glycoprotein that is important for modulating BMP activity during diverse developmental processes such as vertebrate dorsal-ventral patterning, neural induction and differentiation, and skeletogenesis (Brunet et al., 1998; McMahon et al., 1998; Smith and Harland, 1992; Zimmerman et al., 1996). A recent crystal structure of Noggin complexed with BMP7 revealed that noggin binds to the same interface that the ligand uses to interact with both the Type I and Type II receptors, thus physically blocking the ligand-receptor interaction (Groppe et al., 2002). Though the other ligand trap proteins are not structurally conserved, they are thought to interact with BMPs in a similar manner, physically blocking interaction with their receptors.

Chordin [Short gastrulation (SOG) in *Drosophila*] is a much larger protein than Noggin, but like Noggin it binds specifically to BMP2/4/DPP and BMP7/SCW and interferes with the ability of these ligands to interact with their receptors (Holley et al., 1995; Piccolo et al., 1996). An interesting characteristic of this inhibitor is that it is itself regulated by an extracellular protein, a secreted metalloprotease that cleaves Chordin/SOG to either prevent interaction with BMPs or to release BMPs that are already bound. This protease is known as *Drosophila* Tolloid (TLD), *Xenopus* Xolloid (XLD), or human BMP1 or hTLD (Marques et al., 1997; Piccolo et al., 1997). This proteinase, in turn, is regulated by at least two other secreted proteins – Sizzled (SZL) and Olfactomedin-Noelin-Tiarin Protein 1 (ONT1). SZL binds competitively to TLD proteins and inhibits their ability to cleave Chordin/SOG, while ONT1 acts as a scaffolding protein for Tolloid proteins and Chordin to enhance cleavage (Inomata et al.,

2008; Lee et al., 2006). This group of proteins form a complex regulatory system to maintain correct levels of BMP signaling (Figure 1-5).

In *Drosophila*, the combination of SOG and TLD are necessary for proper accumulation of DPP, and also for its subsequent release in a location distant from its synthesis (Ashe and Levine, 1999). In this scenario, high levels of SOG bind to DPP and inhibit its signaling locally, but the inactive complex can also traffic to a location with low SOG levels. In the presence of TLD, the accumulated DPP can then be released to generate a strong, localized signal. This unique mechanism of regulation makes Chordin/SOG appear as an antagonist in some contexts and an agonist in others, and involves multiple interacting proteins in addition to the ones described above, including Twisted Gastrulation (TSG) and Crossveinless-2 (CV-2) (Wu and Hill, 2009). The precise roles these proteins play is still under debate, but it is clear that they modulate Chordin/SOG regulation of BMP/DPP signaling via an unknown but evolutionarily conserved mechanism.

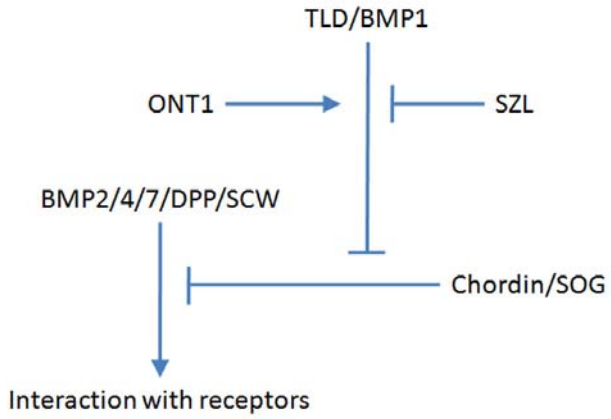

Figure 1-5. Regulation of the BMP inhibitor, Chordin. Chordin/SOG forms a complex with BMP ligands and prevents them from interacting with their receptors. Chordin/SOG is cleaved by Tolloid family proteases (TLD/BMP1), which inhibits binding to BMP ligands. This cleavage is in turn regulated, negatively by Sizzled (SZL) and positively by ONT1.

I.C.4. Regulation of BMP4 actvity via proteolytic activation

In addition to the mechanisms discussed above by which BMP4 activity is regulated in signal receiving cells, activity is also regulated within BMP4 synthesizing

cells, at the level of proteolytic activation. BMPs are synthesized as inactive precursors that are cleaved at specific sites to yield an active, mature protein dimer (Aono et al., 1995). Proteolytic activation of BMP4 is carried out within the secretory system by specific members of the proprotein convertase (PC) family of endoproteases, (discussed below), most likely Furin and PC6 (Constam and Robertson, 1999; Cui et al., 1998). Data from our lab has shown that this is a highly regulated process that may occur differently depending on the tissue in which the protein is being expressed (Goldman et al., 2006).

I.C.4.a. Proteolytic activation of BMP4 via sequential cleavage

Previous data from the Christian lab has shown that proBMP4 is cleaved sequentially at two Furin cleavage motifs, and that this ordered proteolysis regulates the activity and signaling range of mature BMP4 (Cui et al., 2001). ProBMP4 is initially cleaved at an optimal consensus Furin motif adjacent to the mature ligand domain (-R-S-K-R-, denoted the S1 site), and this allows for subsequent cleavage at an upstream minimal Furin motif (-R-I-S-R-, the S2 site; Figure 1-6). In *Xenopus* embryos, proBMP4 carrying a point mutation that renders the upstream site non-cleavable ($BMP4^{S2G}$) generates a ligand that signals over a shorter range, shows less activity *in vivo*, and accumulates at lower levels than does BMP4 cleaved from wildtype precursor. Given that an identical ligand is liberated from the prodomain of wildtype and mutant precursors, these results raise questions as to the mechanism by which a second, upstream cleavage regulates the level of signal that is generated.

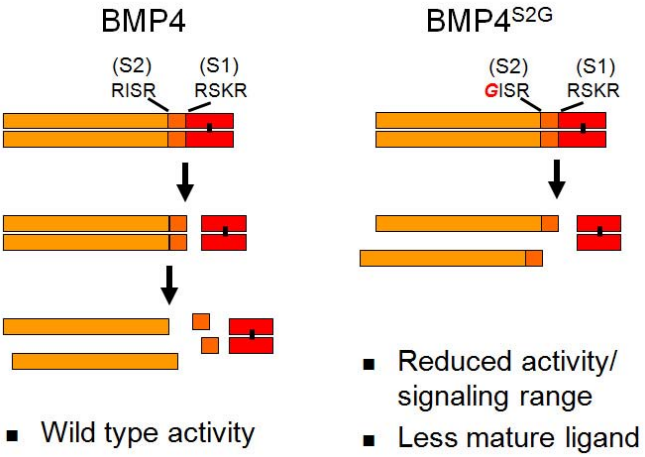

Figure 1-6. BMP4 is cleaved sequentially. Pro-BMP4 is first cleaved adjacent to the mature domain at the S1 site, then upstream within the prodomain at the S2 site. If cleavage at the S2 site is abrogated, less ligand accumulates and thus less activity is generated *in vivo*.

Figure 1-7 outlines published biochemical data from our lab that proposes a mechanism by which cleavage at the upstream site within the prodomain could regulate the activity of the mature ligand (Degnin et al., 2004). First, cleavage of proBMP4 at the S1 site, which most likely occurs in the trans-Golgi network (TGN), releases the mature ligand, but it continues to interact non-covalently with the prodomain. This complex, though signaling competent, is preferentially targeted to the lysosome for degradation. Second, cleavage at the S2 site disrupts the prodomain-ligand interaction and also releases a small internal fragment of unknown function, called the linker domain. The released ligand is no longer targeted to the lysosome. Cleavage at the S2, but not the S1 site, is enhanced by acidic pH, consistent with the possibility that the two cleavages take place in distinct subcellular compartments, possibly by distinct proteases. These studies suggest that cleavage at the S2 site determines how much ligand accumulates, and this in turn dictates the overall level of activity, and how far the ligand can spread *in vivo*.

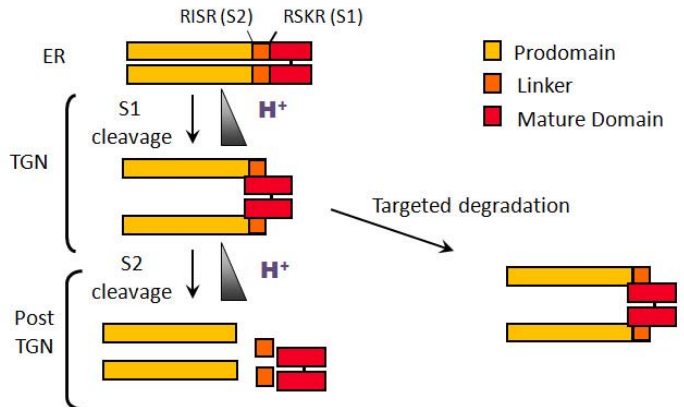

Figure 1-7 Targeted lysosomal degradation as a mechanism of reduced S1-only cleaved BMP4 activity. ProBMP4 is normally cleaved sequentially at S1 then S2. If cleavage occurs at S1 only, the prodomain remains non-covalently associated and the ligand/prodomain complex is preferentially targeted to the lysosome for degredation. See text for details. Modified from (Degnin et al., 2004).

I.C.4.b. Proteolytic activation and signaling activity of BMP4 cleavage mutants in mouse and fly

The ability of cleavages within the prodomain to regulate the signaling range of mature BMP4 is of particular interest because BMP4 and DPP can function as either short- or long-range signaling molecules depending on the tissue in which they are expressed (Neumann and Cohen, 1997). *Xenopus* BMP4, for example, acts over multiple cells within the embryonic mesoderm but acts only within the immediate environment of its synthesis in ectodermal explants (Dosch et al., 1997; Jones et al., 1996). Similarly, DPP acts at long range to pattern the wing disc but signals only to adjacent cells between germ layers of the gut (Neumann and Cohen, 1997; Posakony et al., 1990). Tissue-specific mechanisms that regulate the signaling range of these ligands have not been identified; we hypothesize that selective use of the S2 site generates long versus short range signals in different tissues.

To study the physiological relevance of cleavage at the S2 site, and to test the hypothesis that tissue-specific cleavage at the S2 site regulates BMP4 activity *in vivo*, Goldman et al. generated a cleavage mutant knock-in mouse (*Bmp4*$^{S2G/S2G}$) that carries a point mutation in the *Bmp4* gene that disrupts cleavage of proBMP4 at the S2 site

(Goldman et al., 2006). Characterization of these mice revealed that cleavage at the S2 site is required for normal BMP4 signaling in only a subset of tissues where full BMP4 dosage is known to be necessary (Dunn et al., 1997; Goldman et al., 2006). For example, *Bmp4*$^{S2G/S2G}$ mice show a more severe loss of primordial germ cells and testicular degeneration than that observed in *Bmp4* null heterozygotes (*Bmp4*$^{tm1/+}$). *Bmp4*$^{S2G/S2G}$ mice, however, never display polycystic kidneys, polydactyly, or other skeletal abnormalities that are observed in *Bmp4* $^{tm1/+}$ mice. Furthermore, levels of mature BMP4 protein are decreased in the testes, but not in the limb buds, of *Bmp4*$^{S2G/S2G}$ mice relative to wild-type siblings. Compound *Bmp4* mutants that have one S2G allele and one null allele (*Bmp4*$^{S2G/-}$) die during embryonic development due to defects in ventral body wall closure and abnormalities in the heart and placenta, yet there is no increase in the penetrance or severity of polydactyly or kidney defects compared to *Bmp4* $^{tm1/+}$ mice. These results are consistent with the possibility that the S2 site is selectively cleaved in a tissue-specific fashion. Thus, the tissues that appear unaffected by the S2G mutation (e.g. skeleton and kidneys) may be those in which the S2 site is not normally cleaved. It has not been possible to test this directly, since attempts to generate antibodies that recognize endogenous BMP4 prodomain have not been successful. A knock-in mouse in which the prodomain contains an epitope tag will be indispensable for continuing these studies.

Biochemical as well as phenotypic evidence for tissue-specific cleavage of the S2 site of the invertebrate ortholog of BMP4 has been obtained from studies in flies (Sopory et al., submitted). Sopory and colleagues showed that, like BMP4, DPP is cleaved at two sites, and this dual cleavage is essential for normal development of some but not all

tissues in which DPP activity is necessary. Specifically, a cleavage mutant DPP in which only the S1 site can be processed can rescue defects caused by loss of DPP function in the eye disc and embryonic midgut, but not in the wing or leg disc. Moreover, cleavage of the S2 site of DPP correlates with the requirement for this cleavage as demonstrated in the rescue experiments. Both the S1 and the S2 site of proDPP are cleaved in the wing disc, and this is essential for activation of pMAD multiple cells distant from the DPP source. By contrast, proDPP is cleaved at the S1 site alone in the embryonic midgut, which allows the mature ligand to signal at short range to immediately adjacent cells. These studies provided the first *in vivo* biochemical evidence that the S2 site of proBMP/DPP is cleaved in a tissue-specific manner, and that cleavage at the S2 site coincides with long-range signaling.

I.C.4.c. Tissue-specific regulation of BMP4 cleavage

Our analyses of *Bmp4*$^{S2G/S2G}$ mice and of DPP cleavage in flies support our hypothesis that tissue-specific cleavage of the S2 site can modulate BMP4 ligand activity, but they do not indicate how cleavage at this site is regulated. Several possibilities are being explored.

One hypothesis involves differential trafficking of mature BMP4 vs. S1-only cleaved BMP4. S2 cleavage is enhanced by acidic pH (Degnin et al., 2004), so cleavage of this site might occur only in tissues in which BMP4 sorts from the TGN to the cell surface through an acidic endosomal pathway. Secreted proteins can traffic to the cell surface through endosomal compartments, or they can be delivered directly to the cell surface, bypassing acidic compartments (Futter et al., 1995; Griffiths et al., 1985; Hirschberg et al., 1998; Rodriguez-Boulan et al., 2005 and references therein). If BMP4

sorting is regulated in a tissue-specific manner, cells in which it sorts directly to the cell membrane would generate S1-only cleaved ligand, while cells in which it sorts through the endosomal pathway would generate the fully cleaved, long-range signal.

Alternatively, proteolysis could be regulated at the level of the cleaving enzymes via tissue-specific expression of an S1 or S2 site-specific enzyme. In this situation, the S2 site of BMP4 would only be cleaved to generate the long-range signal in tissues where an enzyme capable of cleaving the S2 site is expressed and active. The enzymes that cleave proBMP4 – the proprotein convertases – are discussed in detail in the following sections.

II. PROPROTEIN CONVERTASES

Proprotein convertases (PCs) are a family of enzymes that cleave various proproteins, including members of the TGFβ family, at specific multibasic sites. Intensive research over the past several decades has focused on identifying and characterizing this important class of enzymes. In 1967 proinsulin, the long-sought insulin precursor, was described, and it became clear that an enzyme must exist that could selectively cleave this and other precursor proteins following multibasic sequences to generate active signaling molecules (Steiner and Oyer, 1967). In 1984, the protease Kex2p, which could cleave pro-α-factor and prokiller toxin after a dibasic motif, was identified in yeast (Fuller et al., 1989; Julius et al., 1984). Soon after, a family of homologous serine protease enzymes, the PCs, was described in mammals.

II.A. Properties of PCs

There are now seven mammalian PC family members that have been identified – Furin [also known as Paired Basic Amino Acid Converting Enzyme (PACE), Subtilisin-like Proprotein Convertase 1 (SPC1), or Proprotein Convertase Subtilisin/Kexin Type 3 (PCSK3)], PC1 (also named as PC3, SPC3, or PCSK1), PC2 (also called SPC2 or PCSK2), PC4 (also known as SPC4 or PCSK4), PACE4 (also called SPC5 or PCSK6), PC6 (also named PC5, SPC6, or PCSK5), and PC7 [also called Lymphoma Proprotein Convertase (LPC), PC8, SPC7, or PCSK7] (Steiner, 1998). Each of these enzymes contains a set of conserved domains, including the highly conserved subtilisin like catalytic domain that defines this family. PC1 and PC2 are secreted enzymes that are active in the regulated secretory pathway of endocrine and neuroendocrine tissues, while *Pc4* is expressed specifically in germ cells. Furin, PACE4, PC6, and PC7, on the other hand, are active in the constitutive secretory pathway and are broadly expressed throughout development.

II.A.1. Conserved domains

Each of the PC family members contains a signal sequence that targets the nascent protein to the endoplasmic reticulum, a minimally conserved prodomain, a highly conserved catalytic domain, a PC-specific P-domain (also called the HomoB or middle domain), and a variable C-terminal domain (Figure 1-8). The prodomain is essential for proper folding of the enzyme and acts as an intramolecular inhibitor until altered cellular conditions and/or proteolytic cleavage results in its dissociation (Anderson et al., 1997; reviewed in Seidah et al., 2008). Both its role as an inhibitor and its removal are discussed in detail below.

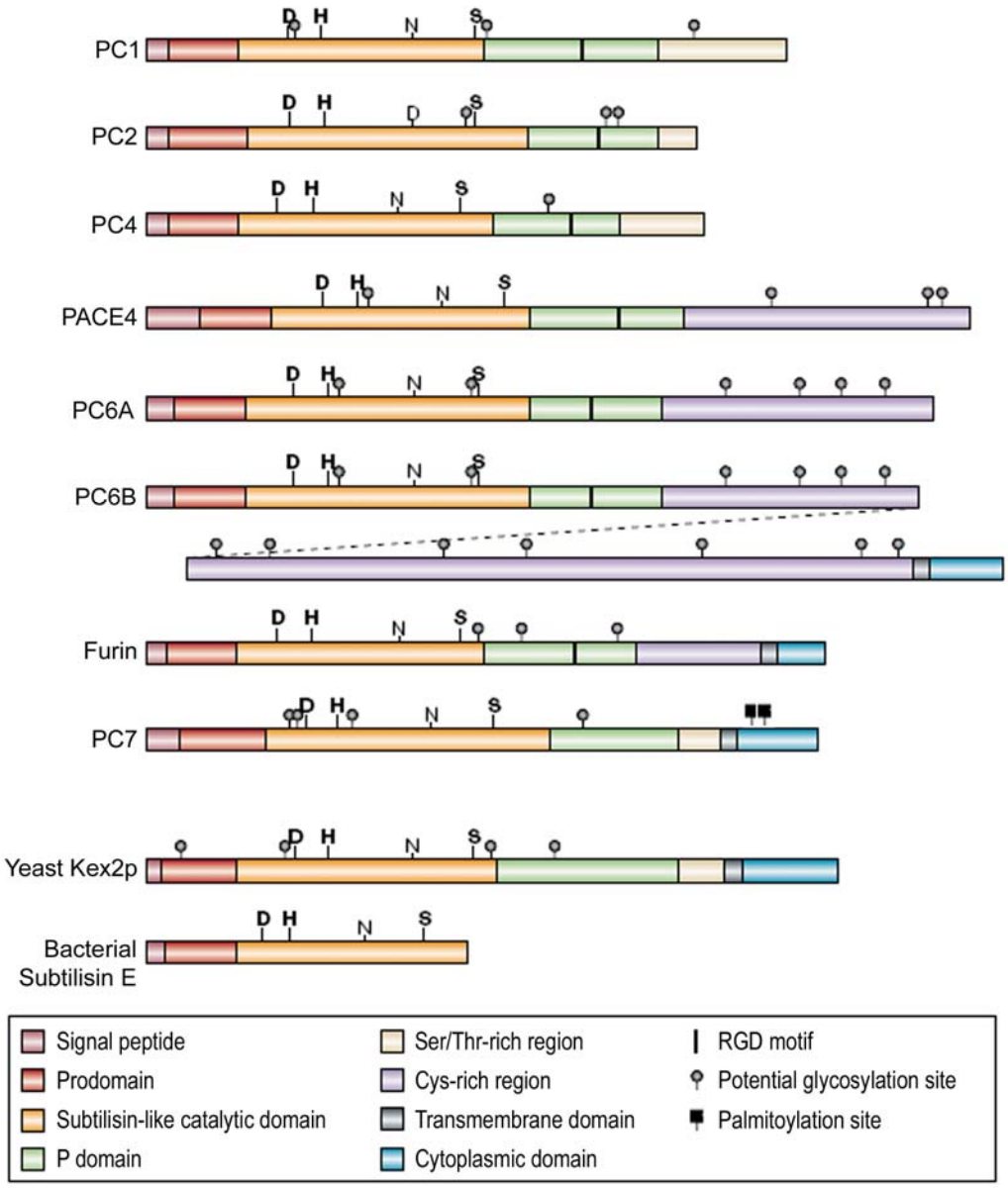

Figure 1-8 Diagram of PC family conserved domains. Shown are schematics of the seven PC family members as well as the evolutionarily conserved yeast Kex2p and bacterial Subtilisin. Also shown are the two main isoforms of PC6 – PC6A and PC6B – generated by alternative splicing. The diagonal dashed line links the two halves of PC6B. The N-terminal half of PC6B contains all of PC6A except for a small portion at the C-terminus that is specific to PC6A. The bold **D**, **H**, and **S** labels indicate the positions of the catalytic triad residues. The non-bold N and D labels identify the oxyanion hole residues. Reprinted with permission (Thomas, 2002).

The P-domain is also necessary for proper folding and enzyme activity (Creemers et al., 1993b; Gluschankof and Fuller, 1994; Zhou et al., 1998). The bacterial subtilisins, which are degradative enzymes, lack this domain, while Kex2p and the PCs, which are selective processing enzymes, all have it. Deletion and domain swapping experiments have implicated the P-domain in stabilizing the catalytic domain, regulating the pH and calcium dependence of the enzymes, and contributing to substrate specificity.

The catalytic domain is the most highly conserved. It includes the essential serine protease catalytic triad (D, H, S) and the oxyanion hole (N) important for stabilization of the acyl-enzyme intermediate (Kraut, 1977). The serine protease mechanism is illustrated in Figure 1-9 and described in the figure legend.

Furin was the first mammalian PC to be identified (Fuller et al., 1989; Roebroek et al., 1986; van den Ouweland et al., 1990), and it has been the best-studied. The C-terminal portion of Furin consists of a region in which the relative position of multiple cysteines is highly conserved into what is termed the cysteine rich domain (CRD). The consensus sequence for the CRD motif is $CX_2CX_3CX_2CX_{5-7}CX_2CX_{10-15}CX_{3-5}C$, and these motifs are separated by 10-16 amino acids (Nakagawa et al., 1993b). The CRD is followed by a transmembrane domain and a cytoplasmic tail that contains multiple sequence motifs important for trafficking (see below).

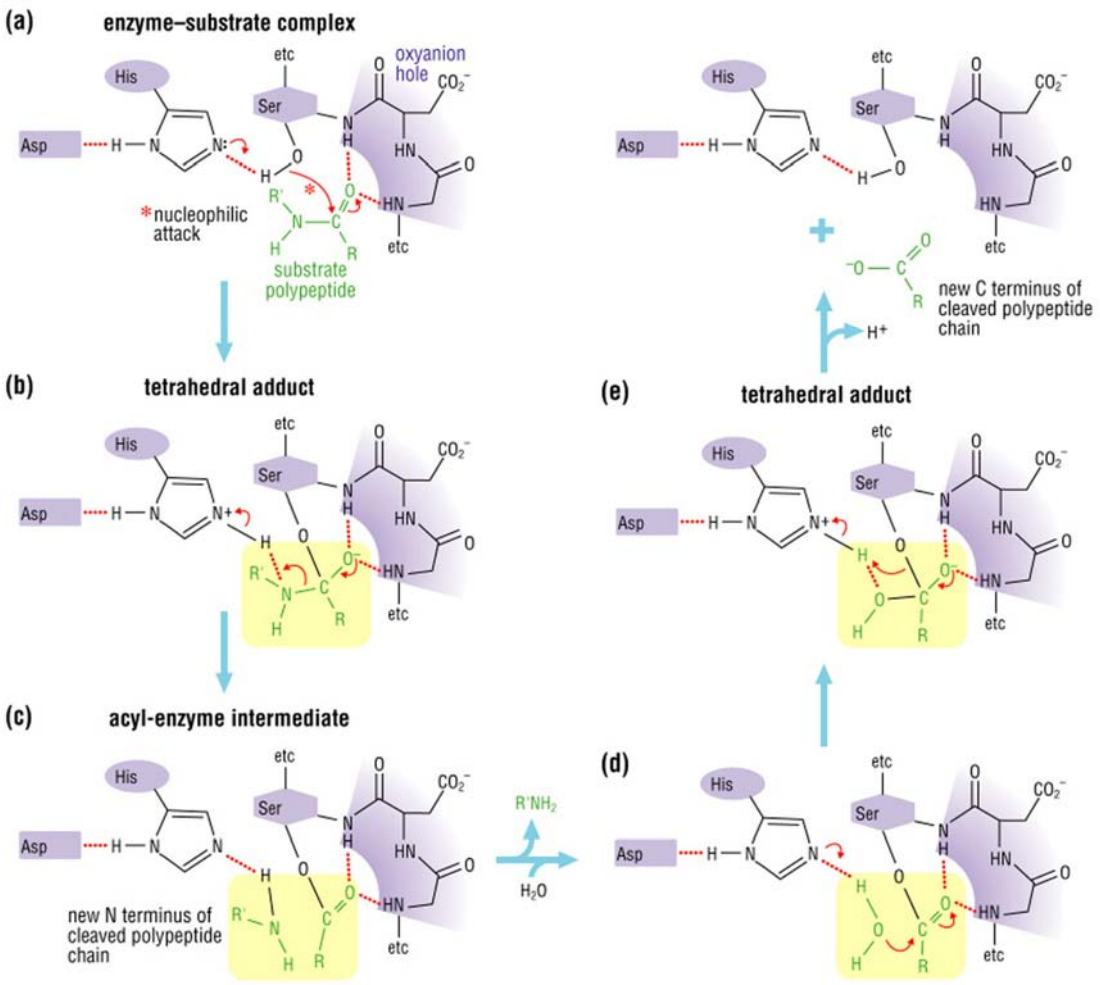

Figure 1-9 Illustration of serine protease mechanism. The reactive site of a serine protease is shown to illustrate the catalytic mechanism used by this family of enzymes. (a) Serine hydroxyl O attacks substrate carbonyl C; histidine N accepts H from serine hydroxyl; carbonyl O accepts electrons; oxyanion hole stabilizes negative charge – tetrahedral adduct is generated. (b) The covalent electrons of the peptide bond attack the histidine H, breaking the bond; the electrons that previously moved from the carbonyl O double bond move back to recreate the bond – acyl-enzyme intermediate is generated. (c) The C-terminal portion of the precursor (mature domain) is released and replaced by water. (d) Water O attacks carbonyl C; histidine N accepts H from water; carbonyl O accepts electrons; oxyanion hole stabilizes negative charge – tetrahedral adduct is generated. (e) Serine O attacks histidine H; electrons from carbonyl double bond move back to recreated bond – N-terminal portion of the precursor (prodomain) is released and active site is regenerated. Reprinted by permission of Oxford University Press from (Petsko and Ringe, 2004).

PC1, PC2, and PC4 were the next PC family members that were identified and described in rapid succession (Nakayama et al., 1992; Seidah et al., 1992; Seidah et al., 1990; Seidah et al., 1991; Smeekens and Steiner, 1990). PC1 and PC2 are secreted proteins with a serine/threonine rich region C-terminal to the P domain rather than the

CRD found in Furin. The function of this domain is not yet clear. There is some evidence that mouse PC4 might be membrane associated, though the nature of this association is unknown (Gyamera-Acheampong et al., 2006). Various splice isoforms of PC4 have been identified in rodents (A-E), but the functional relevance of these is unclear since PC4B and PC4C are truncated, and PC4D and PC4E lack the signal sequence and prodomain (Mbikay et al., 1994; Seidah et al., 1992). Human and *Xenopus* PC4, on the other hand, have an extended C-terminus that contains one CRD motif as well as a transmembrane domain (discussed in Chapter 2).

The next PC family member to be identified was PACE4 (Kiefer et al., 1991). Several splice isoforms of PACE4 have been identified (Creemers et al., 1993a; Kiefer et al., 1991; Mori et al., 1997; Tsuji et al., 1997). Many of the transcripts encode proteins in which the P domain is missing or truncated and are therefore expected to be inactive, but two isoforms have been shown to fold properly and cleave substrates in trans – PACE4A and PACE4E. PACE4A is the predominant protein produced in mammals and is often simply referred to as PACE4; it is broadly expressed, while PACE4E is expressed primarily in the central nervous system (Akamatsu et al., 1997; Kiefer et al., 1991; Zhong et al., 1996). These two proteins differ only in their extreme C-termini (Mori et al., 1997). In both isoforms the CRD is longer than that of Furin (5 repeats rather than two truncated), and neither contains a TMD, though PACE4E may be membrane associated via a cluster of hydrophobic residues at its C-terminus.

PC6 was found next, and multiple splice isoforms have been described for this PC as well (Nakagawa et al., 1993a; Nakagawa et al., 1993b). The PC6A isoform is very similar to PACE4 – they both have 5 CRD repeats, they are secreted, and they associate

with heparin sulfate proteoglycans (HSPGs) on the cell surface (Nour et al., 2005; Tsuji et al., 2003). PC6B is a much longer, membrane-bound form (De Bie et al., 1996; Nakagawa et al., 1993b). It has 22 CRD repeats as well as a cytoplasmic tail with multiple sequence motifs involved in sorting (see below). The N-terminal half of PC6B contains all of PC6A except for a small portion at the C-terminus that is specific to PC6A. Other splice isoforms with variable C-termini have also been described, and those will be discussed in Chapter 2.

PC7 was described most recently, by multiple groups (Bruzzaniti et al., 1996; Constam et al., 1996; Seidah et al., 1996). Human PC7 is encoded by a gene on chromosome 11q23 and was first identified due to a translocation at this site associated with human lymphomas (Meerabux et al., 1996). For this reason, it is also called Lymphoma Proprotein Convertase (LPC). This PC is more similar to yeast Kex2p and bacterial subtilisin than the others are, has a different gene structure than the other PCs, and the C-terminus of its intracellular portion contains an S, T, and C-rich domain rather than the conserved CRD that is found in the other family members that operate in the constitutive pathway (Bruzzaniti et al., 1996; Constam et al., 1996; Goodge et al., 1998). Also, unlike the other family members, PC7 does not contain the conserved RGD integrin binding motif (Bruzzaniti et al., 1996; Seidah et al., 1996). The function of this motif has not yet been elucidated.

II.A.2. Proteolytic activation

PC enzymes are themselves synthesized as inactive precursor proteins that have to be cleaved in order to be activated, and this is tightly coupled to their trafficking through (and sometimes outside of) the cell (Creemers et al., 1993a; De Bie et al., 1996; Leduc et

al., 1992; Mains et al., 1997; Munzer et al., 1997; Rehemtulla et al., 1992; van de Loo et al., 1997). Cleavage is autoproteolytic.

For Furin, there are two consecutive cleavages that are closely linked to its trafficking and activation (Anderson et al., 2002; Anderson et al., 1997; Feliciangeli et al., 2006; Molloy et al., 1994; Vey et al., 1994). The first cleavage occurs in the ER at an optimal consensus motif. This cleavage is necessary for exit out of the ER, but the prodomain remains noncovalently associated with the catalytic domain and inhibits Furin's intermolecular cleavage activity. Once Furin enters the more acidic environment of the TGN, a conformational change occurs to expose a second cleavage site within the prodomain. Cleavage at this site releases the inhibitory prodomain and results in a fully active protease. PC1 and PC6 are activated by a similar sequential cleavage mechanism, and PACE4 is thought to behave the same since it has a predicted second cleavage site that is almost identical to that of PC6 (Nagahama et al., 1998; Nour et al., 2003; Zhou and Lindberg, 1993). PACE4 maturation occurs more slowly than other PCs, and the C-terminus seems to be responsible for this, but the functional consequences of this delay are as yet unknown (Mains et al., 1997).

Similarly, PC7 is autocatalytically cleaved in the ER, which then allows it to traffic to the TGN (Munzer et al., 1997; van de Loo et al., 1997). In this case, though, it is not known if the prodomain remains associated after cleavage, or if so, when it dissociates to release the active enzyme. PC7 does not have a secondary consensus cleavage motif within its prodomain, so it is doubtful that it is activated the same as Furin and PC6. PC4 also lacks an obvious upstream cleavage motif.

PC2 is activated by a different mechanism involving the chaperone protein 7B2 (Mbikay et al., 2001). Unlike the other PCs, proPC2 is not cleaved before exiting the ER. Instead, it associates with 7B2 within the ER, and the two proteins traffic through the secretory system together. When they reach the more acidic compartment of the secretory granules, proPC2 autocatalytically activates itself. The prodomain and 7B2 then dissociate from the enzyme, and PC2 becomes active and able to cleave substrates in trans. 7B2 is not absolutely required for PC2 trafficking and cleavage, but the PC2 enzyme generated in the absence of 7B2 is inactive (Muller et al., 1997). This was recently shown to be due to aggregation of pro- and mature PC2, likely caused by partial unfolding (Lee and Lindberg, 2008). 7B2 is therefore necessary for PC2 to maintain a properly folded conformation as it traffics through the secretory system, until it reaches acidic compartments, where PC2 is able to cleave and activate itself.

II.A.3. Enzymatic properties

Experiments defining the nature and enzymatic properties of PCs revealed that they are Ca^{2+} dependent serine proteases that are active over a broad pH range (Table 1). The optimal [Ca^{2+}] and pH values are indicative of the locations within and outside of the cell where each enzyme is believed to be active. For example, PC1 and PC2 – which are active in the secretory granules of the regulated secretory pathway – require higher [Ca^{2+}] and lower pH, the conditions found in these compartments. On the other hand, PCs that cleave their substrates within the TGN, endosomes, and extracellular space (i.e. Furin, PC4, PACE4, PC6, and PC7) are active at lower [Ca^{2+}] and more neutral pH.

Table 1-1. Optimal calcium concentration and pH for PC enzymatic activity

Enzyme	[Ca^{2+}]	Optimal pH	Reference
PC1	4.0-10mM	5.5-6.0	(Decroly et al., 1996)
PC2	4.0-10mM	5.0-6.0	(Shennan et al., 1991)
PC4	2.0mM	7.0	(Basak et al., 1999)
Furin	1-2mM	6.0-8.5	(Bresnahan et al., 1990; Molloy et al., 1992)
PACE4	0.5-10mM	7.0-8.5	(Decroly et al., 1996);
PC6	0.2-2.5mM	7.0-8.0	(Decroly et al., 1996);
PC7	1-2mM	6.0-7.0	(Munzer et al., 1997)

II.A.4. Inhibitors

Given the important roles that PCs play during development, homeostasis, and pathogenesis, selective and potent inhibitors of these enzymes have become invaluable tools. Much time and energy has been invested in identifying and developing inhibitors as potential therapeutics, as well as inhibitors that can be used to further our understanding of the characteristics of these enzymes, their potential *in vivo* substrates, and the myriad roles they play in biology (reviewed in Fugere and Day, 2005).

II.A.4.a. Proprotein convertase prodomains

As described above, PCs, like their substrates, are synthesized as inactive precursors with an N-terminal prodomain that must be removed to generate an active protease (reviewed in Seidah et al., 2008). The prodomain is necessary for folding and, in the case of PCs, acts as an intramolecular inhibitor to prevent cleavage of substrates in trans until the protease has reached its appropriate location and the prodomain dissociates. It was discovered that these prodomains could also act as inhibitors when added to PCs in trans. Boudreault first tested the ability of the prodomain of PC1 (pPC1) to inhibit its cognate enzyme as well as Furin and PC2 (Boudreault et al., 1998). A

protein fragment encompassing the entire prodomain plus an additional C-terminal 14 amino acids potently inhibited both PC1 and Furin. On the other hand, PC2 was not efficiently inhibited by pPC1; PC2 instead cleaved the PC1 prodomain (Boudreault et al., 1998).

Zhong et al. investigated Furin and PC7 prodomains (pFurin, pPC7) for their ability to selectively and efficiently inhibit PCs, and they found that both inhibited their parent molecules with IC_{50} values in the nanomolar range (Bhattacharjya et al., 2000; Zhong et al., 1999). The prodomains were not completely selective, though, as they also inhibited PCs that are not the parent molecule. The more selective pPC7 inhibited PC7 > PC6 ≈ PACE4 ≈ Furin > Kexin, while pFurin inhibited PC5 > Furin > PC7 > PACE4 > Kexin. The C-terminal 10 amino acids were sufficient for inhibition *in vitro*, but they were less potent and selectivity was altered, suggesting that other residues within the prodomain are also important for maximal inhibition. Nour et al. observed the same for pPC6, and another group observed similar results when they compared the ability of each of the seven mammalian prodomains to inhibit PC6A and soluble forms of Furin and PC7 (Fugere et al., 2002; Nour et al., 2003). Also, cleavage of Furin substrates – nerve growth factor (NGF) and brain-derived neurotrophic factor (BDNF) – was blocked in cells overexpressing a construct encoding pFurin with a signal sequence (ppFurin), suggesting that the prodomain expressed in trans is able to fold and interact with PCs within the secretory pathway (Zhong et al., 1999).

II.A.4.b. Endogenous small peptide inhibitors

7B2 is a protein that acts as a chaperone for PC2 and is necessary for its activation (discussed above), but the C-terminal portion of this protein is also a very potent and specific inhibitor of that PC (Lindberg et al., 1995). A similar endogenous inhibitor of PC1 has been identified named proSAAS (Cameron et al., 2000b). Unlike 7B2, proSAAS is not required for PC1 activation, but it has an analogous C-terminal peptdide that acts as a specific inhibitor of PC1.

II.A.4.c. Serpins

Serine protease inhibitors (serpins), are a class of proteins that act as competitive suicide inhibitors by forming an equimolar complex with their target proteases (Huntington et al., 2000; Perlmutter and Pierce, 1989) (Figure 1-10). Upon formation, the complex undergoes a major structural rearrangement, trapping the protease in an inactive conformation by a covalent, SDS-stable interaction (acyl-enzyme intermediate, shown in step (c) of Figure 1-9). The reactive site loop (RSL) of the serpin is the portion that interacts with the catalytic domain of the protease and therefore largely determines the target specificity. This characteristic has been used to identify potential endogenous inhibitors as well as to generate specific, potent inhibitors of PCs.

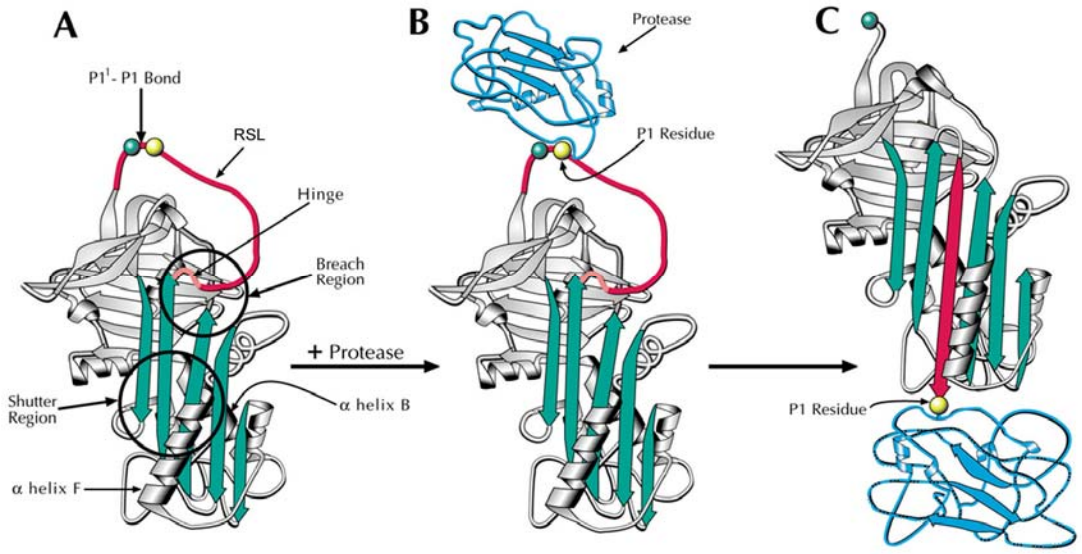

Figure 1-10. Illustration showing irreversible serpin inhibition of a serine protease. A. Ribbon diagram of a serpin highlighting the bond within the reactive site loop (RSL) that will be cleaved by the protease as well as regions of the serpin that will undergo conformational changes. B. The protease recognizes and binds to the primary sequence of the RSL and cleaves the P_1-P_1' bond. C. Cleavage of the RSL results in a conformational change in which the the RSL inserts into the β-sheet within the shutter region and displaces α helices B and F, generating a stable serpin-protease complex. Illustration reprinted with permission from Pepro Tech Inc. 2007 Update (http://www.peprotech.com/content/focusarticles.htm?id=134).

II.A.4.c.i. Potential endogenous serpins

Protease Inhibitor 8 (PI8) is a naturally occurring ovalbumin type serpin that contains two minimal PC consensus motifs in its RSL (P_4-P_1: -R-N-S-R- and P_1-P_3': -R-C-S-R-) (Sprecher et al., 1995). It is a potent inhibitor of Furin with physiologically significant kinetic constants (Dahlen et al., 1998). It is not clear how PI8 and Furin might interact, though, since PI8 does not have a typical N-terminal signal sequence directing it to the secretory pathway and is instead localized to the nucleus of differentiated squamous epithelial cells and monocytes, and to the cytoplasm of some neuroendocrine cells as determined by immunohistochemistry of human tissue sections (Strik et al., 2002). However, excellent evidence for endogenous Furin-PI8 interaction was demonstrated in one cell type: upon stimulation of human platelets, both proteins are

rapidly released and immediately begin to form an SDS-stable complex that coincides with loss of Furin activity (Leblond et al., 2006). It will be interesting to see if a molecular and functional interaction can be demonstrated in other cell types as well.

Another potential endogenous serpin was first described in *Drosophila*. The *Spn4* gene encodes eight different serpin proteins, with four different RSL sequences (Bruning et al., 2007; Kruger et al., 2002). The most interesting isoform with respect to PCs is Spn4A, which has an optimal Furin recognition sequence in its RSL (-R-R-K-R-). It also has an N-terminal signal sequence and a C-terminal ER retrieval motif, suggesting that it is retained in the secretory pathway. *In vitro*, Spn4A is able to form SDS-stable complexes with *Drosophila* PC2 and human Furin (*Drosophila* Furin was not tested), and it is a very potent inhibitor of these PCs (Oley et al., 2004; Osterwalder et al., 2004; Richer et al., 2004). Also, overexpression of *Spn4A* in flies resulted in a phenotype resembling PC2 loss of function, suggesting that this could be a bona fide inhibitor. However, the closest mammalian homolog, neuroserpin, does not have a Furin recognition sequence in its RSL (-A-I-S-R-), so it is not clear if an analogous, PC-specific serpin exists in vertebrates (Osterwalder et al., 2004). Spn4A is a very potent inhibitor, though, and may be a useful experimental tool.

II.A.4.c.ii. Engineered serpin variants

α_1-antitrypsin (α_1-AT) is a naturally occurring serpin that targets neutrophil elastase. It functions as a major antielastase in the lower respiratory tract (Perlmutter and Pierce, 1989). A naturally occurring mutation that converts the RSL sequence of human α_1-AT from -A-I-P-M^{358}- to -A-I-P-R^{358}- renders the serpin ineffective against elastase and converts it to a potent inhibitor of thrombin. Patients with this α_1-AT Pittsburg (α_1-

PIT) mutation have a severe bleeding disorder. Anderson and colleagues took advantage of this ability to alter target specificity and introduced another mutation that changes the RSL of α_1-PIT to a minimal PC recognition motif (-R-I-P-R^{358}-) (Anderson et al., 1993). This variant, called α_1-AT Portland (α_1-PDX), is inactive against elastase and thrombin but specifically inhibits Furin with a K_i of 1.4 nM and a stoichiometry of inhibition (SI) of 2 (Anderson et al., 1993; Jean et al., 1998). α_1-PDX is able to inhibit cleavage of known PC targets, such as F protein of measles virus and *Pseudomonas* exotoxin A (PEA) (among others), when cells are cotransfected with α_1-PDX and F protein or treated with exogenous α_1-PDX prior to addition of PEA (Jean et al., 1998; Watanabe et al., 1995).

Although α_1-PDX inhibits Furin most efficiently, it is also an effective inhibitor of other PCs, especially PC6 (Jean et al., 1998). It is less effective against PC1 and PC2, and ineffective against PC7. This is expected since PC7 requires a basic residue in the P_2 position (van de Loo et al., 1997). It was also thought to be ineffective against PACE4, but another group later showed that higher concentrations of α_1-PDX can inhibit PACE4 effectively (Jean et al., 1998; Tsuji et al., 1999a; Tsuji et al., 2002). Since α_1-PDX is able to inhibit multiple PCs, several groups attempted to improve Furin inhibition or increase differential specificity for other PCs by making additional mutations within the RSL. Dufour and colleagues found that a variant with a P_2 arginine (-R-I-R-R-, α_1-EK1) is slightly more effective against Furin than α_1-PDX (Dufour et al., 2001). A similar variant with a P_2 lysine (-R-I-K-R-, α_1-EK4), though, is only effective at higher concentrations because it is a better substrate (i.e. is cleaved by Furin) than an inhibitor (SI = 13). Similarly, Tsuji and colleagues used the rat α_1-AT (RSL sequence -A-V-P-

M^{352}-) as a starting point and introduced mutations corresponding to α_1-PDX (-R-V-P-R^{352}-) and α_1-EK1 (-R-V-R-R^{352}-) as well as a novel mutation (-A-V-R-R^{352}-) (Tsuji et al., 2002). As expected, the variant containing -R-V-P-R^{352}- in its RSL inhibited Furin, PC6, and PACE4, while that containing -R-V-R-R^{352}- inhibited Furin and PACE4. Surprisingly, the -R-V-R-R^{352}- variant was not an effective inhibitor of PC6 (IC_{50} = 620nM). Also, the -A-V-R-R^{352}- variant was able to inhibit Furin and PC6, but it did not inhibit PACE4; it was efficiently cleaved by PACE4 and did not form an SDS-stable complex with this enzyme. Therefore, although some differences in inhibitory properties have been identified *in vitro* and in cell culture, it is unknown how useful these differences will be for inhibition of specific PCs in a whole organism where multiple PCs are likely present in any given tissue.

II.A.4.d. Engineered protein-based inhibitors

Proteins other than serpins have also been explored as backbones for potential PC inhibitors, one of which – Eglin c – is particularly promising both experimentally and therapeutically. Eglin c is a polypeptide protease inhibitor from the leech *Hirudo medicinalis* that efficiently inhibits subtilisins (Bae and Sturtevant, 1995; Seemuller et al., 1981). It is an excellent starting point for engineered protein-based inhibitors because it is small (70 amino acids) and lacks disulfide bonds, yet is thermally stable (Tm ~86°C), so that robust expression is possible. Komiyama and Fuller introduced a series of substitutions in the eglin RSL (-G-S-P-V-T-L^{45}-) and found that a protein in which the P_1 and P_4 residues are replaced with arginine (R_4R_1-eglin) is a stable and potent reversible competitive inhibitor of Furin (Komiyama and Fuller, 2000). R_4R_1-eglin forms a complex with Furin that is stable over a physiological pH range (~6.0 – 7.4) and has a

half-life of approximately one hour. Substitution of the P_2 or P_6 residues of this variant with basic amino acids further enhanced the affinity of the protein for Furin, but the interaction is temporary due to cleavage of the inhibitor. Because R_4R_1-eglin forms a stable complex with Furin, it was hoped that this complex might be internalized to inhibit intracellular as well as extracellular Furin-mediated processing. However, very high concentrations (~1,000-fold greater than the K_i) of exogenously applied eglin were necessary to inhibit cleavage of intracellular PC targets, suggesting that it does not enter cells efficiently (Komiyama et al., 2005).

In order to enhance the affinity of eglin variants for Furin and to potentially generate variants with differential specificity for each PC via improved adventitious contacts, Komiyama and collegues identified and generated random mutations at residues that were likely to contact the bound enzyme (Komiyama et al., 2003). Of these, substitutions at only four sites resulted in improved Furin affinity, the best of which was a combination of D33V and Y49D (Val-33-Asp-49-R_4R_1-eglin). This variant was ~40-fold more potent against Furin than PC7 while the Trp-49-R_4R_1-eglin was ~20-fold more potent against PC7 than Furin. In additon, substitutions at the P_6 position resulted in cleavage by Furin, as previously observed, but not by PC7. This set of variants could therefore be very useful for discriminating between the effects of these two related PCs

II.A.4.e. Engineered peptide inhibitors

Peptide-based inhibitors have also been an active area of research. They are relatively easy to synthesize and multiple peptides have proven to be potent inhibitors.

II.A.4.e.i. Polybasic peptides

The Lindberg lab performed a systematic screen of peptide combinatorial libraries to identify optimal inhibitory small molecules for six of the mammalian PCs – PC1, PC2, Furin, PACE4, PC6, and PC7 (Apletalina et al., 1998; Cameron et al., 2000a; Fugere et al., 2007; Kacprzak et al., 2004). From a hexapeptide library, they found one peptide (Ac-LLRVKR-NH_2) that is a potent inhibitor of both PC1 and PC2 but is relatively ineffective against Furin, suggesting that this molecule could be useful for discriminating between these PCs (Apletalina et al., 1998). Further studies revealed that hexapeptides with basic residues in all six positions preferentially inhibit Furin (Cameron et al., 2000a). In addition, it was found that the dextrorotatory peptide Hexa-D-Arginine (D6R) is as effective an inhibitor of Furin as the standard levorotatory version (L6R), but the L6R peptide is cleaved and inactivated by Furin while D6R is not. Finally, Fugere et al. screened a library of hexapeptides to measure their ability to inhibit PC6 and PC7 and concluded that longer, poly-basic peptides with the D rather than the L conformation are the best inhibitors of these PCs, as they are for Furin (Fugere et al., 2007). D6R is non-toxic and can efficiently inhibit PC-mediated cleavage and activation of *Pseudomonas aeruginosa* exotoxin A (PEA) and anthrax toxin protective antigen (PA) in cell culture and in animal models (Sarac et al., 2002; Sarac et al., 2004). Thus, D6R has a high therapeutic potential when blocking Furin, PC6, and PC7 is necessary or at least tolerated.

II.A.4.e.ii. Chloromethyl ketones

Peptidyl chloromethyl ketones (CMKs) are peptides in which the C-terminal residue has been modified with a CH_2Cl group. The CMK reacts with serine proteases

irreversibly by forming a covalent bond with the active site histidine and serine (see Figure 1-11 for reaction scheme) (Basak, 2005). Garten et al. found that by changing the sequence of the peptide to a dibasic motif (FAKR-CMK), they were able to inhibit cleavage of influenza virus hemagglutinin (HA) *in vitro* and in cells, and that if they add a hydrophobic moiety to the N-terminus – palmitic acid in this case (pal-FAKR-CMK) – they were able to use a much lower concentration (100μM vs. 10mM) to achieve an equivalent level of inhibition (Garten et al., 1989). The same group of researchers later identified Furin as a potential protease responsible for cleaving fowl plague virus HA. They created a modified peptidyl CMK that incorporated a Furin consensus cleavage site and a decanoic acid (dec-REKR-CMK), and showed that it inhibited Furin much more efficiently than dec-FAKR-CMK (Stieneke-Grober et al., 1992). They also showed that it effectively inhibited cleavage of human immunodeficiency virus 1 envelope glycoprotein-160 (HIV-1 gp160) and prevented gp160-mediated infectivity in cells (Hallenberger et al., 1992). It was later shown that these tri-basic peptidyl CMKs actually inhibit all of the PCs very efficiently (Denault et al., 1995; Fugere et al., 2002; Jean et al., 1998). The lack of specificity, along with their short half-life and their irreversible interaction with enzymes that are likely important for cell survival make them unattractive therapeutic candidates (Garten et al., 1994). They are, however, very useful for research purposes and are frequently used as a control PC inhibitor.

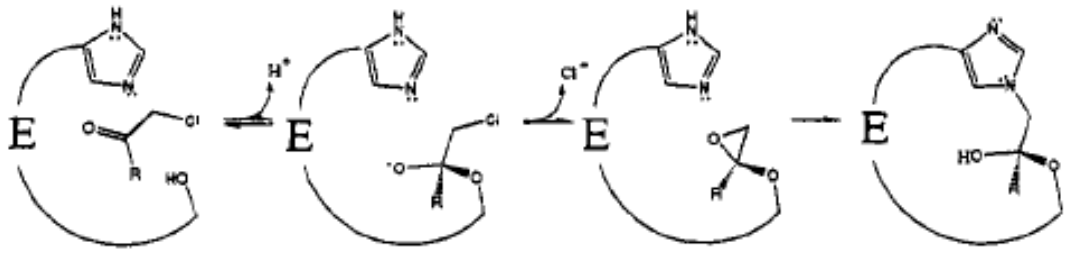

Figure 1-11. Reaction scheme showing irreversible interaction of chloromethyl ketone with the active site of a serine protease. (1) The active site serine OH attacks the CMK carbonyl carbon, (2) the hemiketal oxyanion displaces chloride to give an epoxy ether intermediate, (3) the active site histidine attacks the CMK methylene carbon , and (4) the hemiketal is regenerated. Reprinted with permission (Kreutter et al., 1994).

In summary, multiple protein and peptide-based inhibitors are continually being developed with the hope of finding a set of molecules that potently and selectively inhibit each of the PCs, and that are non-toxic and therefore potentially suitable for therapeutic purposes. Currently, the most frequently used inhibitors for experimental situations are the pan-PC inhibitor dec-RVKR-CMK and the Furin/PC6 partially selective serpin α_1-PDX.

II.B. Substrate specificity and proteolytic targets

PCs have been implicated in the proteolytic activation of a wide variety of targets during development, adult tissue homeostasis, and disease (reviewed in Taylor et al., 2003). Since most PCs recognize a common basic cleavage motif, substrate specificity is likely to arise from multiple factors, including enzyme-substrate interactions outside of the catalytic cleft, co-localization within (or outside of) a cell, and co-expression within a tissue. These observations, combined with loss of function studies for each of the PCs, have suggested potential targets that are important during development.

II.B.1. Cleavage site specificity

The defining feature of PCs is that they selectively cleave their substrates following a multibasic motif. Cleavage occurs at the sissile bond C-terminal to a basic residue; that basic residue and those N-terminal to it are designated P_1, P_2, etc., while those C-terminal to the cleavage site are designated P_1', P_2', etc. Furin has been shown to cleave multiple substrates following an optimal consensus motif of -R-X-R/K-R-, listed P_4 to P_1, where X is any amino acid except cysteine (Brennan and Nakayama, 1994; Krysan et al., 1999; Molloy et al., 1992; Rehemtulla and Kaufman, 1992). It can also cleave following a minimal motif (-R-X-X-R-), and occasionally a P_6 basic residue in addition to a P_2 basic residue can substitute for the P_4 arginine (-R/K-X-X-X-R/K-R). A crystal structure for Furin has been resolved and shows multiple acidic residues in the active site cleft, explaining the preference for basic residues (Henrich et al., 2003).

PC1 and PC2 primarily cleave following a dibasic motif (-R/K-R-), while PC4 prefers sequences similar to Furin (-K-X-X-R-, -R-X-R/K-R-, or -R/K-X-R-X-X-R-) (Basak et al., 2004; Benjannet et al., 1991). A comparative study of cleavage specificity for multiple PCs confirmed these observations and showed that PACE4 and PC6 also cleave following a minimal or optimal Furin consensus motif (-R-X-X/R/K-R-) (Remacle et al., 2008). PC7, on the other hand, requires a P_2 basic residue (Munzer et al., 1997; van de Loo et al., 1997). In addition to the P_1 arginine, PC7 prefers lysine over arginine in the P_2 position, and prefers motifs containing an arginine in the P_6 position (-R-X-X/R-X-K-R) over those containing an arginine only in the P_4 position (-X-X-R-X-K-R). Lysine is not well-tolerated in either the P_4 or the P_6 position.

II.B.2. Subcellular/extracellular trafficking and localization

PCs are active in multiple compartments within the cell, as well as outside the cell in some cases. Furin, for example, has been shown to localize primarily to the TGN, but some protein is present in late endosomal/pre-lysosomal vesicles and at the cell surface (Figure 1-12). Several groups have demonstrated that the cytoplasmic tail of Furin is necessary and sufficient to determine this localization (Bosshart et al., 1994; Chapman and Munro, 1994; Molloy et al., 1999; Molloy et al., 1994). It was subsequently demonstrated that Furin is actively trafficking between the TGN and the plasma membrane in a complex bi-cycling pattern involving tyrosine-based (YXXL) and leucine/isoleucine-based internalization motifs as well as an acidic cluster, which is phosphorylated on two serines by casein kinase II (Jones et al., 1995; Molloy et al., 1999 and references therein; Molloy et al., 1998) (Figure 1-13). This motif binds to Phosphofurin Acidic Cluster Sorting Protein 1 (PACS-1) as well as various other interacting proteins (Crump et al., 2001; Liu et al., 1997; Scott et al., 2003; Wan et al., 1998). In addition to the transient population of membrane-bound Furin available to cleave extracellular substrates at the cell surface, a shed form of Furin, generated by cleavage within the C-terminus of the luminal domain, has also been observed (Denault et al., 2002; Plaimauer et al., 2001; Vey et al., 1994) (Figure 1-12).

PACE4 and PC6A are both secreted molecules that have been shown to associate with heparin sulfate proteoglycans (HSPGs) in the extracellular matrix via their cysteine rich domains (CRDs) (Nour et al., 2005; Tsuji et al., 2003) (Figure 1-12). PC6A has also been shown to sort to regulated secretory granules in some cells, while a membrane-bound isoform (PC6B) has only been reported in the constitutive secretory pathway (De

Bie et al., 1996). PC6B undergoes a similar trafficking pattern to that of Furin, except that it cycles between a post-TGN compartment and the cell surface (Xiang et al., 2000) (Figure 1-12). A membrane proximal acidic cluster directs TGN localization in a PACS-1 dependent fashion while a second, PACS-1 independent, acidic cluster in the C-terminus is responsible for the post-TGN localization (Figure 1-13). It is not known, however, what proteins or trafficking systems are utilized to affect this latter localization. A tyrosine-based internalization motif in the N-terminal portion of the cytoplasmic tail was also shown to be important, and another potential tyrosine-based motif may contribute to PC6B trafficking. Also, like Furin, PC6B is cleaved within the C-terminus of the luminal domain to generate a shed form (De Bie et al., 1996) (Figure 1-12).

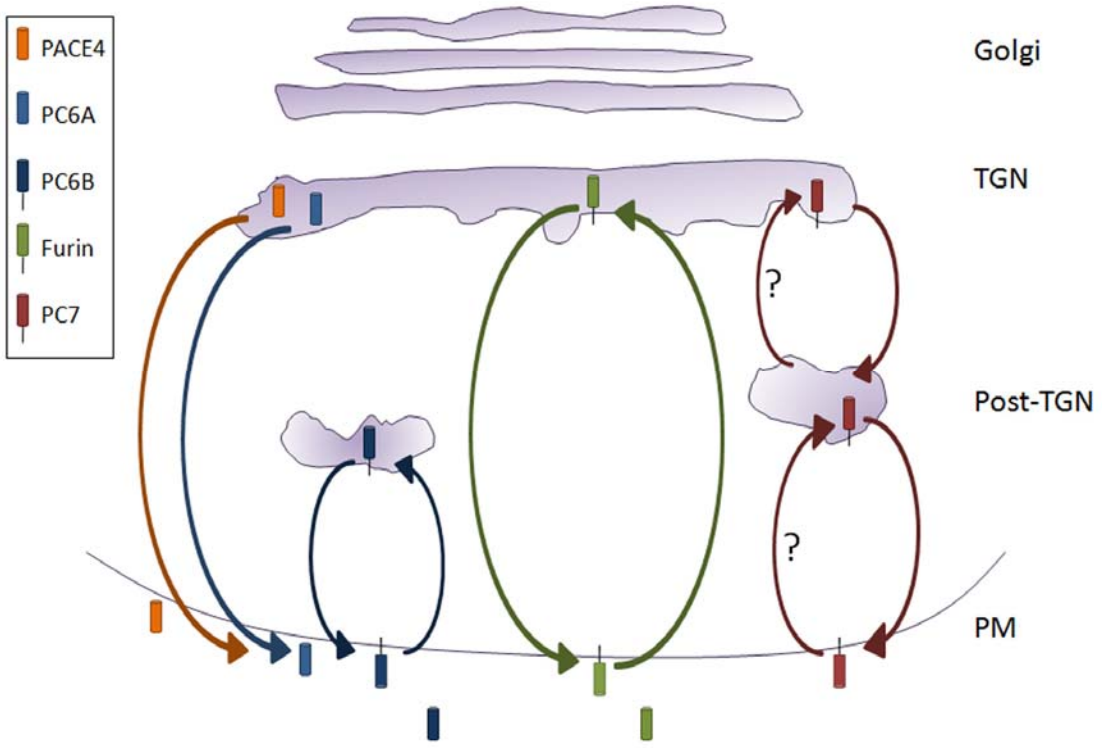

Figure 1-12. Simplified representation depicting trafficking and localization of candidate BMP4 PCs. PACE4 and PC6A are secreted and associate with the plasma membrane (PM) via HSPGs. PC6B cycles between a post-TGN compartment and the PM, and Furin cycles between the TGN and the PM; both can also be shed into the extracellular space. PC7 can be localized to the TGN, a post-TGN compartment, or the cell surface. It is unknown if this PC cycles or if the post-TGN compartment is the same as that in which PC6B is found. See text for details.

PC7 is a type 1 transmembrane protein similar to Furin and PC6B, though it is not cleaved to generate a shed form (Bruzzaniti et al., 1996; Constam et al., 1996). Like Furin, PC7 is predominantly localized to the TGN, although antibody uptake experiments show that it can traffic to the plasma membrane and be internalized, and subcellular fractionation suggests that a significant proportion of PC7 is found in post-TGN vesicles (Jean et al., 2000; van de Loo et al., 1997; Wouters et al., 1998) (Figure 1-12). The cytoplasmic tail of PC7 lacks conserved leucine/isoleucine- or tyrosine-based internalization motifs (Figure 1-13). Also, it is not phosphorylated and lacks the acidic cluster found in Furin's cytoplasmic tail that mediates TGN retrieval in a phosphorylation dependent fashion, suggesting that PC7 uses an alternate, PACS1-independent mechanism for TGN localization (van de Loo et al., 1997).

One possible mechanism controlling PC7 trafficking involves the palmitoylation motif that is found only in the cytoplasmic tail of this PC family member (Figure 1-13) (van de Loo et al., 1997; van de Loo et al., 2000). Palmitate is a fatty acid that can be linked to cysteine residues via a reversible thioester linkage, and it has been implicated in controlling localization and stability of various proteins (reviewed in Linder and Deschenes, 2007). Van de Loo et al identified the two N-terminal cysteines in the cytoplasmic tail of PC7 as sites of palmitoylation and showed that the moiety is added in a late compartment of the exocytic pathway, likely in the TGN. When palmitoylation was disrupted, PC7 still localized primarily to the TGN, but the protein had a reduced half life (van de Loo et al., 2000). More recently, McCormick et al showed that palmitoylation is essential for sorting and trafficking of the lysosomal receptors cationic-independent mannose 6-phosphate (CI-MPR) and sortilin (McCormick et al., 2008).

Without palmitoylation, these proteins cannot interact with the retromer complex that is responsible for their retrograde transport from late endosomes to the Golgi, and they are therefore degraded in the lysosome. It is possible that an analogous mechanism is involved in PC7 trafficking, which would explain the reduced half-life and the lack of gross mislocalization observed upon disruption of palmitoylaton.

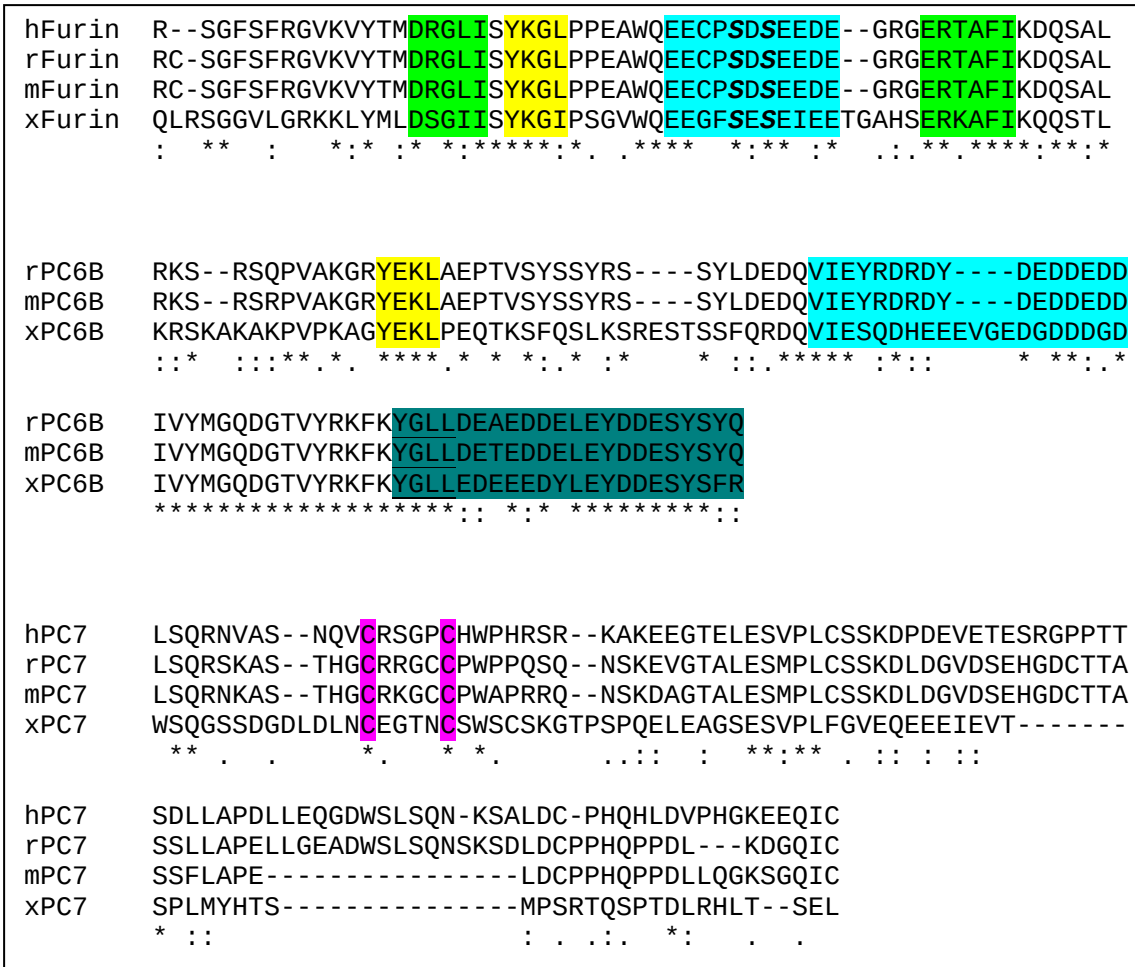

Figure 1-13. Sequence aligments of Furin, PC6B, and PC7 cytoplasmic tails indicating sorting motifs. Experimentally validated YXXL internalization motifs are highlighted in yellow. A potential YXXL motif within an acidic cluster (AC) of PC6B is underlined. Experimentally validated leucine/isoleucine internalization motifs are highlighted in green. PACS-1 interacting ACs are highlighted in blue (phosphorylated serines in Furin AC are italicised), and the PACS-1 independent AC2 of PC6B is highlighted in teal. The palmitoylated cysteines in the PC7 cytoplasmic tail are highlighted in pink. Sequences are from human, rat, mouse, and *Xenopus* genbank accession numbers: hFurin NP_002560, rFurin NP_062204, mFurin NP_035176, xFurin translated from NM_001088801, rPC6B XP_001078022, mPC6B XP_129214, xPC6B AAW83025, hPC7 translated from NM_004716, rPC7 translated from NM_019246, mPC7 translated from NM_008794, xPC7 NP_001090019.

II.B.3. Tissue localization

PC1 and PC2 are active within the regulated secretory pathway of neuroendocrine tissues, while PC4 is active within the constitutive secretory pathway specifically within reproductive tissues (Seidah et al., 1992; Seidah et al., 1990; Seidah et al., 1991). For this reason, and because their preferred cleavage site sequences do not include the -R-X-X-R- motif found at the S2 site of BMP4, these three PCs are not likely candidates for BMP4 processing enzymes and will not be discussed further.

Furin is a strong candidate for an endogenous BMP4 convertase; its transcripts are broadly expressed throughout development. In mice, the earliest expression is detected during implantation (E4.5) in the primitive endoderm (Mesnard et al., 2006). By E5.5, expression is restricted to extraembryonic visceral endoderm and ectoderm. At E7.5, *Furin* is primarily seen in extraembryonic tissues – including extraembryonic ectoderm, anterior visceral endoderm, and allantois – and in the proximal region of the embryo (Roebroek et al., 1998). Transcripts are also detected in the precardiac mesoderm, the anterior intestinal portal (AIP), the ventral notochordal plate, and the node (Roebroek et al., 1998). At E8.5, strong expression persists in the allantois, the visceral yolk sac, the primitive heart, and the AIP (from where ventral closure proceeds caudally; Roebroek et al., 1998). Posteriorly, *Furin* is detected in the hindgut and the caudal intestinal portal (CIP). Expression patterns in *Xenopus* will be described in Chapter 2.

Like *Furin*, *Pace4* is broadly expressed and is first detected in mice at E4.5, but *Pace4* is expressed specifically in the trophectoderm lineage (Mesnard et al., 2006). At E6.5, transcripts are detected in extraembryonic ectoderm, at E8.0 in the chorion, and by E8.5 in the definitive endoderm of the foregut and in the splanchnic mesoderm (Constam

and Robertson, 2000a). *Pace4* is broadly expressed in *Xenopus* as well (Birsoy et al., 2005). mRNA is present in the oocyte – localized to the vegetal hemisphere – and persists in endoderm precursors during gastrulation. At tadpole stages, transcripts are specifically detectable in the olfactory bulb, the brain, and the notochord.

Pc6 expression in mice begins later than that of *Furin* and *PACE4*, with transcripts first detected at E6.5 in the trophoblast (Essalmani et al., 2006; Rancourt and Rancourt, 1997). At E8.5, transcripts are detected in the most posterior somites, a staining pattern that moves caudally with the developing embryo. At E9.5, *Pc6* is also seen in the lung bud; and by E10.5 and beyond, transcripts are detectable in multiple tissues, including the first branchial arch, pancreatic primordium, nasal pits, intestine, adrenal primordium, heart, and in developing vertebral, limb, and craniofacial skeleton. In addition, the two main isoforms of *Pc6* – *Pc6A* and *Pc6B* – have been shown to be differentially expressed in adult mice (Essalmani et al., 2006). *Pc6A* is the predominant isoform in most tissues and is broadly, if not ubiquitously, expressed with highest levels in the adrenal gland. *Pc6B* is less abundant overall and is primarily detected in kidney, liver, and intestines. Additional splice isoforms were found in *Xenopus*, and their expression will be described in Chapter 2.

In some tissues, expression of *Pace4* and *Pc6* appears complementary. For example, *Pace4* is found in the intestinal villus mesenchyme while *Pc6* is in the villus epithelium (Constam et al., 1996). Some regions of *Pace4* and *Pc6* expression overlap with those of *Bmp2*, *4*, and *7*, consistent with the possibility that they activate these TGFβ family growth factors.

Pc7 appears to be ubiquitously expressed throughout development. In mice, it is present in embryonic stem cells as well as in post-implantation stage embryos and whole animals from E7.5-E16.5 (Constam et al., 1996). In addition, *Pc7* was found to be broadly expressed in multiple adult tissues from human, mouse, and rat, including heart, testis, and intestine (Bruzzaniti et al., 1996; Meerabux et al., 1996; Seidah et al., 1996). *Pc7* expression in *Xenopus* will be described in Chapter 3.

II.B.4 . Potential targets

Hundreds of targets for PC cleavage have been proposed from *in silico, in vitro,* and *ex vivo* studies. Experiments *in vitro* and using cotransfection in cell culture have demonstrated numerous potential endogenous as well as pathogenic targets, but definition of bona fide enzyme-substrate pairs is still not straightforward since the physiological relevance of these overexpression results is questionable (Seidah and Chretien, 1999). PC loss of function experiments have also been performed to attempt to identify important endogenous targets during development (reviewed in Scamuffa et al., 2006). Though phenotypic analyses of PC knockout mice are complicated by the loss of activation of multiple targets and partial compensation by other PCs, these *in vivo* studies have provided valuable insight into potential substrates for each PC.

The *Furin* knockout mouse, for example, displays a subset of defects that are also observed in Bmp4 mutants, such as failed chorioallantoic fusion, as well as additional unique phenotypes (Goldman et al., 2006; Roebroek et al., 1998; Winnier et al., 1995). *Furin* null mice die at approximately E10.5 due to severe ventral body wall closure defects, failure of the heart tube to fuse or loop, and failure to complete axial rotation. *Bmp4* null mice die earlier, about E7.5, and lack posterior mesoderm.

The *Furin* homologues in *Drosophila – Dfur1* and *Dfur2* – have also been knocked down (Kunnapuu et al., 2009). RNAi directed toward each transcript individually and together in S2 cells resulted in reduced DPP processing at both sites, suggesting that both enzymes are important for DPP activation and both are capable of cleaving minimal and optimal consensus motifs.

The *Pace4* loss of function phenotype is less severe than that of Furin (Constam and Robertson, 2000a). Approximately 25% of homozygous null animals die before birth, likely due to severe heart malformations. A subset of those that survive display mild situs abnormalities (lungs, visceral organs, heart, and during embryonic turning) and/or craniofacial malformations, including cyclopia. These phenotypes were proposed to be due, at least in part, to loss of Nodal function since mice heterozygous for one null allele and one hypomorphic allele of *Nodal* are able to complete gastrulation but display defects in left-right asymmetry and anterior patterning similar to those observed in *Pace4* null embryos (Lowe et al., 2001). Furthermore, removal of one allele of *Nodal* in *Pace4* mutants enhances the penetrance and severity of phenotypic defects, consistent with a role for PACE4 in proteolytic activation of this precursor protein (Constam and Robertson, 2000a). The Nodal knockout mouse, however, shows more severe defects than do *Pace4* mutants, arresting during gastrulation without forming mesoderm (Conlon et al., 1991; Conlon et al., 1994). Thus, it is probable that a second PC functions redundantly with PACE4 to cleave Nodal.

Pace4 has also been knocked-down in *Xenopus*, and the resulting phenotypes include delayed gastrulation, loss of mesoderm and anterior patterning defects (Birsoy et al., 2005), all of which are also seen when *Xenopus* Nodal function is impaired (Osada

and Wright, 1999). In addition, cleavage of several TGFβ family members is disrupted in PACE4 depleted embryos. Specifically, mRNA encoding potential cleavage substrates was injected into embryos in which maternal *Pace4* had been knocked down using antisense oligonucleotides. Cleavage of the substrates was then evaluated by Western blot, and the results showed that *Xenopus* Nodal related 1 (Xnr1), Xnr2, Xnr3, and Vg1 are cleaved less efficiently in the absence of PACE4 while Xnr5, ActivinB, and Derriere are cleaved normally.

A role for both Furin and PACE4 in cleaving Nodal is strongly supported by analysis of mice mutant for both enzymes. *Pace4* and *Furin* double mutants phenocopy *Nodal* mutants in that they lack mesoderm and fail to express Nodal target genes (Beck et al., 2002; Conlon et al., 1991; Conlon et al., 1994). Furthermore, whereas PCs secreted from wild type ES cells can cleave recombinant Nodal precursor protein, those secreted from *Furin* and *Pace4* mutant ES cells cannot.

Several mutant alleles of *Pc6* have been generated, including ubiquitous deletion of exon 4, which encodes a portion of the catalytic domain, or of the proximal promoter and exon 1, embryo-specific deletion of the same region, and a point mutation within the P-domain that results in ER retention (Essalmani et al., 2006; Essalmani et al., 2008; Szumska et al., 2008). Whereas mice homozygous for the exon 4 deletion were reported to die between E4 and E7.5, subsequent analysis of null alleles revealed that mutants survive at least until E18.5 but die pre- or postnatally. Detailed analysis of embryos revealed a pleiotropic phenotype, including axial skeletal, limb, and cardiac malformations, renal and palatal agenesis, pulmonary hypoplasia, and ventral body wall closure defects. A subset of these phenotypes are also observed in mice lacking GDF11,

another member of the TGFβ family (Esquela and Lee, 2003; McPherron et al., 1999). They possess additional thoracic and lumbar vertebrae, as well as additional ribs attached to the sternum, but they have few to no sacral and caudal vertebrae. Also, the palate and kidneys fail to form. These phenotypic observations, as well as expression studies showing that *Gdf11* and *Pc6* are often expressed in the same or adjacent tissues and cleavage experiments demonstrating that PC6 is capable of cleaving GDF11 *in vitro* and in cells, suggest that at least a subset of the defects resulting from PC6 loss of function are due to lack of GDF11 cleavage and activation (Constam et al., 1996; Essalmani et al., 2006; Essalmani et al., 2008; McPherron et al., 1999; Nakashima et al., 1999; Szumska et al., 2008). Other phenotypes, though, are not explained by loss of GDF11. Specifically, abdominal hernias and incomplete fusion of the sternum were observed, indicative of a defect in ventral body wall closure. Also, several cardiac abnormalities were seen, including atrioventricular septal defects and common arterial trunk (Szumska et al., 2008). These phenotypes are also observed in mice deficient for *Bmp4* (Goldman et al., 2009; Goldman et al., 2006; Jiao et al., 2003; Liu et al., 2004). In addition, like *Gdf11*, *Bmp4* is often expressed in the same or adjacent tissues as *Pc6*, and PC6 is able to cleave BMP4 *in vitro* (Constam et al., 1996; Cui et al., 1998; Essalmani et al., 2006; Johansson and Wiles, 1995; Jones et al., 1991; Winnier et al., 1995). Together, these data suggest that the cardiac and ventral body wall defects resulting from PC6 loss of function could be due to lack of BMP4 cleavage and activation, and that PC6 is therefore necessary to cleave BMP4 in these tissues.

Furin and PC6 have not been specifically knocked down in *Xenopus*, but overexpression of the Furin and PC6 selective inhibitor, α_1-PDX, in the ventral marginal

zone of 4-cell embryos results in conversion of cells fated to form ventral derivatives such as blood and mesenchyme to more dorsal fates, i.e. muscle (Cui et al., 1998). Also, α_1-PDX expression induces neural markers in ectodermal explants. These phenotypes are identical to those seen when BMP4 signaling is blocked, and they can be reversed by co-expression of BMP4 downstream signaling molecules.

Mice lacking *Pc7* are reported to develop normally, suggesting that this enzyme does not function as the sole convertase to cleave essential precursors (Taylor et al., 2003). PC7 loss of function analyses have not been performed in *Xenopus*.

III. Thesis Overview

The work presented herein aims to test the hypothesis that a site-specific PC cleaves BMP4 as a mechanism to regulate its signaling range and activity, which is thought to differ depending on the tissue in which it is expressed. We have proposed three potential models for how tissue-specific cleavage of the S2 site could be achieved, which are summarized below and illustrated in Figure 1-14. The first two models rely critically on the observation that the S1 site of BMP4 is cleaved in a neutral environment, while the S2 site is cleaved under more acidic conditions, thereby suggesting that the S1 site of BMP4 is cleaved in the TGN whereas cleavage at the S2 site can only occur in a more acidic, post-TGN compartment (Degnin et al., 2004). Secreted proteins can traffic to the cell surface from the TGN either directly or via endocytic intermediaries (reviewed in Rodriguez-Boulan et al., 2005), and the first model proposes that S2 cleavage is regulated by subcellular trafficking machinery. Specifically, in a subset of cells, BMP4 is proposed to traffic from the TGN to the cell surface via endocytic vesicles, such that both

sites are cleaved, while in other cells, BMP4 is proposed to traffic via a pathway that bypasses the acidic compartment, such that only the S1 site is cleaved (Figure 1-14A). Notably, in this model, tissue specific cleavage of the S2 site is not determined by the identity of the enzymes that cleave the S1 and/or S2 sites and thus my studies do not test this model.

The second model proposes that selective cleavage of the S2 site is mediated by tissue-specific expression of a convertase that resides in the more acidic post-TGN compartment in which the S2, but not the S1, site is cleaved (Figure 1-14B). Specifically, since Furin is broadly expressed and localizes primarily to the TGN while PC6B is concentrated in a post-TGN compartment, it is possible that Furin and PC6B cleave the S1 and S2 sites of BMP4, respectively (Thomas, 2002 and references therein; Xiang et al., 2000). Thus, BMP4 would be cleaved at both sites in all tissues except those that lack PC6B.

The third model proposes that an S1-site specific protease exists, and that BMP4 will be cleaved at the S1 site alone in any tissue where this protease is the sole active PC. Notably, whereas Furin, PACE4 and PC6 can all cleave both the optimal motif (-R-X-R/K-R-) at the S1 site and the minimal motif (-R-X-X-R-) at the S2 site of BMP4 *in vitro*, PC7, which requires a basic residue at the P_2 position, can cleave only the optimal motif (-R-X-R/K-R-) at the S1 site (Cui et al., 1998; van de Loo et al., 1997). Thus, in this model BMP4 would be constitutively cleaved at the S1 site by PC7, and would be cleaved at both the S1 and S2 sites in tissues that also express an enzyme capable of cleaving the minimal sequence (Figure 1-14C).

We began exploring the question of tissue-specific S2 cleavage by first cloning and characterizing PCs in *Xenopus*, then identifying those PCs that cleave BMP4 *in vivo* and determining which, if any, act as an S2-specific enzyme. The results of these studies are described in the following two chapters.

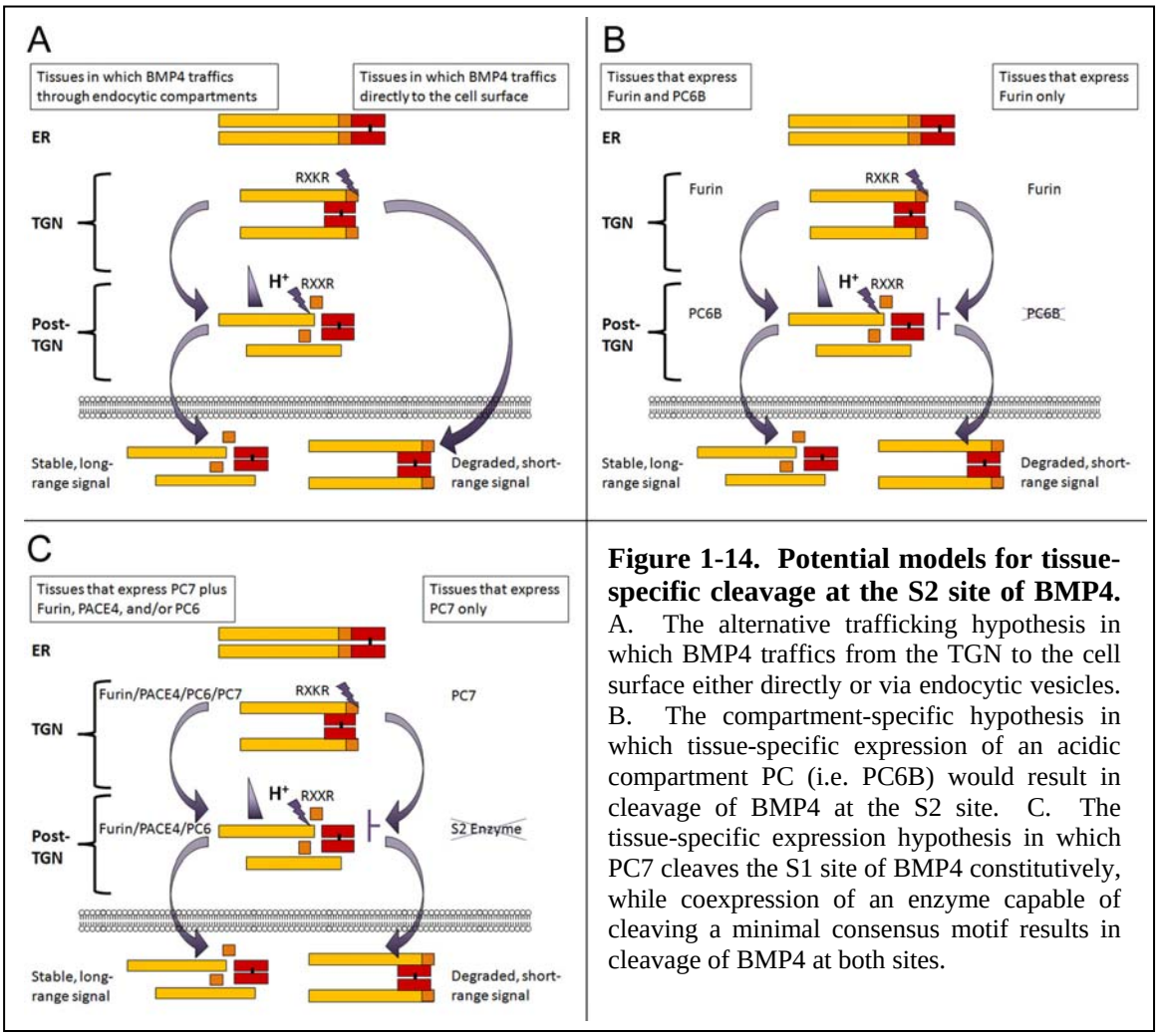

Figure 1-14. Potential models for tissue-specific cleavage at the S2 site of BMP4. A. The alternative trafficking hypothesis in which BMP4 traffics from the TGN to the cell surface either directly or via endocytic vesicles. B. The compartment-specific hypothesis in which tissue-specific expression of an acidic compartment PC (i.e. PC6B) would result in cleavage of BMP4 at the S2 site. C. The tissue-specific expression hypothesis in which PC7 cleaves the S1 site of BMP4 constitutively, while coexpression of an enzyme capable of cleaving a minimal consensus motif results in cleavage of BMP4 at both sites.

Chapter 2

Proprotein Convertase Genes in *Xenopus* Development

Sylvia Nelsen[1,§], Linnea Berg[2,§], Crispin Wong[2,§], and Jan L. Christian[2]

Departments of Molecular & Medical Genetics[1] and Cell & Developmental Biology[2], Oregon Health & Science University, Portland, Oregon, USA

[§]These authors contributed equally

Published in Developmental Dynamics 2005 Jul;233(3):1038-44

Received 17 December 2004; Revised 31 January 2005; Accepted 1 February 2005

PREFACE

This work was published in the July 2005 issue of Developmental Dynamics by Sylvia Nelsen, Linnea Berg, Crispin Wong, and Jan L. Christian.

My contributions to the manuscript include cloning *Xenopus Pc6* isoforms, analyzing the sequence variations, and describing their spatiotemporal patterns of expression (Figures 2-2 to 2-4).

Linnea Berg contributed to this work by cloning and analyzing expression of *Pc4* (Figure 2-5).

Crispin Wong contributed to this study by analyzing the spaciotemporal patterns of *Furin* expression (Figure 2-1).

Jan L. Christian contributed to this study by cloning *Xenopus Furin* and performing sequence alignments (including Table 2-1), and by writing the manuscript. She also provided advice and suggestions on experimental design and data analysis, as well as the space, equipment, and supplies with which to perform the experiments.

SUMMARY

Proprotein convertases (PCs) are a family of serine endoproteases that proteolytically activate many precursor proteins within various secretory pathway compartments. Loss of function studies have demonstrated a critical role for these proteases in embryonic patterning and adult homeostasis, yet little is known about how substrate selectivity is achieved. We have identified *Xenopus* orthologs of three PCs: *Furin, Pc6* and *Pc4*. In addition to previously described isoforms of *Pc6* and *Furin*, four novel splice isoforms of *Pc6*, that are predicted to encode constitutively secreted proteases, and a putative transmembrane isoform of PC4 were identified. *Furin* and *Pc6* are expressed in dynamic, tissue-specific patterns throughout embryogenesis while *Pc4* transcripts are restricted primarily to germ cells and brain in adult frogs.

INTRODUCTION

Proprotein convertases (PCs), also known as subtilisin-like proprotein convertases (SPCs), are a family of calcium-dependent serine proteases with catalytic domains that are similar to that of bacterial subtilisin. They are responsible for proteolytic activation of a wide variety of precursor proteins, including hormone and neuropeptide precursors, growth factors, receptors, adhesion molecules, proteases, bacterial toxins, and viral surface glycoproteins (Taylor et al., 2003; Thomas, 2002).

PCs have been highly conserved throughout evolution, with seven known family members in mammals including Furin (also known as SPC1), PC2 (also known as SPC2), PC1 (also known as PC3 or SPC3), PACE4 (also known as SPC4), PC4 (also known as SPC5), PC6 (also known as PC5 or SPC6), and PC7 (also known as LPC, PC8 or SPC7).

PCs share a common domain structure consisting of a prodomain followed by a catalytic domain, a P domain and one or more carboxy (C)-terminal domains (Taylor et al., 2003; Thomas, 2002). The prodomain is required for proper folding and maintains the precursor in an inactive state until it is autocatalytically removed once the zymogen has reached the proper subcellular compartment (Anderson et al., 2002). The catalytic domain contains a canonical D, H, S catalytic triad at the active site and a negatively charged substrate binding pocket which contributes to substrate selectivity. Cleavage of substrates occurs following a dibasic (-R/K-R-) or multibasic (-R-X-X-R-; where X is any amino acid) motif. The P domain appears to structurally stabilize the catalytic domain and contribute to substrate specificity (Lipkind et al., 1998; Zhou et al., 1998). The C-terminal domains are the most divergent among PCs and are dispensible for catalytic activity. Furin, PACE4, and PC6 all contain a cysteine-rich (Cys-rich) domain consisting of a variable number of repeated motifs, each ~50 amino acids in length and containing a well conserved Cys topography (Roebroek et al., 1992). The function of this domain is unknown. Furin, PC6B (a splice isoform of PC6) and PC7 contain a transmembrane domain and a cytoplasmic tail that directs trafficking between different subcellular compartments. The remaining PC family members are secreted, either via the constitutive (PACE4) or the regulated (PC1, PC2, PC4 and PC6A) pathway.

Three members of the PC family are expressed exclusively in neuroendocrine tissues (*Pc1* and *Pc2*) or are restricted to reproductive organs (*Pc4*). The remaining PCs are broadly expressed in mammalian embryos and adults (Taylor et al., 2003). *Furin*, *Pace4* and *Pc6* are co-expressed in many tissues and all recognize an identical consensus motif in vitro (-R-X-X-R-), yet loss of function studies suggest that individual family

members selectively cleave only a subset of substrates that contain this motif in vivo (Beck et al., 2002; Birsoy et al., 2005). It is likely that colocalization of a PC and its substrate at the tissue and/or subcellular level contributes to substrate selectivity.

Analyses of mice mutant for *Furin* and/or *Pace4* have been invaluable in defining developmental roles of these enzymes (Beck et al., 2002; Constam and Robertson, 2000a; Constam and Robertson, 2000b; Roebroek et al., 1998; Taylor et al., 2003). These studies have provided only limited information on substrate specificity, however, due to the complexity of phenotypes, early lethality and difficulty detecting endogenous candidate substrates at the protein level. We have chosen to explore expression patterns of PCs in *Xenopus laevis* because of the power of this organism as a model system. The large size of *Xenopus* eggs and embryos, coupled with rapid, external development enable a multitude of studies that complement and extend those that are possible in mice. The temporal and spatial pattern of expression of *Xenopus Pace4* has recently been published (Birsoy et al., 2005). In the current studies, we report structural characteristics and developmental patterns of expression of *Xenopus* orthologs of *Furin*, *Pc6* and *PC4*.

RESULTS AND DISCUSSION

Xenopus Furin is dynamically expressed throughout development

A cDNA encoding *Xenopus* Furin (xFurin) was identified in the NCBI expressed sequence tag (EST) database (EST BG233070) and the coding region was sequenced. A partial length version of this same cDNA (designated *xFurinB*) as well as a closely related cDNA (*xFurinA*) have previously been reported (Korner et al., 1991). These two cDNAs most likely represent duplicate copies of a single gene as they encode proteins

that are >95% identitical at the amino acid level. *Xenopus* and mouse Furin (mFurin) share 70% amino acid identity overall with the greatest degree of conservation in the catalytic domain (Fig. 2-1A). Both proteins contain a predicted transmembrane domain and a poorly conserved, short cytoplasmic tail. Despite the low overall amino acid identity within this domain, the sequence motifs that direct intracellular trafficking of Furin are conserved across species. These motifs include di-leucine like and tyrosine based internalization signals (Fig. 2-1B, green) and an acidic cluster motif (yellow) containing two phosphorylatable serines (black dots) that direct trafficking between the *trans*-Golgi network (TGN) and cell surface (Molloy et al., 1999).

TABLE 2-1. Amino Acid Identity Between *Xenopus* and Mouse PC Family Members

mFurin								
xFurin	70							
mPC4	55	52						
xPC4	50	49	58					
mPACE4A	44	45	46	43				
xPACE4A	44	44	44	41	70			
mPC6A	44	45	46	42	56	57		
xPC6A	44	45	46	43	57	57	75	
mPC7	33	33	34	30	34	33	34	34
	mFurin	xFurin	mPC4	xPC4	mPACE4A	xPACE4A	mPC6A	xPC6A

Northern blot analysis was used to examine the temporal profile of expression of *Furin* in developing *Xenopus* embryos. Consistent with previous reports (Korner et al., 1991), *Furin* is maternally expressed, with transcripts of ~6 kb and 3 kb being detected in oocytes (Fig. 2-1C). The larger transcript persists at fairly uniform levels throughout embryogenesis while the smaller transcript becomes barely detectable during neurula stages (st. 15-23) but then reappears by the tadpole stage (st. 41). Based on the size of existing cDNAs, the 6 kb transcript encodes the membrane bound Furin isoform that we report here. The size of the smaller transcript is sufficient to encode an identical protein with a shorter 3′ untranslated region, although it could also represent a splice isoform that

encodes a structurally different protein. Distinct isoforms of Furin have not been reported in mammals with the exception of C-terminally truncated proteins that arise as the result of defective splicing in mutant cell lines (Spence et al., 1995).

Spatial patterns of expression of *Furin* were examined by hybridizing digoxygenin-labeled antisense riboprobes to developmentally staged *Xenopus* embryos. *xFurin* transcripts are ubiquitously expressed throughout gastrulation (data not shown and (Cui et al., 1998) but become restricted primarily to non-neural ectoderm and somitic mesoderm by stage 15 (Figure 2-1D). *xFurin* is also expressed at lower levels in lateral plate and ventral mesoderm and throughout the endoderm at stage 15 but is excluded from the most dorsal mesodermal (prospective notochord) and ectodermal (neural) tissues (Fig. 1D, lower right panel). In tailbud stage embryos (Fig. 2-1E-F), *xFurin* transcripts are localized to dorsal regions of the eye, the otic vesicle, pharyngeal arches, pronephric duct and mesenchymal cells of the dorsal fin. This pattern of expression is apparent by stage 26 and persists throughout the tailbud and into the early tadpole (st. 36) stages.

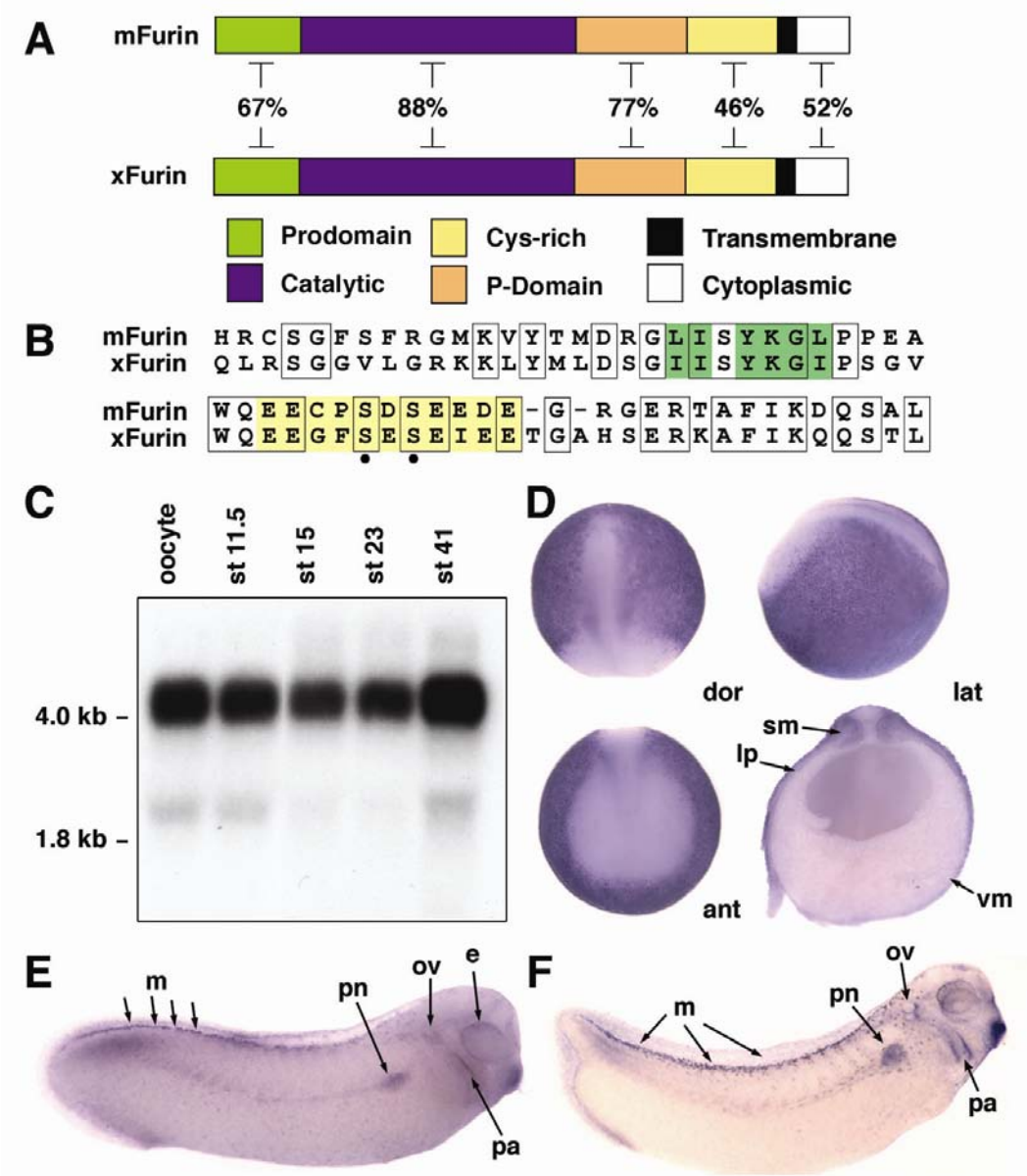

Figure 2-1. Analysis of temporal and spatial patterns of expression of *xFurin* in developing *Xenopus* embryos. A: Schematic illustration of domain structure and amino acid identity shared by *Xenopus* and mouse Furin. **B:** Sequence alignment of the cytoplasmic tail domain of *Xenopus* and mouse Furin showing conservation of internalization signals (green shading), acidic clusters (yellow shading) and phosphorylated serines (black dots) that direct subcellular trafficking. **C-F:** Analysis of *xFurin* expression by Northern blot analysis (C) or whole mount in situ hybridization (D-F). (D) Dorsal (dor), lateral (lat), anterior (ant) and midsagittal (lower right) views of neurula stage (st. 18) embryos are shown. sm; somatic mesoderm, lp; lateral plate mesoderm, vm; ventral mesoderm. (E-F) Lateral views of tailbud stage (st. 28-32) embryos. The embryo shown in F has been cleared. pn, pronephric duct; ov, otic vesicle; m, fin mesenchyme; pa, pharyngeal arches; e, eye.

Xenopus embryos express multiple isoforms of *Pc6*

The primary *Pc6* transcript undergoes tissue-specific alternative splicing to generate multiple PC6 isoforms (Nakagawa et al., 1993b; Nie et al., 2003), two of which have been characterized. *Pc6A* encodes a soluble protein that enters the regulated secretory pathway (De Bie et al., 1995) whereas *Pc6B* encodes a C-terminally extended and membrane bound protein which traffics between the cell surface and a post-TGN compartment (Xiang et al., 2000). An ~6 kb cDNA encoding the *Xenopus* ortholog of *Pc6A* was identified in the NCBI EST database (EST BG022872) and the coding region was sequenced. *Xenopus* PC6A (xPC6A) and mouse PC6A (mPC6A) share greater than 80% amino acid identity across all domains with the exception of the Cys-rich region (Fig. 2-2A). Although this domain is less well conserved overall, the number and relative position of all cysteine residues is identical between the two proteins. The C-terminal PC6A-specific residues, which are required for sorting into the regulated secretory pathway (De Bie et al., 1995), are highly conserved between mouse and *Xenopus*.

Primers complementary to sequence encoding a portion of the Cys-rich region of PC6A which is shared between the A and B isoforms were used to amplify an *xPc6B* cDNA by 3′ Rapid Amplification of cDNA Ends (RACE) (Fig. 2-2B). xPC6B has an extended Cys-rich domain that shares less than 50% identity with that of mPC6B, yet the number and relative position of each cysteine residue within this domain is absolutely conserved. xPC6B also contains a predicted transmembrane spanning region and a short cytoplasmic tail. Within the cytoplasmic domain, the tyrosine based internalization motif (Fig. 2-2C, green shading) and the two acidic clusters (yellow shading) that direct

subcellular localization to Golgi and post-Golgi compartments (Xiang et al., 2000) are conserved between mouse and *Xenopus* PC6B.

Four additional RACE products were identified that encode C-terminally truncated isoforms of PC6B, designated PC6C-F (Fig. 2-2B). Each of these clones terminates with a stop codon and includes unique 3′ untranslated sequence. Furthermore, each clone was amplified in a minimum of two independent RACE reactions using different cDNA pools suggesting that they are bona fide transcripts. The cDNAs encode proteins that differ from each other primarily in the number of Cys-rich repeats that they contain, although PC6C, E, and F also contain a short stretch of unique sequence at the C-terminus. The transmembrane domain is absent in PC6C-F, suggesting that these isoforms are constitutively secreted.

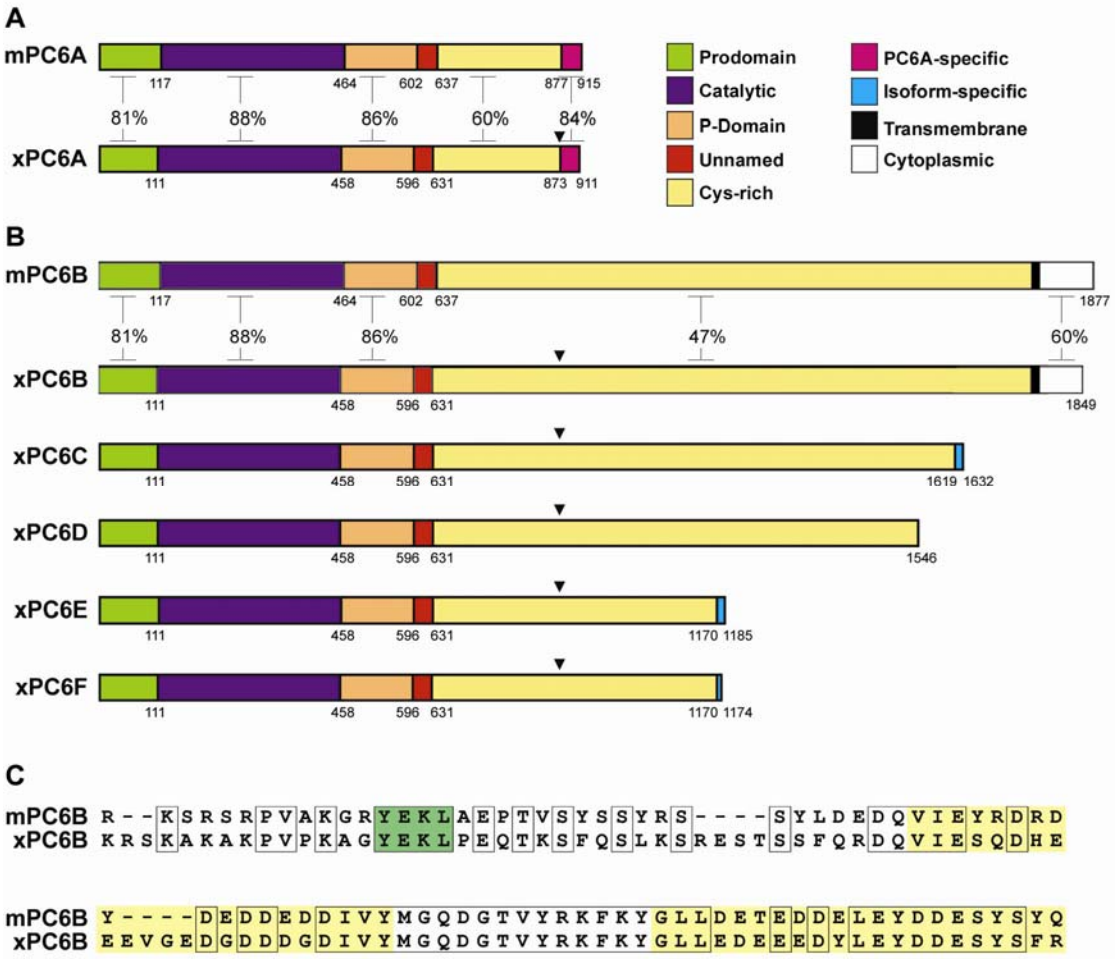

Figure 2-2. Comparison of *Xenopus* and mouse PC6 isoforms. A,B: Schematic illustration of domain structure and amino acid identity shared by *Xenopus* and mouse PC6A**,** PC6B and four novel PC6 isoforms (xPC6C-F) that were identified in the current studies. Arrowheads indicate the point of divergence between xPC6A and other isoforms. **C:** Sequence alignment of the cytoplasmic tail domain of *Xenopus* and mouse PC6B showing conservation of internalization signals (green shading) and acidic clusters (yellow shading) that direct subcellular trafficking.

Pc6 is widely expressed throughout development

The temporal pattern of expression of *Pc6* was analyzed in *Xenopus* embryos by Northern blot and ribonuclease protection assays. In initial studies, duplicate blots of developmentally staged RNA were hybridized with a full length *Pc6A* riboprobe (Fig. 2-3A), which recognizes transcripts encoding all of the PC6 isoforms that we have identified, or with a probe corresponding to the 3′ end of *Pc6F* (Fig. 2-3B), which cross

reacts with transcripts encoding PC6B-F, but not PC6A. Consistent with what has been observed in mouse (Nakagawa et al., 1993b; Nie et al., 2003), the pan-PC6 probe recognized multiple transcripts ranging in size from approximately 3.5 kb to 10 kb (Fig. 2-3A). By contrast, the probe specific for *Pc6B-F* detected only the 8 and 10 kb transcripts (Fig. 2-3B). The 8 kb transcript is maternally expressed at low levels, is barely detectable during neurula through tailbud stages (st. 18-24), and is upregulated by the tadpole stage (st. 41), while the 10 kb transcript is zygotically expressed and is maintained at low levels throughout embryogenesis. Based on this analysis, and consistent with the size of existing cDNAs, the dominant 6 kb transcript encodes PC6A whereas the 8 and 10 kb transcripts encode one or more of the carboxy-terminally extended isoforms. The 3.5 kb transcript may encode a unique PC6 isoform that has not yet been characterized at the molecular level, or it may represent a form of PC6A with a shorter 3′ untranslated region, as is observed in mouse (Nakagawa et al., 1993b; Nie et al., 2003).

To further characterize the developmental pattern of expression of different PC6 isoforms, RPAs were conducted using probes that are specific for *xPc6A* or for *xPc6B, C* and *D* (illustrated in Fig. 2-3C), together with a probe that recognizes the *Xenopus fibroblast growth factor receptor* (*FGFR*) as a loading control. Consistent with the results of Northern blot analysis, *xPc6A* is expressed at fairly uniform levels in oocytes and throughout embryonic development (Fig. 2-3D). By contrast, *xPc6B, C* and/or *D* are barely detectable in oocytes and early embryos but are abundantly expressed by the tadpole stage (stage 41) (Fig. 2-3E).

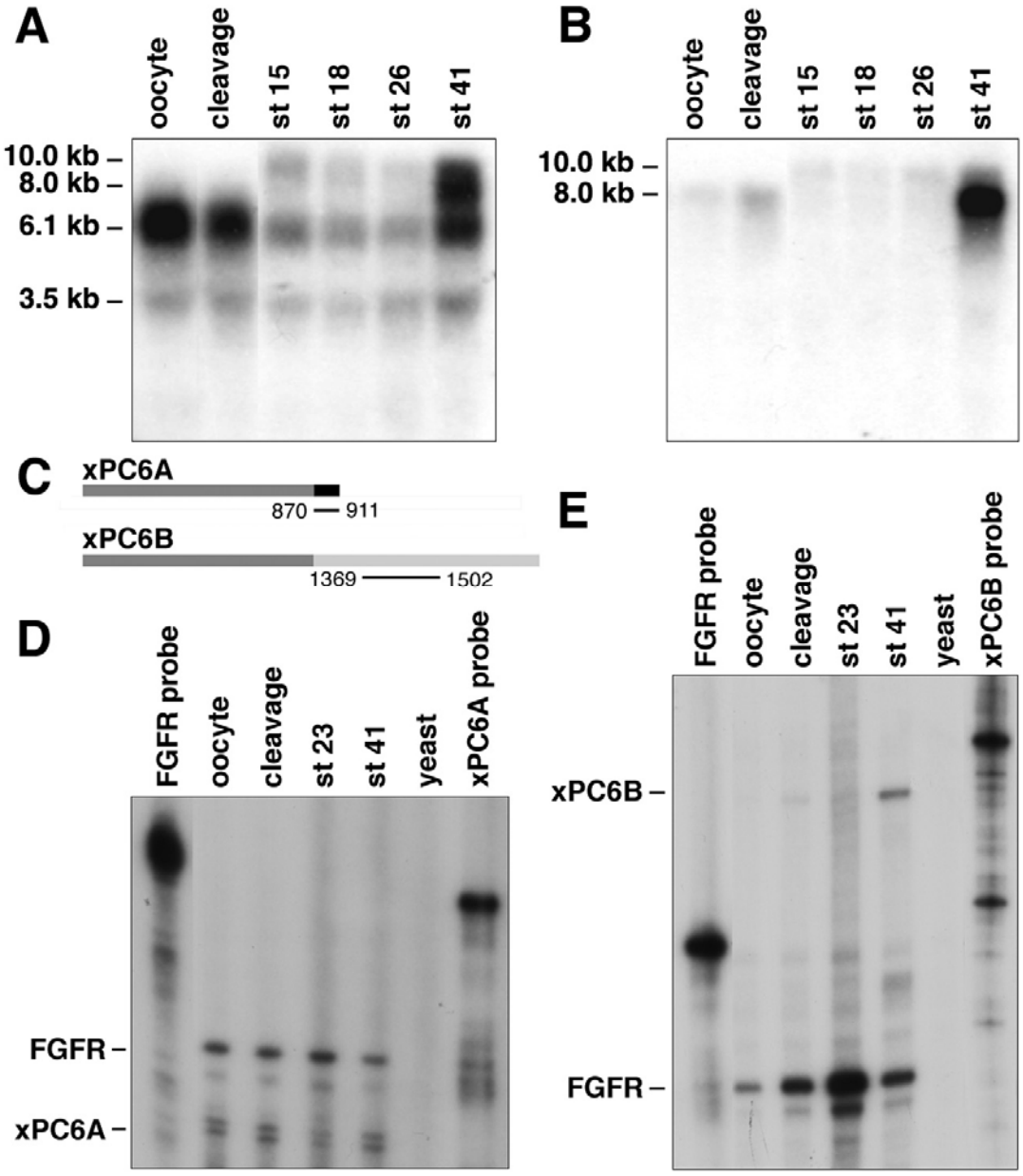

Figure 2-3. Distinct temporal patterns of expression of *PC6* isoforms during *Xenopus* embryogenesis. A,B: Northern blots of developmentally staged RNA hybridized with a probe that recognizes all *xPC6* isoforms (A) or with a probe specific for *xPC6B-F* (B). Approximate size of transcripts is indicated to the left of each blot. **C-E:** Ribonuclease protection analysis of expression of *xPC6A* (D) and *xPC6B-D* (E) using probes illustrated schematically in panel C. Numbers correspond to amino acids encoded by the DNA fragment that was transcribed to generate each probe, sequence that is unique to PC6A or PC6B is indicated by black or light gray shading, respectively. FGFR serves as a loading control.

The spatial localization of *xPc6* transcripts was examined by in situ hybridization using either a probe that recognizes all *xPc6* isoforms (Fig. 2-4A-F) or that detects only *xPc6B-D* (Fig. 2-4G, H). *xPc6* transcripts are ubiquitously distributed up until the end of gastrulation (data not shown) but become enriched in prospective neural tissue shortly thereafter (Fig. 2-4A, B and data not shown). By stage 18, *xPc6* transcripts are most abundant in the neural folds, neural crest and prospective eyes (Fig. 2-4A, B). During tailbud stages (st 26-32, Fig. 2-4C-E), *xPc6* is expressed in the eye, otic vesicle, pronephric duct, notochord and pharyngeal arches. Transcripts are also detected in specific regions of the brain (Fig. 2-4D-E, arrowheads), the nasal placode, lateral line and in scattered mesenchymal cells located on the surface of the embryo immediately posterior and ventral to the pharyngeal arches (Fig. 2-4C,E, open arrowheads). At the tadpole stage (Fig. 2-4F), *xPc6* is most abundantly expressed in the otic vesicle, lateral line, kidney (not shown) and gill slits. Transcripts encoding C-terminally extended isoforms of *xPc6* (*xPc6B-D*) were first detected at the tailbud stage and were restricted to the otic vesicle, the kidney and a subset of lateral line cells (Fig. 2-4G, H). This signal was considerably weaker than that detected with the pan-PC6 probe, suggesting that most of the staining shown in panels A-F represents expression of *xPc6A*. This is consistent with the results shown in Fig. 2-3 and with studies in mice showing that *mPc6A* is expressed at much higher levels than is *mPc6B* (Nakagawa et al., 1993b).

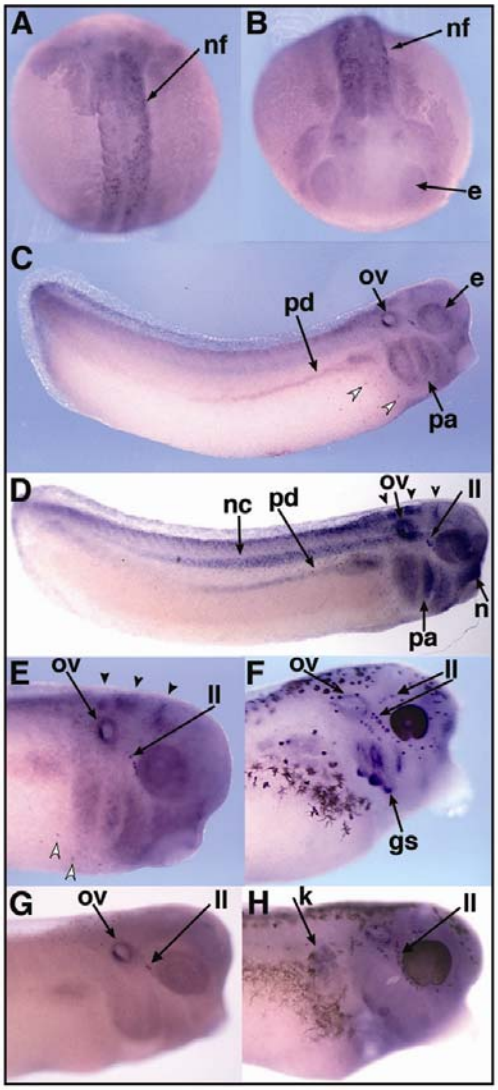

Figure 2-4. Spatial distribution of *PC6* transcripts during *Xenopus* embryogenesis.
A-H: In situ hybridization of probes specific for all *xPC6* isoforms (A-F) or for *xPC6B-D* (G, H) to whole *Xenopus* embryos. Dorsal (A) and dorsoanterior (B) views of neurula (st. 18) stage embryos or lateral views of tailbud (st. 28-30; C-E, G) and tadpole (st. 36; F and H) stage embryos are shown. The embryo shown in D was cleared to visualize internal structures. nf, neural fold; e, eye; pd, pronephric duct; ov, otic vesicle; pa, pharyngeal arches; nc, notochord; n, nasal placode; ll, lateral line; gs, gill slits; k, kidney. Arrowheads denote staining of specific stripes of cells in the brain, open arrowheads indicate staining of mesenchymal cells posterior to the pharyngeal arches.

***Xenopus PC4* encodes a membrane bound protein expressed primarily in germ cells.**

A cDNA encoding an apparent *Xenopus* ortholog of *PC4* (*xPC4*) was obtained using a combination of polymerase chain reaction (PCR) and library screening (see methods). The degree of homology between *Xenopus* and mouse PC4 (58% amino acid identity) is significantly lower than that observed for *Xenopus* and mammalian orthologs of other PCs (70-75% amino acid identity; Table 2-1). Furthermore, the domain structure of xPC4 differs from that of any murine PC4 (mPC4) isoforms described to date (Fig. 2-

5A). A human PC (hPC; accession no. AAQ89322) that shares a domain organization identical to that of xPC4 was recently identified in a screen for novel secreted or transmembrane proteins (Clark et al., 2003). This protein appears to be an isoform of PC4 based on overall sequence identity with mPC4 within the prodomain, catalytic domain, and P domain (Fig. 2-5A). In addition to these domains, xPC4 and hPC4 contain an extended Cys-rich domain, a putative transmembrane domain and a cytoplasmic tail. There is almost no sequence conservation within the putative cytoplasmic tails of xPC4 and hPC4, and both lack classical internalization or trafficking motifs (data not shown).

Semi-quantitiative RT-PCR was used to examine temporal and spatial patterns of expression of *xPc4* since we were unable to detect transcripts by Northern analysis or whole mount in situ hybridization. In the mouse, *Pc4* is expressed only in testicular germ cells and somatic cells of the ovary, but not in oocytes (Tadros et al., 2001; Torii et al., 1993). By contrast, *xPc4* transcripts are detected in RNA isolated from whole ovaries and, at ~4-fold lower levels, in enzymatically defolliculated oocytes (Fig. 2-5B) at all stages of oogenesis (data not shown). This suggests that *xPc4* is expressed in both somatic cells and germ cells within the ovary. Equivalent amounts of *xPc4* are detected in RNA isolated from dissected animal and vegetal halves of oocytes, showing that the transcripts are not localized (Fig. 2-5B). Although x*Pc4* transcripts are readily detected in oocytes, expression is much lower in unfertilized eggs and early embryos (Fig. 2-5C), suggesting that *xPc4* RNA is rapidly degraded upon oocyte maturation. Oocyte maturation has been shown to trigger degradation and/or regulate translation of other maternal RNAs (Wickens, 1990). *xPc4* transcripts persist at low levels until gastrulation (st. 11) at which time they become undetectable (Fig. 2-5B). In adult frogs, expression of

xPc4 is restricted primarily to ovaries and testes, although low levels of *xPc4* are detected in the brain (Fig. 2-5C).

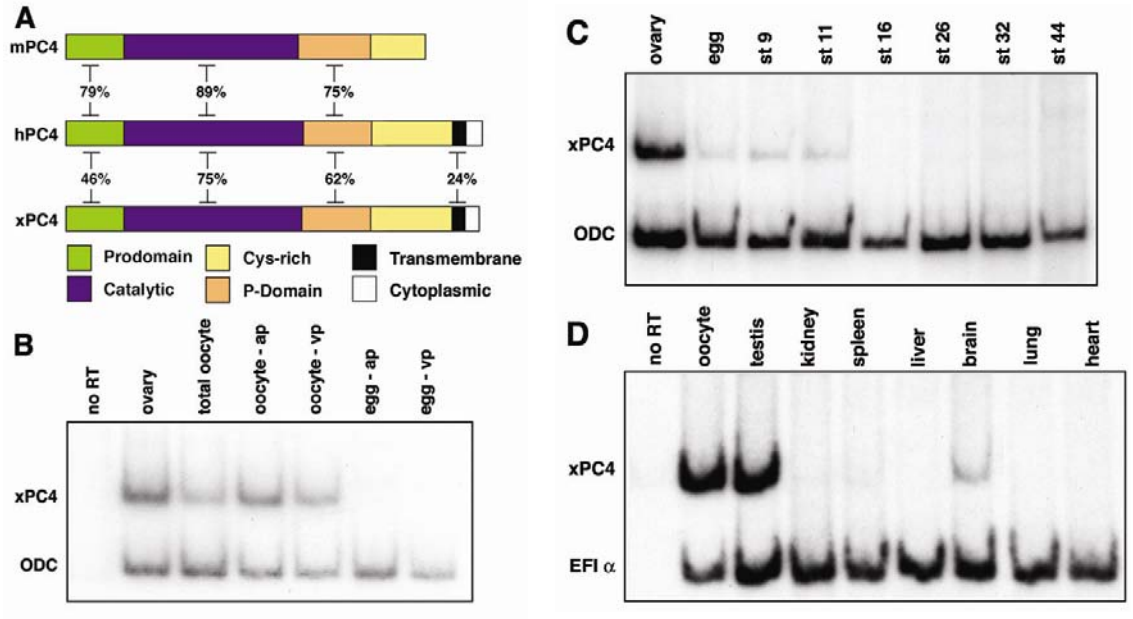

Figure 2-5. Domain structure and expression pattern of *Xenopus Pc4*. A: Schematic illustration of domain structure and amino acid identity shared by mouse, *Xenopus* and human PC4. **B-D:** Analysis of expression of *xPc4* in oocytes, embryos and adult tissues by RT-PCR. (B) RNA was isolated from oocytes that had been dissected into vegetal pole (vp) or animal pole (ap) halves. EF-1α and ornithine decarboxylase (ODC) serve as loading controls.

The results reported here show that overall structural characteristics and expression patterns of Furin, PC6 and PC4 are similar in mammals and *Xenopus*, with a few exceptions. *Furin* and *Pc6*, for example, show dynamic and overlapping, yet unique patterns of expression during embryogenesis in mice and rats (Constam et al., 1996; Roebroek et al., 1998; Zheng et al., 1994) as well as in frogs. By contrast, *Pc4* is expressed exclusively in male germ cells and somatic cells of the ovary in rodents (Tadros et al., 2001; Torii et al., 1993), but is expressed in the brain and in germ cells of both sexes in *Xenopus*.

Structurally, Furin, PC6A and PC6B show an identical domain organization across species whereas xPC4 differs from that reported in mice by the addition of an extended Cys-rich region, transmembrane domain, and cytosolic tail. The Cys-rich domain has been reported to be a unique feature of Furin, PACE4 and PC6 (Taylor et al., 2003), although mPC4 does contain a number of conserved cysteine residues near the C-terminus. The novel isoform of xPC4 described in this study contains an extended Cys-rich domain that is identical to that of Furin in terms of the number and topography of cysteine residues. Multiple splice variants of mouse and rat *Pc4* have been reported (Mbikay et al., 1994; Seidah et al., 1992), including one that encodes a protein with a hydrophobic stretch at the extreme C-terminus which might function as a transmembrane anchor. None of these, however, include the extended Cys-rich region or the cytoplasmic tail contained in xPC4 and hPC4. Finally, we report several new isoforms of PC6 that encode C-terminally truncated, and thus presumably secreted, versions of PC6B. Previous studies have shown the existence of multiple PC6 transcripts in mammals, only a subset of which cross-react with probes specific for the 3′ end of PC6A or PC6B (Nakagawa et al., 1993b; Nie et al., 2003). Our identification of cDNAs encoding novel PC6 isoforms may explain the molecular basis of the observed diversity. Further analysis of the unique PC6 transcripts identified on Northern blots of RNA isolated from mice will be required to determine whether the novel splice isoforms we have identified in *Xenopus* are conserved in mammalian species. The data reported in this study provide necessary background information for further analysis of developmental functions and identification of in vivo substrates for individual PC family members in *Xenopus*.

MATERIALS AND METHODS

Isolation of PC cDNAs

Gene searches were conducted through NCBI (http://ncbi.nlm.nih.gov). Furin and PC6A EST clones were obtained from Open BioSystems on behalf of the IMAGE consortium (Lennon et al., 1996) (http:///image.llnl.gov).

Oligonucleotide primers complementary to sequence encoding C-terminal portions of the Cys-rich domain of xPC6A were designed and 3′ RACE was performed as described (Frohman, 1993) to obtain cDNAs encoding *xPc6B-F*. RACE products were subcloned into pGEM-T EZ. Multiple cDNAs specific for each isoform were obtained and sequenced.

Degenerate oligonucleotides were designed based on sequence motifs conserved among multiple members of the PC family (Birsoy et al., 2005) and a partial length *xPc4* clone was amplified from oocyte cDNA. This clone was used to screen a *Xenopus* oocyte library and a nearly full length *xPc4* cDNA was isolated. This cDNA lacked sequence encoding the extreme N-terminus based on alignment with PC4 from other species. cDNAs encoding a single xPC4 amino terminus were obtained using 5′ RACE and three independent clones were sequenced. Complete sequences of all cDNAs reported here can be accessed in GenBank (accession nos. xFurin: AY901983; xPC6A AY901985; xPC6B AY901986; xPC6C AY901987; xPC6D AY901988; xPC6E AY901989; xPC6F AY901990; xPC4 AY901984).

Analysis of *PC* expression

RNA was isolated from embryos and subjected to ribonuclease protection analysis as described (Cui et al., 1995). Northern blots containing 20 μg of RNA per lane were hybridized to ^{32}P-labeled cRNA probes as described (Christian et al., 1991). Semi-quantitative reverse transcription (RT)-PCR was performed according to Nakayama et al. (Nakayama et al., 1998). xPC4-specific primers were as follows: downward 5′-GAACACTCAGTACTGAGCGA-3′; upward 5′-TGTTGTTTCATCATAGGTGG-3′. The sequences of EF-1α (Tsuneizumi et al., 1997) and ODC (Nastos et al., 1998) primers have been reported. Results were visualized by autoradiography. Wholemount in situ hybridization was performed as described (Harland, 1991) using BM Purple AP substrate (Roche). Embryos were staged according to Nieuwkoop and Faber (Nieuwkoop and Faber, 1967).

ACKNOWLEDGEMENTS

J.L.C. and S.M.N. were funded by the NIH.

Chapter 3

Site-specific cleavage of BMP4 by Furin, PC6 and PC7

Sylvia M. Nelsen[1] and Jan L. Christian[2]

Departments of Molecular & Medical Genetics[1] and Cell & Developmental Biology[2],

Oregon Health & Science University, Portland, Oregon, USA

Manuscript in press in the Journal of Biological Chemistry

Received for publication, June 1, 2009; Accepted for publication August 2, 2009

PREFACE

This work is currently in press in the Journal of Biological Chemistry by Sylvia M. Nelsen and Jan L. Christian.

My contributions to this study include all experiments and manuscript preparation except as detailed below.

Jan L. Christian cloned *Xenopus Pc7*, designed all antisense oligonucleotides (except for *Pace4* which was previously published), and performed Northern analyses for *Furin*, *Pace4*, and *Pc6* (Figure 3-1). She also co-wrote the manuscript and provided advice and suggestions on experimental design and data analysis, as well as the space, equipment, and supplies with which to perform the experiments.

SUMMARY

Bone morphogenetic proteins (BMPs) require proteolytic activation by members of the proprotein convertase (PC) family. ProBMP4 is initially cleaved at a site adjacent to the mature ligand domain (S1), and then at an upstream site (S2) within the prodomain. Cleavage at the S2 site, which appears to occur in a tissue-specific fashion, regulates the activity and signaling range of mature BMP4. To test the hypothesis that tissue-specific cleavage of proBMP4 is regulated by differential expression of a site-specific protease, we identified the PCs that cleave each site *in vivo*. In *Xenopus* oocytes, Furin and PC6 function redundantly to cleave both the S1 and S2 sites of proBMP4, as evidenced by the results of antisense-mediated gene knockdown and use of the Furin and PC6 selective inhibitor, α_1-PDX. By contrast, α_1-PDX blocked cleavage of the S2 but not the S1 site of proBMP4 in embryos, suggesting the existence of a developmentally regulated S1 site-specific convertase. This protease is likely to be PC7 based on knowledge of its required substrate cleavage motif and resistance to α_1-PDX. Consistent with this prediction, an α_1-PDX variant engineered to target PC7, in addition to Furin and PC6, completely inhibited cleavage of BMP4 in oocytes and embryos. Further studies showed that *Pc7* transcripts are expressed and polyadenylated, and that the PC7 precursor protein undergoes efficient autocatalytic activation in both oocytes and embryos. These results suggest that PC7, or a convertase with similar substrate specificity, functions to selectively cleave the S1 site of proBMP4 in a developmentally regulated fashion.

INTRODUCTION

Bone morphogenetic protein 4 (BMP4) is a cell to cell signaling molecule that was originally isolated for its ability to induce ectopic bone formation (Wozney et al., 1988). More recent studies demonstrate diverse roles for BMP4 during development of the skeleton and other organs, and in bone homeostasis after birth (Hogan, 1996).

The bioactivity of BMP4 is regulated post-translationally, at the level of proteolytic activation. BMP4 originates as an inactive dimeric precursor that is cleaved by specific members of the proprotein convertase (PC) family of endoproteases (Constam and Robertson, 1999; Cui et al., 1998) to yield prodomain fragments along with the carboxyl-terminal mature ligand. In mammals, seven members of the PC family have been characterized. Among these only Furin (also known as PACE, SPC1, or PCSK3), PACE4 (also named SPC4 or PCSK6), PC6 (also called PC5, SPC6, or PCSK5) and PC7 (also known as PC8, LPC, SPC7, or PCSK7) are broadly expressed and active within the constitutive, as opposed to the regulated, secretory pathway, making them appropriate candidates for endogenous BMP4 convertases (Steiner, 1998; Thomas, 2002). Furin prefers to cleave proproteins at the carboxy-terminal side of the optimal consensus sequence -R-X-R/K-R-, but can also cleave following the minimal sequence -R-X-X-R- (Molloy et al., 1992). PACE4 and PC6 recognize the same optimal and minimal Furin consensus motifs, whereas PC7 has a strict requirement for a basic residue in the P_2 position (counting back from the cleavage site), and can thus only cleave substrates containing an optimal Furin motif (Rockwell et al., 2002; van de Loo et al., 1997).

We have shown that BMP4 is sequentially cleaved at two sites within its prodomain and that this ordered proteolysis regulates both the activity and signaling

range of mature BMP4 (Cui et al., 2001). BMP4 is cleaved first following an optimal Furin motif adjacent to the mature domain (-R-X-K-R-, the S1 site), and this allows for subsequent cleavage at an upstream minimal site within the prodomain (-R-X-X-R-, the S2 site). In *Xenopus* embryos, proBMP4 carrying a point mutation that renders the upstream site non-cleavable generates a less active ligand that signals over a shorter range, and accumulates at lower levels compared to BMP4 cleaved from wild type precursor.

More recent studies from our lab suggest that differential cleavage of proBMP4 regulates the activity of the mature ligand by directing its intracellular trafficking to either degradatory or secretory/recycling pathways (illustrated schematically in Figure 3-1) (Degnin et al., 2004). Cleavage of proBMP4 at the S1 site, which is presumed to occur in the trans-Golgi network (TGN), generates a non-covalently associated ligand/prodomain complex that is then trafficked to a post-TGN compartment where the more acidic environment makes the S2 site accessible, possibly by triggering a conformational change. Cleavage at the S2 site liberates mature BMP4 from the prodomain, which promotes protein stability. If cleavage of the upstream S2 site does not occur, the prodomain/ligand complex is preferentially targeted to the lysosome for degradation,

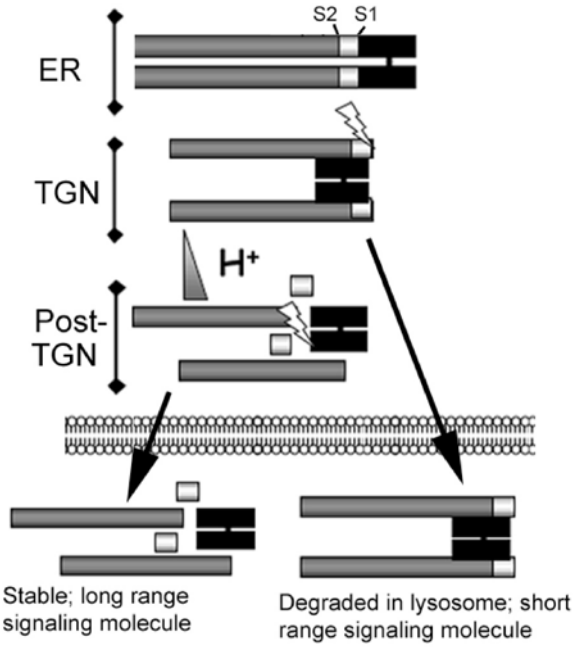

Figure 3-1. Model for regulation of BMP4 activity by sequential cleavage. See text for details.

either directly within the biosynthetic pathway or via the endocytic pathway following secretion, receptor activation and reuptake. As a consequence, less mature ligand is available, resulting in lower levels of BMP4 activity.

Analysis of mice carrying a knock-in point mutation in *Bmp4* (*Bmp4*^{S2G}) that allows for cleavage at the S1 site (generating a wild type ligand) but prevents S2 processing has shown that cleavage of the S2 site is essential for normal development and, more importantly, suggests that this site might be selectively cleaved in a tissue-specific fashion (Goldman et al., 2006). Specifically, these mice display phenotypic defects in only a subset of tissues where full *Bmp4* dosage is known to be important. For example, *Bmp4*$^{S2G/S2G}$ mice show a greater loss of primordial germ cells and more severe testicular degeneration than that observed in *Bmp4* null heterozygotes (*Bmp4*$^{+/-}$) (Dunn et al., 1997). *Bmp4*$^{S2G/S2G}$ mice, however, never display polycystic kidneys, polydactyly, or other skeletal abnormalities that are observed in *Bmp4*$^{+/-}$ mice. Furthermore, levels of mature BMP4 protein are decreased in the testes but not in the kidneys of *Bmp4*$^{S2G/S2G}$ mice relative to wild type siblings.

The above studies illustrate the importance of proteolytic processing in regulating BMP4 activity, yet the PCs that cleave the S1 and/or S2 site have not been definitively identified. Recombinant Furin, PACE4 and PC6 are all capable of cleaving the S1 and S2 sites of proBMP4 *in vitro*, whereas PC7 can only recognize and cleave following the optimal motif present at the S1 site (Cui et al., 1998). Ectopic expression of the selective PC inhibitor, α_1-PDX, in *Xenopus* embryos phenocopies loss of BMP4 function. Furthermore, this same inhibitor prevents cleavage of BMP4 in an oocyte translation assay (Cui et al., 1998). α_1-PDX is a genetically engineered mutant form of the naturally

occurring serine protease inhibitor (serpin), α_1-antitrypsin (α_1-AT), that contains in its reactive site the amino acids -R-I-P-R-, the minimal consensus motif for efficient processing by Furin (Anderson et al., 1993). As with all serpins, α_1-PDX functions as a suicide substrate inhibitor, forming a tight, stable complex with, and eventually being cleaved by the protease(s) it targets. α_1-PDX is a potent and selective inhibitor of Furin and PC6 *in vitro*, with K_i values of 0.6 nM and 2.3 nM, respectively (Jean et al., 1998). It can also inhibit the activity of ectopically expressed PACE4 (Tsuji et al., 1999b), but not PC7 (Jean et al., 1998), when overexpressed in cultured cells. Collectively, these studies identify Furin and PC6 as the most likely endogenous BMP4 convertases, but do not rule out the possibility that PACE4 and/or PC7 contribute to cleavage of one or both sites.

Phenotypic analysis of *Furin* or *Pc6* mutant mice is consistent with the possibility that these enzymes contribute to proteolytic activation of BMP4 *in vivo*. *Furin* null mutants die by E11.5 and show an early defect in chorioallantoic fusion (Roebroek et al., 1998) similar to that observed in *Bmp4* deficient mice (Goldman et al., 2009; Goldman et al., 2006). However, loss of *Furin* has less severe consequences than loss of *Bmp4* (Winnier et al., 1995), suggesting that additional PCs function redundantly to cleave this precursor. Mice homozygous for null alleles of *Pc6* die between E15.5 and birth due to defects in multiple organ systems (Essalmani et al., 2008; Szumska et al., 2008). Some defects in *Pc6* mutants have been attributed to deficiencies in GDF11 whereas others, including defects in ventral body wall closure and cardiac abnormalities, phenocopy those observed in *Bmp4* mutants (Goldman et al., 2009; Goldman et al., 2006; Jiao et al., 2003; Liu et al., 2004). By contrast, mice lacking *Pace4* show laterality defects that have been attributed primarily to loss of Nodal processing (Constam and Robertson, 2000a). *Pc7*

mutants develop normally (Taylor et al., 2003), demonstrating that this protease does not function independently to activate proBMP4.

The mechanism through which tissue-specific cleavage of the S2 site of BMP4 is achieved is unknown, but one possibility involves differential expression of site-specific convertases. For example, selective cleavage of the S2 site could be mediated by tissue-specific expression of a convertase that resides in the more acidic post-TGN compartment in which the S2, but not the S1 site is cleaved. Furin is broadly expressed and resides predominantly in the TGN (Thomas, 2002), whereas PC6B (a membrane-bound isoform of PC6) is expressed in only a few tissues (Essalmani et al., 2008) and is localized to a distinct, post-TGN compartment (Xiang et al., 2000). Thus, it is possible that the S1 site is constitutively cleaved by Furin, whereas the S2 site is cleaved only in tissues that co-express PC6B. Alternatively, it is possible that Furin, PC6 and/or PACE4 cleave both sites, whereas PC7 cleaves only the S1 site *in vivo*, similar to what has been demonstrated *in vitro*. In this scenario, BMP4 would be cleaved at both sites in all tissues except for those in which PC7 is the sole convertase. To begin to test potential mechanisms for tissue-specific regulation of S2 cleavage, we used loss-of-function approaches along with protein-based inhibitors to ask which PCs cleave the S1 and S2 sites of BMP4 *in vivo*.

RESULTS

Furin and PC6 function redundantly to cleave both sites of BMP4 in oocytes

We developed an *in vivo* assay in oocytes to definitively identify the endogenous PCs that cleave the S1 and/or S2 site of BMP4 (illustrated in Figure 3-2A). Oocytes were injected with phosphorothioate-modified antisense oligonucleotides specific for *Furin, Pc6*

(all known isoforms, Nelsen et al., 2005), *Pace4*, and *Pc7*, and these were shown to reduce the levels of their target mRNAs by 90-95% (Figure 3-2B). Injected oocytes were cultured for 3 days to allow for turnover of endogenous PC proteins, and then injected with RNA encoding epitope-tagged BMP4 together with [^{35}S]Met/Cys. The following day, precursor protein and cleavage products were immunoprecipitated from oocyte lysates using antibodies specific for the HA tag in the prodomain or the myc tag in the mature domain. Immunoprecipitated proteins were then analyzed by SDS-PAGE under non-reducing conditions and imaged by autoradiography (Figure 3-2C, position of precursor dimer, precursor monomer, and S1 + S2 cleaved prodomain and mature ligand are illustrated to the right of the gel). Because dimerization and folding of proBMP4 is relatively slow and is rate-limiting for cleavage, levels of precursor monomer were not affected by the depletion of endogenous convertases over the short time course of this analysis. Thus, the precursor monomer band (second panel from the top) served as a loading control. Levels of dimerized BMP4 precursor increased significantly in oocytes depleted of Furin, and this effect was accompanied by a corresponding decrease in the levels of both the fully cleaved prodomain and mature BMP4 (Figure 3-2C). Levels of cleaved prodomain and mature BMP4 were slightly decreased in oocytes depleted of PC6 alone, and were strongly decreased in oocytes depleted of both Furin and PC6. By contrast, there was no significant loss of BMP4 cleavage in oocytes depleted of PACE4 or PC7. These data show that Furin and PC6 function redundantly to cleave both the S1 and the S2 sites in oocytes, and rule out a model in which PC6B selectively cleaves the S2 site.

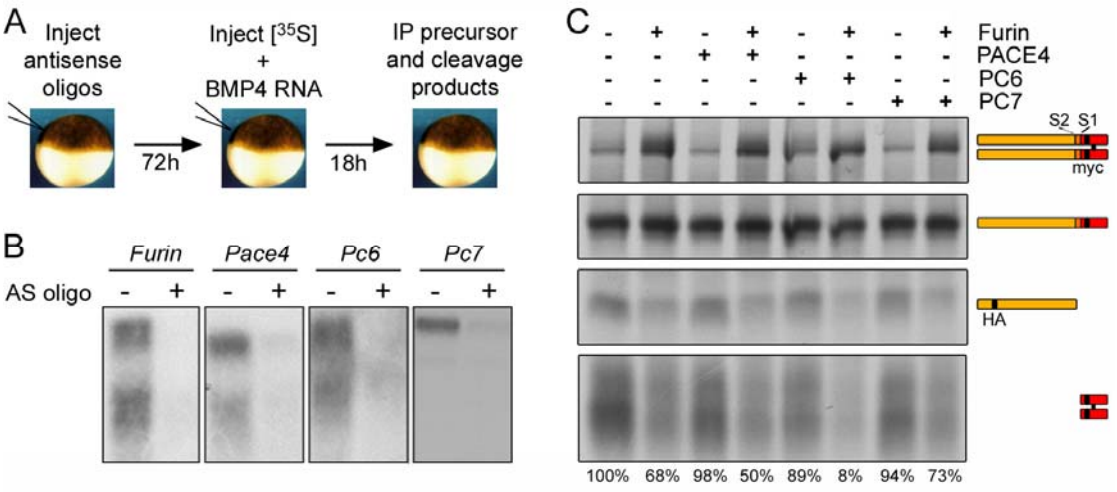

Figure 3-2. Furin and PC6 function redundantly to cleave both sites of BMP4 in Oocytes. (A) Schematic illustration of PC knockdown assay. B) Northern analysis of *Pc* expression in oocytes 24 h after injection of antisense oligonucleotides (AS oligo) specific for each *Pc* as indicated. (C) Radiolabeled proBMP4 precursor dimers and monomers, prodomain and mature domain fragments (indicated to right of gel) were immunoprecipitated from uninjected oocytes or oocytes injected with antisense oligonucleotides specific for Furin, PACE4, PC6 and/or PC7 as indicated and separated by SDS-PAGE under non-reducing conditions. Prodomains were deglycosylated with PNGase-F. Mature BMP4 dimers appear as fuzzy bands due to variable glycosylation. Below each lane, levels of cleaved mature BMP4 normalized to precursor monomer are expressed as percent of that observed in uninjected oocytes. Results were reproduced in at least three experiments.

An α_1-PDX-insensitive enzyme acts redundantly with Furin and PC6 to cleave the optimal site of BMP4 in embryos, but not oocytes

To ask whether Furin and PC6 are the sole convertases responsible for cleaving proBMP4 throughout development, we analyzed BMP4 cleavage products in oocytes and embryos in the presence of the selective PC inhibitor α_1-PDX. As described previously, α_1-PDX is a potent inhibitor of Furin and PC6 but is ineffective against PC7. *Xenopus* oocytes were injected with 1 ng of RNA encoding epitope-tagged proBMP4, proBMP4^{S2G} (which can only be cleaved at the S1 site) or proBMP4^{S1G} (which can only be cleaved at the S2 site) alone or together with increasing amounts of RNA encoding α_1-PDX. Western blots of oocyte extracts were then probed with antibodies specific for the HA tag

in the prodomain of BMP4. When we expressed α_1-PDX in oocytes at doses of 0.5 ng or greater, cleavage of both the S1 and the S2 site of wild type BMP4 was blocked (Figure 3-3, top panels; position of precursor, S1-only cleaved prodomain, and S1 + S2 cleaved prodomain are illustrated to the right of the gel). Cleavage of proBMP4^{S2G} and proBMP4^{S1G} at the S1 or S2 sites, respectively, was ablated at similar doses of α_1-PDX. We do not detect any increase in BMP4 precursor levels concomitant with the loss of cleavage products in oocyte lysates because proBMP4 is present primarily in monomeric form inside of cells, and this pool is impervious to inhibitors of cleavage. These findings are consistent with the results of our antisense depletion experiments (Figure 3-2C), and with our previous studies using this inhibitor (Cui et al., 1998) in showing that Furin and PC6 are fully responsible for cleavage of BMP4 in oocytes. A different result was obtained, however, when we analyzed BMP4 cleavage in embryos (Figure 3-3, lower panels). In these experiments, RNA encoding epitope-tagged proBMP4, proBMP4^{S2G} or proBMP4^{S1G} (1 ng) was injected near the animal pole of four-cell embryos either alone or together with RNA encoding increasing doses of α_1-PDX. At the mid-gastrula stage, fluid was aspirated and pooled from the blastocoel of 10 embryos in each group, and Western blots of blastocoel fluid were probed with antibodies specific for the HA tag in the prodomain of BMP4. ProBMP4 is cleaved intracellularly and thus precursor proteins are detected only in the intact cells of embryo homogenates, whereas the cleaved prodomain and mature ligand are secreted into the blastocoel. In the absence of α_1-PDX, BMP4 precursor protein was not detected in the blastocoel fluid, but a prodomain fragment generated by cleavage at both the S1 and the S2 sites was observed (Figure 3-3, lower panels). In the presence of increasing doses of α_1-PDX, uncleaved precursor began to

accumulate in the blastocoel, consistent with a loss of Furin- and PC6-meditated cleavage of at least a fraction of proBMP4. This was accompanied by complete loss of the S1 + S2 cleaved prodomain band, and a concomitant increase in the level of S1-only cleaved prodomain. The S1-only cleaved prodomain fragment generated from wild type BMP4 or $BMP4^{S2G}$ persisted even at the highest doses of α_1-PDX. By contrast, cleavage of the S2 site of wild type BMP4, or of $BMP4^{S1G}$ was completely inhibited by α_1-PDX at doses of 0.5 ng or greater. Taken together, these results suggest that Furin and PC6 are the only active BMP4 convertases in oocytes and that they cleave both the S1 and the S2 sites of this precursor. By the mid-gastrula stage, however, an additional α_1-PDX insensitive convertase, that is either not present or not active in oocytes, functions redundantly with Furin and PC6 to cleave the optimal (-R-S-K-R-) motif at the S1 site, but not the minimal (-R-I-S-R-) motif at the S2 site, of BMP4. We hypothesize that this enzyme could be PC7 based on previous studies showing that PC7 is unique among PC family members in having a stringent requirement for a P_2 basic residue (which is present at the S1 but not the S2 site of BMP4), and based on its known insensitivity to inhibition by α_1-PDX (Jean et al., 1998; van de Loo et al., 1997).

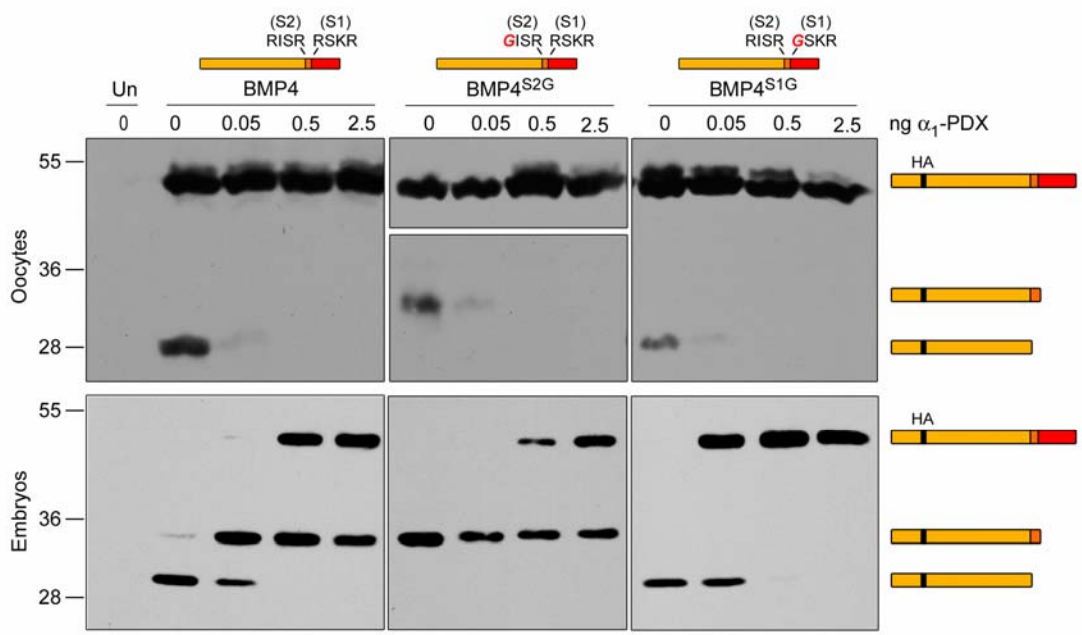

Figure 3-3. An α_1-PDX insensitive enzyme acts redundantly with Furin and PC6 to cleave the optimal site of BMP4 in embryos. Western blot of oocyte lysates (top panels) or blastocoel fluid from embryos (bottom panels) not injected (Un) or injected with RNA encoding wildtype or cleavage mutant forms of proBMP4 (illustrated above each panel) either alone or together with increasing doses of α_1-PDX as indicated. Blots were probed with HA- specific antibodies to detect precursor proteins and cleaved prodomain fragments (illustrated schematically to right of gel). Monomeric forms of proBMP4 are present at significantly higher levels than cleavage products in oocyte lysates, and thus when Western blots are exposed for sufficient periods of time to visualize cleavage products, bands corresponding to precursor proteins are overexposed. This is particularly true in the case of BMP^{S2G}, since cleavage products are unstable, and thus two different exposures of the same Western blot are shown. Results were reproduced in at least three experiments.

The α_1-PDX resistant protease present in embryos requires an optimal PC7 motif for cleavage

To more stringently test whether the α_1-PDX resistant activity we observe in embryos but not oocytes is only able to cleave substrates following an optimal (-R-X-K/R-R-) motif, consistent with the known minimal consensus site for cleavage by PC7, we analyzed processing of BMP4 cleavage site variants in the presence and absence of α_1-PDX. Specifically, we assayed cleavage of BMP4 variants (illustrated at the top of Fig. 4) that contain optimal ($BMP4^{S2K}$), or minimal ($BMP4^{S1I}$) Furin motifs at both the S1 and the

S2 sites, or in which the order of the optimal and minimal motifs is reversed ($BMP4^{S2K/S1I}$). Oocytes or embryos were injected with RNA encoding epitope-tagged wild type or cleavage variant proBMP4 (1 ng), either alone or together with RNA (0.05-2.5 ng) encoding α_1-PDX. Precursor proteins and cleavage products present in oocyte homogenates or blastocoel fluid were analyzed by Western blot as described above, using antibodies directed against the HA tag to detect precursor and cleaved prodomain, or against the myc tag to detect the cleaved mature domain. In the absence of α_1-PDX, all precursor proteins were efficiently cleaved at both the S1 and the S2 site to generate prodomain and mature BMP4 (Figure 3-4, precursor and cleavage products are illustrated to the right of the gel). Ligand generated from each variant was active *in vivo*, as assayed by the ability to ventralize *Xenopus* embryos and induce expression of the BMP target gene, *Xbra*, in Xenopus ectodermal explants (data not shown and Cui et al., 2001).

In oocytes, α_1-PDX blocked proteolysis of both the S1 and the S2 site of wild type and cleavage variant proBMP4 at doses of 0.5 ng of RNA or greater (Figure 3-4, top panel). In embryos, however, α_1-PDX blocked cleavage of minimal Furin motifs, whereas cleavage at optimal motifs was partially preserved even in the presence of the highest doses of α_1-PDX, regardless of their position (S1 versus S2) within the protein. Specifically, prodomain fragments generated by cleavage at both of the optimal (-R-X-K-R-) motifs in $BMP4^{S2K}$ and at the S2 optimal motif of $BMP4^{S2K/S1I}$ persisted even at the highest doses of α_1-PDX. By contrast, α_1-PDX completely inhibited cleavage at both of the minimal (-R-X-X-R-) motifs present in $BMP4^{S1I}$ and at the S1 minimal motif in $BMP4^{S2K/S1I}$. These results confirm that the α_1-PDX resistant protease present in embryos

requires a P2 basic residue in order to cleave a substrate, consistent with our hypothesis that this protease is PC7.

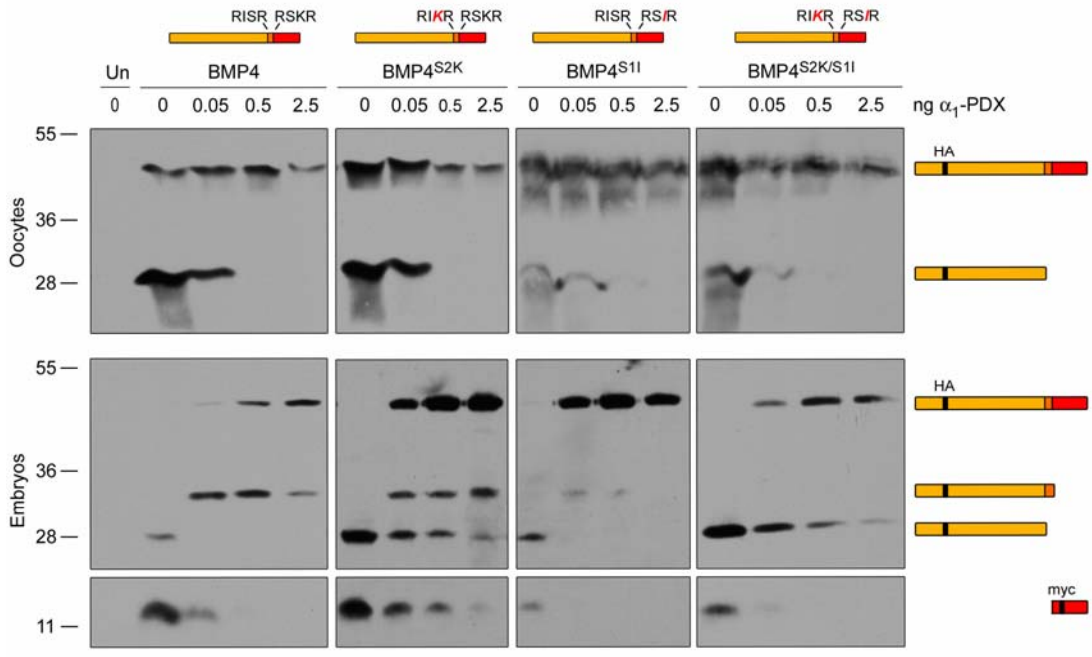

Figure 3-4. The α_1-PDX resistant protease present in embryos requires an optimal PC7 motif for cleavage. Western blot of oocyte lysates (top panels) or blastocoel fluid from embryos (bottom panels) that were not injected (Un) or were injected with RNA encoding wildtype or cleavage variant forms of proBMP4 (illustrated above each panel) either alone or together with increasing doses of α_1-PDX. Blots were probed with HA-specific antibodies to detect precursor proteins and cleaved prodomain fragments or with myc-specific antibodies to detect mature BMP4 (illustrated to right of gel). Results were reproduced in at least three experiments.

An α_1-PDX variant predicted to target PC7 as well as Furin and PC6 fully inhibits BMP4 cleavage in oocytes and embryos

To begin to test our hypothesis that PC7 functions redundantly with Furin and PC6 to cleave the S1 site of BMP4, we initially attempted to knock down expression of all three proteases individually and in combination in embryos using translation blocking morpholino antisense oligonucleotides. We were not, however, able to deplete BMP4 convertase activity in early (gastrula stage) embryos to any detectable degree using this

technology (Christian, unpublished data), presumably because all three of these enzymes are expressed maternally (Figure 3-2B) and have relatively long half lives. As an independent method of testing whether PC7, or an enzyme with similar substrate selectivity, contributes to cleavage of the S1 site of BMP4 in embryos, we asked whether an α_1-PDX variant containing a P_2 basic residue in its reactive site loop could fully inhibit cleavage of BMP4 in embryos. As described previously, α_1-PDX is modeled after the naturally occurring serpin, α_1-AT, but contains in its reactive site the minimal consensus motif for efficient processing by Furin (illustrated in Figure 3-5A). This serpin is a potent inhibitor of Furin and PC6, but it does not bind or inhibit PC7, most likely due to the lack of the P_2 basic residue that is required for recognition by PC7 (Anderson et al., 1993; Jean et al., 1998). The serpin α_1-EK4, which has been further modified to include a P_2 basic residue (Figure 3-5A), has been shown to interact with and inhibit Furin (Dufour et al., 2001) and is predicted to inhibit PACE4, PC6, and PC7 as well. Oocytes or embryos were injected with RNA encoding epitope tagged proBMP4 (1 ng), either alone or together with increasing amounts (0.05-5 ng) of RNA encoding α_1-PDX or α_1-EK4. Precursor proteins and cleavage products present in oocyte homogenates or blastocoel fluid were analyzed by Western blot as described above. As shown in Figure 3-5B, α_1-PDX and α_1-EK4 were both able to fully inhibit the endogenous convertases that cleave the S1 and S2 sites of proBMP4 in oocytes. In embryos, however, α_1-PDX inhibited the endogenous convertases responsible for cleavage of the S2 but not the S1 site, whereas α_1-EK4 inhibited the convertases responsible for cleaving both of these sites. To test the possibility that α_1-EK4 is merely more effective because it is expressed at higher levels than α_1-PDX, Western blots were stripped and reprobed with antibody specific for α_1-AT.

In both oocytes (Figure 3-5B, top section, lower panel) and embryos (Figure 3-5B, bottom section, lower panel), steady state levels of α_1-PDX protein were reproducibly higher than those of α_1-EK4 following injection of equivalent amounts of RNA. Furthermore, whereas the vast majority of the α_1-PDX that was detected was the fully active form (asterisk), approximately 50% of α_1-EK4 had been converted to the inactive, cleaved form (double asterisk). This finding is consistent with previous studies showing that whereas α_1-PDX forms a highly stable, SDS resistant complex with its substrates (Jean et al., 1998), α_1-EK4 more readily dissociates to yield the active enzyme and cleaved inhibitor (Dufour et al., 2001). Thus, the ability of α_1-EK4, but not α_1-PDX, to block cleavage of the S1 site of proBMP4 *in vivo* likely reflects differences in substrate selectivity rather than potency. These results further support our hypothesis that PC7, or an enzyme with similar selectivity, functions redundantly with Furin and PC6 to cleave the S1 site of BMP4 in embryos, but not in oocytes.

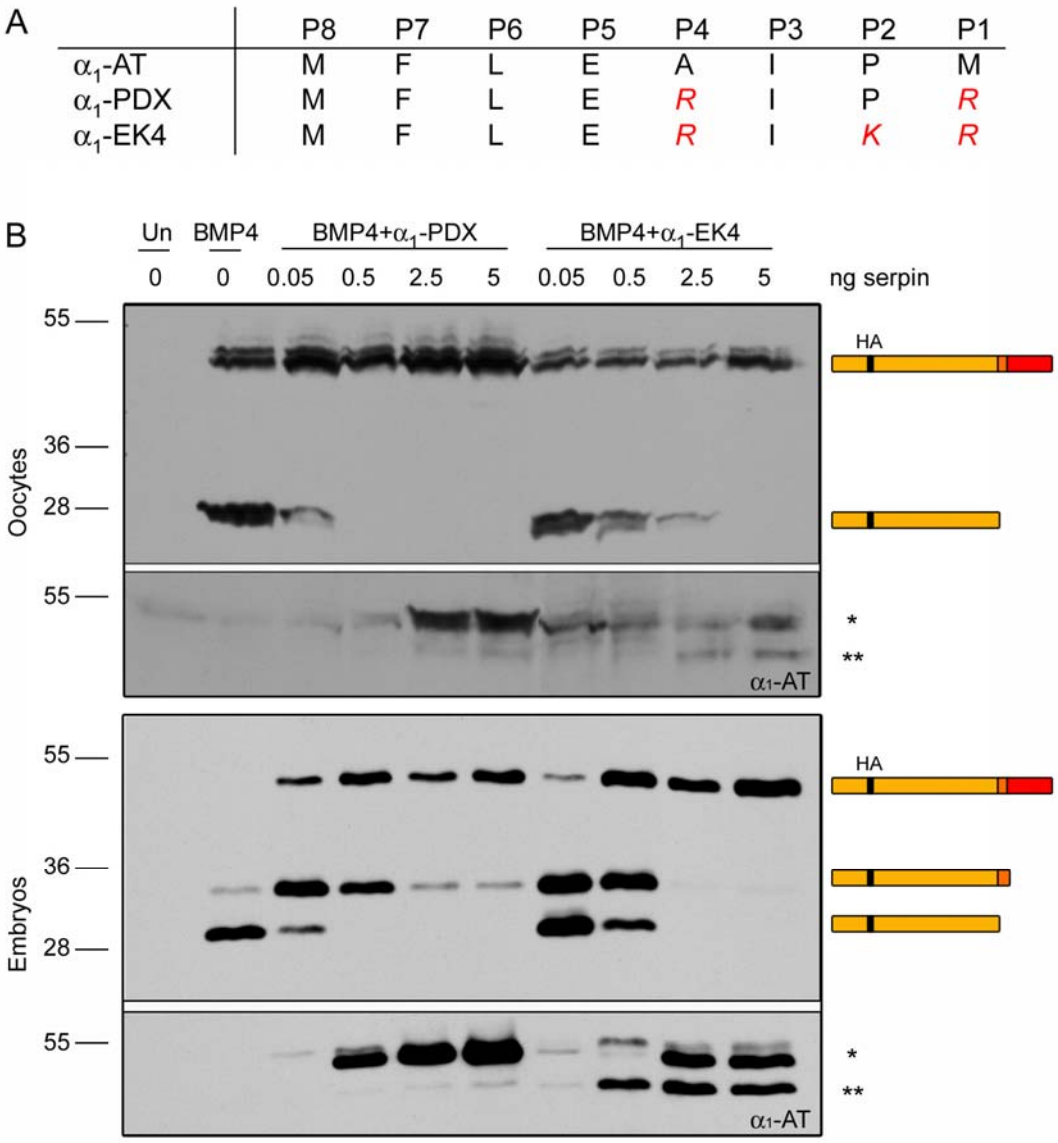

Figure 3-5. EK4 fully inhibits cleavage of both the optimal and minimal sites of BMP4 in oocytes and embryos. (A) Sequence surrounding the reactive site loop of α_1-AT and genetically engineered variants. (B) Western blot of oocyte lysates (top two panels) or blastocoel fluid from embryos (bottom three panels) that were not injected (Un) or were injected with RNA encoding proBMP4 either alone or together with increasing doses of α_1-PDX or α_1-EK4. Blots were probed with HA-specific antibodies to detect precursor proteins and cleaved prodomain fragments (illustrated to right of gels). Blots were reprobed with antibodies specific for α1-AT to detect the intact (asterisk) and cleaved form (double asterisk) of each serpin. Results were reproduced in at least two experiments.

α_1-PDX fully inhibits cleavage of both the S1 and the S2 sites of proBMP4 in oocytes

One possible explanation for why PC7-like activity is detected in embryos but not oocytes is that this enzyme might cleave substrates at the cell surface, as they are being secreted. If this were the case, cleavage products would not be detected in oocyte lysates, but would only be present in embryonic blastocoel fluid or in culture media from oocytes, the latter of which was not assayed on Western blots due to technical limitations. In order to test this possibility, we used a more sensitive assay to ask whether prodomain fragments generated by cleavage of proBMP4 at the S1 site alone are present in the culture media from oocytes made to express α_1-PDX. Oocytes were injected with [^{35}S]Met/Cys and RNA encoding epitope tagged proBMP4 (1 ng), either alone or together with increasing amounts (0.05-5 ng) of RNA encoding α_1-PDX. The following day, BMP4 precursor protein and cleavage products were immunoprecipitated from oocyte lysates or media using antibodies specific for the HA tag in the prodomain. Immunoprecipitated proteins were then analyzed by SDS-PAGE under reducing conditions and imaged by autoradiography. In the absence of α_1-PDX, a prodomain fragment generated by cleavage at both the S1 and the S2 sites was observed in oocyte lysates and media, whereas BMP4 precursor protein was detected primarily in oocyte lysates (Figure 3-6). In the presence of increasing doses of α_1-PDX, uncleaved precursor protein began to accumulate in the media, and this was accompanied by complete loss of all prodomain fragments in the culture media, similar to what is observed in cell lysates. These results suggest that the PC7-like activity we detect in embryos is either not present or not active in oocytes.

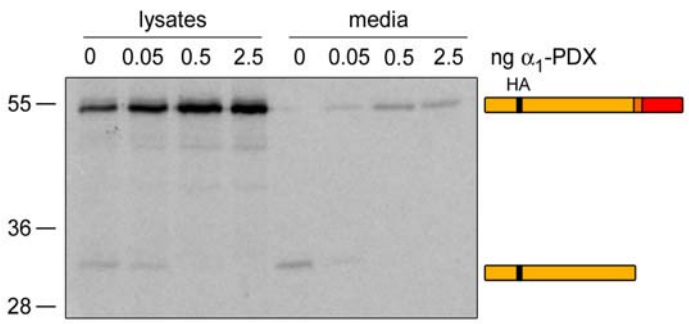

Figure 3-6. PC7-like activity is not detected in oocytes, even wen extracellular BMP4 cleavage products are analyzed. Radiolabeled pro-BMP4 precursor and prodomain fragments (indicated to right of gel) were immunoprecipitated from lysates and media of uninjected oocytes or oocytes injected with increasing doses of α_1-PDX, and separated by PAGE under reducing conditions.

PC7 transcripts are present and polyadenylated in both oocytes and early embryos

To begin to ask whether *Pc7* expression is developmentally regulated at the level of transcription, which might account for our results showing that a PC7-like activity is absent in oocytes but present by mid-gastrula stages, we analyzed the temporal and spatial patterns of expression of this enzyme. *Pc7* transcripts of ~5.8 kb, ~3.8 kb and ~ 2 kb were present in oocytes and persisted at fairly equivalent levels at least through early gastrula stages (St. 10.5) as assayed by Northern blot analysis (Figure 3-7A). The largest and most abundant transcript corresponds in size to full length ESTs published in the NCBI database. The abundance of *Pc7* transcripts decreased by the mid-gastrula stage (St. 11) and remained at these levels until the tailbud stage (St. 32). Transcripts were ubiquitously distributed in embryos as analyzed by in situ hybridization of PC7 probes to developmentally staged embryos, and by Northern blot analysis of dissected embryos (data not shown). Thus, the acquisition of PC7-like activity during gastrula stages cannot be accounted for by an increase in *Pc7* transcription or localized accumulation of transcripts in embryos relative to oocytes.

An alternate explanation for the appearance of PC7-like activity in early embryos might be that maternally inherited *Pc7* transcripts are not translated in oocytes but are

translated in embryos. Early animal development is controlled in part by maternal RNAs that are initially stored in a dormant state, but then undergo elongation of their poly(A) tail and mobilization onto polysomes upon oocyte maturation or after fertilization (Radford et al., 2008). To test whether PC7 is post-transcriptionally regulated via this mechanism, we used a PCR-based poly(A) tail (PAT) assay (Salles et al., 1999) (illustrated in Figure 3-7B) to compare the polyadenylation status of endogenous *Pc7* transcripts in *Xenopus* oocytes and gastrula stage embryos. Polyadenylation of endogenous *Furin* was analyzed in parallel as a positive control since our data show that this enzyme is active in oocytes. RNA was isolated from *Xenopus* oocytes and gastrula stage embryos and reverse transcribed using an oligo(dT) linker primer. The resultant cDNA was then amplified using primers that anneal to sequences located ~300 nucleotides from the end of the 3′ untranslated region (UTR) of the PC of interest (lightly shaded arrows) in combination with primers that anneal to either the 3′ linker sequence (black arrow) to generate PAT PCR products, or to the extreme 3′ end of the UTR (darkly shaded arrow) to generate control PCR products. Specific products were then detected by hybridizing Southern blots with a radiolabeled probe generated from the 3′ UTR of each PC. As shown in Figure 3-7B, the length of the poly(A) tail on *Pc7* transcripts was identical in oocytes relative to gastrula stage embryos, and the same was true for *Furin* transcripts. Antibodies that recognize endogenous PC7 are not available, and thus we are unable to definitively rule out the possibility that maternally inherited *Pc7* transcripts are not translated until after fertilization. The above results, however, demonstrate that maternal *Pc7* is not translationally regulated at the level of poly(A) tail elongation.

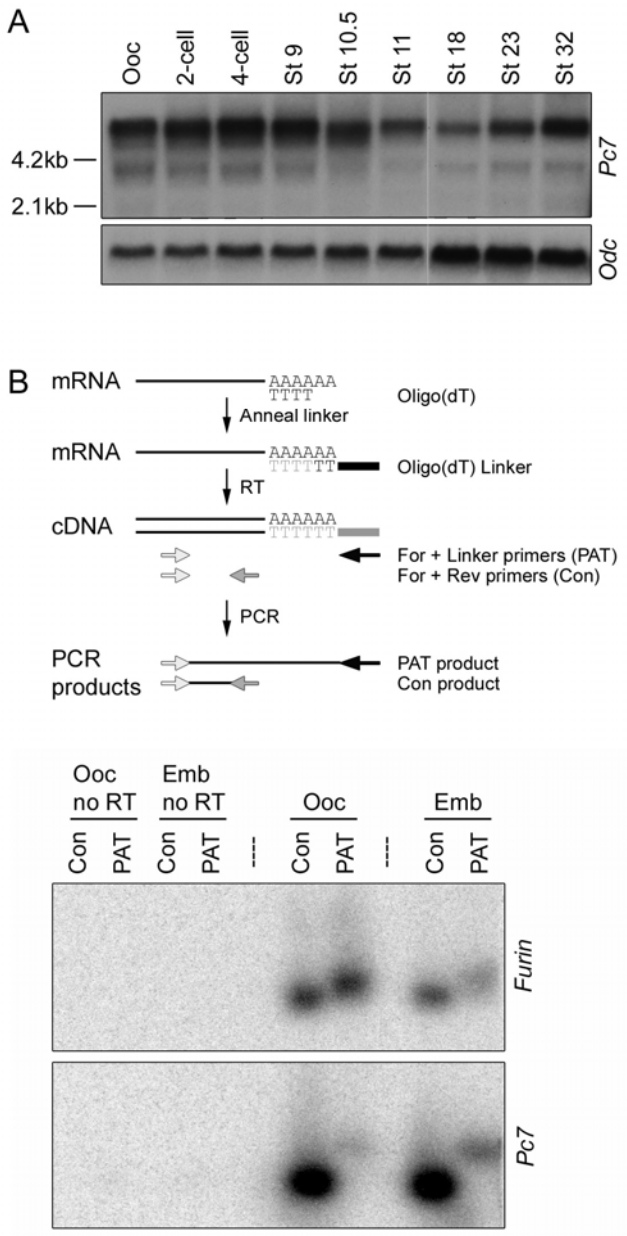

Figure 3-7. *Pc7* transcripts are expressed and polyadenylated to a similar extent in oocytes and embryos. (A) Northern blot analysis of *Pc7* and *ornithine decarboxylase* (*Odc*, as a loading control) expression in Xenopus oocytes (Ooc) and developmentally staged embryos. Vertical line between St 11 and St 18 indicates position where a lane was removed due to degraded RNA. (B) Analysis of poly(A) tail length of *Furin* and *Pc7* transcripts in oocytes and embryos (Emb) using the PCR-based assay illustrated schematically above the gel (see text for details). cDNA was synthesized in the presence or absence (no RT) of reverse-transcriptase and amplified via PCR using gene-specific forward and reverse primers (For + Rev) to generate a control band (Con) or the same gene-specific forward primer with a common reverse primer that anneals to the linker (For + Linker) to analyze poly(A) tail (PAT) length. Southern blots of PCR products were hybridized with radiolabeled cDNA probes specific for the 3′ untranslated region of *Furin* or *Pc7*. For Con lanes, 1/10th reaction was loaded. Results were reproduced in at least two experiments.

The cleaved form of PC7 is present in both embryos and oocytes

An alternate mechanism by which PC7 might be differentially regulated in oocytes versus embryos is at the level of proteolytic activation. All members of the PC family are generated as inactive zymogens that must be autocatalytically cleaved within the biosynthetic pathway to generate an enzyme that is capable of cleaving substrates in

trans (Thomas, 2002). To analyze the ability of Furin and PC7 to undergo autocatalytic cleavage, we injected RNA encoding FLAG tagged forms of *Xenopus* Furin and PC7 into oocytes and embryos and cultured them overnight. We then looked at whether the mature, cleaved form of each enzyme was generated *in vivo* by probing Western blots of membrane-enriched extracts with antibodies directed against the FLAG tag. As a size control for the uncleaved zymogen form, we analyzed cleavage mutant (cm) forms of Furin and PC7 (in which the consensus motif for cleavage had been disrupted) in parallel. As shown in Figure 3-8, all of the PC7 and most of the Furin detected in oocytes was the mature form, demonstrating that autocatalytic cleavage is rapid and nearly complete. In embryos, a small fraction of both Furin and PC7 persisted in the uncleaved zymogen form, but the mature, cleaved form of PC7 was the predominant species in membrane extracts from embryos (Figure 3-7) while mature cleaved Furin was detected primarily as the shed form in blastocoel fluid (data not shown), rather than membrane extracts. Thus, the activity of PC7 is not developmentally regulated at the level of autocatalytic activation. Notably, the presence of cleaved PC7 does not definitively prove that the enzyme is active in either oocytes or embryos.

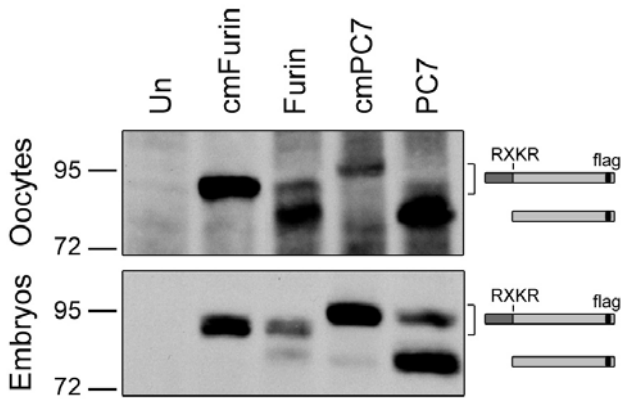

Figure 3-8. The cleaved form of PC7 is present in both embryos and oocytes. Western blot of membrane proteins from oocytes or embryos that were injected with native or cleavage mutant (cm) forms of flag-tagged *Xenopus* Furin or PC7. M2 antibody was used to detect the flag epitope in the mature domain. Position of precursor and cleaved mature proteins indicated to the right. Results were reproduced in at least three experiments. Left two lanes of oocyte panel are from the same blot washed two extra days and redeveloped.

DISCUSSION

In this study, we provide the first definitive evidence that Furin and PC6 are the primary endogenous BMP4 convertases, and that they function redundantly to cleave both the S1 and the S2 site of this precursor protein. These two enzymes are necessary and sufficient to activate BMP4 in *Xenopus* oocytes. By the early gastrula stage, however, an additional convertase activity that selectively cleaves only the optimal motif at the S1 site of BMP4 becomes apparent. This site-specific protease is likely to be PC7, or a closely related enzyme, based on its substrate selectivity and inhibitor sensitivity. The current studies provide insight into a potential mechanism by which the S2 site of BMP4 might be cleaved in a tissue-specific fashion. In addition, they highlight the fact that substrate selectivity of PCs is highly regulated at levels other than cleavage motif recognition or tissue-specific transcription, and provide essential information that sets the stage for further studies into how this occurs.

These studies do not definitively rule out the possibility that the S1-selective cleavage activity detected in embryos but not oocytes is PACE4 rather than PC7. Since PACE4 is capable of cleaving both the S1 and the S2 sites of BMP4 *in vitro*, however, (Cui et al., 1998), it is improbable that it cleaves only the S1 site *in vivo*. Furthermore, the phenotypes of mouse or *Xenopus* embryos depleted of *Pace4* are not consistent with a major role for this enzyme in proteolytic activation of BMP4 or related family members (Birsoy et al., 2005; Constam and Robertson, 2000a). Finally, proBMP4 is still cleaved in early gastrula stage mice lacking both *Pace4* and *Furin*, thereby eliminating PACE4 as an essential BMP4 convertase in the early embryo (Beck et al., 2002).

Pc7 is maternally expressed and yet our data suggest that this convertase is first active in embryos. This implies that PC7 expression or activity is regulated at a post-transcriptional level, although initial analyses revealed that this does not occur at the level of polyadenylation or autocatalytic activation. At least three alternative mechanisms by which PC7 expression or activity might be developmentally regulated can be envisioned. First, it is possible that PC7 expression is regulated at the level of translation, but that this occurs independent of poly(A) tail lengthening. Definitive evidence for or against translational control will require the development of antibodies that can detect endogenous *Xenopus* PC7. Second, PC7 might require a binding protein that is expressed in embryos but not oocytes in order to generate an active enzyme following autocatalytic cleavage. Precedent for the necessity of accessory proteins for PC activation is seen in the case of PC2, which requires its binding partner 7B2 for production of an active enzyme species (Mbikay et al., 2001). In the absence of 7B2, proPC2 can fold, transit the secretory system and undergo cleavage, but the mature enzyme that is generated remains incapable of cleaving substrates in trans. Recent studies suggest that 7B2 functions as a chaperone that prevents partially unfolded proPC2 from aggregating (Lee and Lindberg, 2008). It is likely that other PC family members utilize similar chaperones and our data are consistent with the possibility that a PC7-specific chaperone is expressed in embryos, but not oocytes. A third potential mechanism by which PC7 expression or activity could be developmentally regulated is at the level of post-translational modifications. PC7 is unique among members of the PC family in that it is reversibly modified by palmitoylation of its cytoplasmic tail (van de Loo et al., 1997). In the context of transmembrane proteins such as PC7, palmitoylation serves a variety of functions including binding to specific

lipid or protein domains in the membrane compartment in which the palmitoylated protein resides, aiding in folding, preventing aggregation and/or stabilizing the protein (Linder and Deschenes, 2007). The functional consequences of palmitoylation of PC7 are unknown, but it appears to promote protein stability since a form of PC7 that cannot be palmitoylated is more rapidly degraded (van de Loo et al., 1997). Alternatively, or in addition, palmitoylation may be required to anchor PC7 to the subcellular compartments or plasma membrane domains where it encounters its substrates. If PC7 is palmitoylated in embryos, but not oocytes, this might explain why PC7 activity can be detected in the former but not the latter. Further studies, that are beyond the scope of the current work, will be required to determine whether PC7 requires specific binding partners or post-translational modifications to become active.

The current studies suggesting that Furin and PC6 function redundantly to cleave both the S1 and S2 sites of BMP4, while PC7 contributes to cleavage of the S1 site alone, are consistent with the possibility that tissue-specific cleavage of the S2 site of BMP4 is regulated by differential expression of active Furin, PC6, and PC7. Specifically, it is possible that Furin and PC6 function redundantly to cleave both the S1 and the S2 site of BMP4 in all tissues where one or both of these enzymes are expressed, while BMP4 is cleaved at the S1 site alone in tissues that express PC7 exclusively. Analysis of $Bmp4^{S2G/S2G}$ mice, which carry a knock-in point mutation that allows for cleavage at the S1 site but prevents cleavage at the upstream S2 site, suggests that cleavage at both sites is essential for normal BMP4 function in many tissues (Goldman et al., 2009; Goldman et al., 2006). This is consistent with the observation that both *Furin* and *Pc6* are broadly expressed, and their expression domains often overlap with those of *Bmp4* (Constam et al.,

1996). The two tissues in which cleavage at the S2 site appears to be dispensable for vertebrate BMP4 function are the skeleton and the kidneys (Goldman et al., 2006). If BMP4 is cleaved at the S1 site alone in these tissues, and if, as hypothesized, this occurs because active PC7 (but not Furin or PC6) is co-expressed with BMP4 in these tissues, then *Pc7* mutants would be expected to show phenotypic abnormalities in the skeleton and kidneys similar to those observed in *Bmp4* mutants. The skeletal and kidney phenotypes in mice with reduced *Bmp4* dosage are incompletely penetrant and fairly subtle, however (Dunn et al., 1997; Goldman et al., 2006). Thus, although *Pc7* null mutants are reported to have no overt abnormalities, a detailed analysis has not been published (Taylor et al., 2003) and similar defects may exist in *Pc7* mutants. Closer examination of *Pc7* null mice, or of compound mutants that lack potentially compensatory PCs, may define more clearly the role of PC7 in development in general and in BMP4 cleavage in particular.

MATERIALS AND METHODS

cDNA constructs and antisense oligonucleotides

cDNAs encoding HA- and myc-tagged native and cleavage mutant forms of proBMP4 have been described previously (Degnin et al., 2004; Sopory et al., 2006). cDNAs encoding other cleavage site variants were made using the splicing by overlap extension method (Horton et al., 1990) or by PCR-mediated introduction of appropriate restriction sites. A full length *Xenopus Pc7* cDNA (accession no. NM_00196550) was identified by searching the NCBI database (http://ncbi.nlm.nih.gov) and obtained from Open BioSystems on behalf of the IMAGE consortium (http://image.hudsonalpha.org) (Lennon et al., 1996). The coding region of *Xenopus Pc7* or *Furin* (Nelsen et al., 2005)

was amplified and sequence encoding a FLAG tag inserted at the extreme carboxy-terminus using PCR-based approaches. Cleavage mutant forms of Furin and PC7, in which the consensus cleavage motif (-R-X-K-R-) was changed to -R-X-K-G- and -G-X-K-R-, respectively, were generated using a Quick Change mutagenesis kit (Stratagene). All cDNAs were subcloned into the vector pCS2+ and regions of cDNAs generated by PCR were sequenced. Antisense oligonucleotides specific for *Furin* (5′-A*C*T*TGCTGCTCCAAC C*A*G), *Pc6* (5′-A*T*A*CCACATGCTTGGC*C*A) and *Pc7* (5′-T*C*C*AGCAAGTTCATCA*G*G) (where residues with phosphorothioate bonds are indicated by an asterisk), were purchased from Invitrogen. The antisense oligonucleotide specific for *Pace4* has been described previously (Birsoy et al., 2005).

Embryo culture and manipulation

Ovulation was induced by injecting female frogs with human chorionic gonadotropin (Sigma). Embryonic stages are according to Nieuwkoop (Nieuwkoop and Faber, 1967). Capped synthetic mRNA was synthesized by in vitro transcription of linearized template cDNAs using a MegaScript kit (Ambion) and injected into embryos as described previously (Moon and Christian, 1989). *Xenopus* ventralization and ectodermal explant assays were performed as described (Cui et al., 2001).

Expression and analysis of radiolabeled proteins in oocytes

Xenopus oocytes (stage VI) were isolated and cultured at 18°C as described (Degnin et al., 2004). For PC-depletion experiments, oocytes were injected with antisense oligonucleotides (10 ng), cultured for 3 days, and then injected with RNA encoding BMP4 (10 ng) together with [^{35}S]Met/Cys (700 nCi). For experiments testing α_1-PDX inhibition of BMP4 cleavage, oocytes were injected with [^{35}S]Met/Cys (700 nCi) together with RNA

encoding BMP4 (1 ng) alone or with increasing doses of RNA encoding α_1-PDX (0.05 ng – 2.5 ng). For both experiments, oocytes were cultured overnight and radiolabeled BMP4 precursor proteins and cleavage products were immunoprecipitated from clarified lysates by incubation with antibodies specific for HA (12CA5 hybridoma cell supernatant, 1:10) or myc epitope tags (9E10 hybridoma cell supernatant, 1:10) and Protein A Sepharose 4B beads as described (Degnin et al., 2004). Samples immunoprecipitated with anti-HA antibodies were deglycosylated using Peptide: N-glycosidase F (PNGase F) according to the manufacturer's instructions (New England BioLabs). Immunoprecipitated proteins were analyzed by SDS-PAGE (11% acrylamide) under non-reducing conditions and imaged by autoradiography. Radiolabeled bands were visualized with a Molecular Dynamics phosphorimager and quantified using the Macintosh IP Lab Gel program.

Western blot analysis of proteins expressed in oocytes and embryos

Oocytes were injected with appropriate RNAs and cultured overnight. Ten oocytes in each group were triturated in 100 µl of lysis buffer [50 mM Tris-HCl, pH 7.5; 150 mM NaCl; 1 mM EDTA; 1% Triton X-100; 0.1% SDS; 2.5% Igepal CA-630 (Sigma), 1x Complete Mini Protease Inhibitor Cocktail (Roche)]. Lysates were centrifuged twice in a microcentrifuge for 10 min each. Embryos were injected with RNA and cultured to the gastrula stage (stage 11) at which time fluid was aspirated and pooled from the blastocoel of 10 embryos in each group, as described (Birsoy et al., 2005). Proteins were deglycosylated by incubation with PNGase-F, resolved by SDS-PAGE (12% acrylamide), and transferred onto PVDF membrane. Membranes were probed with anti-myc (9E10 hybridoma cell supernatant, 1:250), anti-HA (3F10, Roche, 1:000), anti-FLAG (M2,

Sigma, 1:1000), and/or anti-α_1-AT antibodies (Calbiochem, 1:1000). Immunoreactive proteins were detected using Enhanced Chemiluminescence reagent (Pierce).

Western blot analysis of PCs in crude membrane extracts from oocytes and embryos

Oocytes and embryos were injected with appropriate RNAs and cultured overnight. Twenty oocytes or embryos were triturated in 200 µl of homogenization buffer [0.25 M sucrose; 50 mM Tris-HCl, pH 7.5; 5 mM KOAc; 5 mM MgOAc; 1x Complete Mini Protease Inhibitor Cocktail (Roche)], and lysates were centrifuged at 800g for 5 min at 4°C to remove nuclei. Supernatants were then centrifuged at 70,000 rpm for 30 min at 4°C in a TLA-100 rotor (~180,000g). Pelleted proteins were deglycosylated with PNGase F, resolved by SDS-PAGE (8% acrylamide), and transferred onto PVDF membrane. Membranes were probed with anti-FLAG antibodies (M2, Sigma, 1:1000). Immunoreactive proteins were detected using Enhanced Chemiluminescence reagent (Pierce).

Northern blot analysis

RNA was extracted from oocytes or embryos and Northern blots hybridized with antisense riboprobes as described previously (Christian and Moon, 1993).

Poly(A)-tail assay

The Linkage-Mediated Poly(A)-Tail assay was performed as described (Salles et al., 1999). Briefly, total RNA was extracted from oocytes or embryos as described (Christian and Moon, 1993), and 250 ng of RNA was incubated with phosphorylated oligo$(dT)_{12\text{-}18}$ at 42°C for 30 min in the presence of T4 DNA ligase. Oligo(dT)-linker primer [5′-GAGAGAACTAGTCTCGAG$(T)_{18}$] was added to the reaction, which was then incubated at 14°C for 2 h before addition of AMV-Reverse Transcriptase and further

incubation for 1 h at 42°C. The resulting cDNAs were subjected to PCR amplification using *Furin*- (5′-TATTGCATTGCACAGAGACATATC) or *Pc7*-specific primers (5′-CCTATTGGACCAACTGGGATG), which are targeted 314 and 241 nucleotides, respectively, upstream of the 3′ end of their respective mRNAs, together with a primer specific to the oligo(dT)-linker (5′-GAGAGAACTAGTCTCGAGT), or together with primers complementary to the extreme 3′ end of *Furin* (5′-CTATTCAATTGTATATCCACATCC) or *Pc7* transcripts (5′-CAGGTTTGCCTCAGTTTCTAGG), respectively. The following PCR conditions were used: 94°C for 5 min, followed by 30 cycles at 94°C for 30 sec; 60°C for 30 sec; and 72°C for 1 min, followed by incubation at 72°C for 7 min. PCR products were separated by agarose gel electrophoresis, and Southern blots of PCR products were hybridized with radiolabeled cDNA probes specific for the 3′ untranslated region of *Furin* or *Pc7* as described (Tian et al., 1999).

ACKNOWLEDGEMENTS

We thank Richard Leduc for the α_1-EK4 cDNA and for helpful discussions and T. O'Hare, M. Wong and D. Goldman for critical reading of the mansucript. This work was supported in part by grants from the Shriners Hospitals for Children (#8530) and NIH (RO1HD037976) to JLC and by a predoctoral fellowship from the American Heart Association to SMN.

Chapter 4

Discussion and Conclusions

I. SUMMARY

BMP4 is a member of the TGFβ family of cell signaling molecules. It is essential for ventral patterning of all germ layers, as well as for development and maintenance of multiple organ systems (reviewed in Hogan, 1996). As with other members of this family, BMP4 is generated as an inactive precursor protein that must be cleaved in order to generate an active signaling ligand (Aono et al., 1995). Unlike most other BMPs, though, BMP4 is cleaved twice – first adjacent to the mature ligand (S1) then upstream within the prodomain (S2) (Cui et al., 2001). Previous work from our lab showed that cleavage at the S1 site alone generates a noncovalently associated prodomain-mature ligand complex that can only signal at short-range because it is targeted for rapid degradation, such that little active ligand is present at steady state (Cui et al., 2001; Degnin et al., 2004). Conversely, cleavage at both the S1 and the S2 sites generates a more stable ligand, and the higher steady state levels are compatible with long-range signaling. We also showed that S2 cleavage is necessary for development and occurs in a tissue-specific manner, a potential explanation for the short- vs. long-range BMP4 signal that is observed depending on the tissue examined (Goldman et al., 2006; Sopory et al., submitted). The mechanisms regulating tissue-specific cleavage at the S2 site are unknown and are the focus of the work presented here.

One possible mechanism by which cleavage of the S2 site could be differentially regulated is tissue-specific expression of an S1 or S2 site-specific enzyme. To begin to test this idea, we first cloned and characterized the expression patterns of four candidate PCs – Furin, PACE4, PC6, and PC7 – from our animal model of choice, *Xenopus laevis* (Chapters 2, 3, and Birsoy et al., 2005). We showed that each of these PCs is broadly

expressed, from oocytes through the tailbud stage, confirming their candidacy. We next used antisense knockdown and specific α_1-PDX inhibition of these PCs to determine which are responsible for BMP4 cleavage *in vivo* and showed that Furin and PC6 function redundantly to cleave both the S1 and the S2 sites (Chapter 3). Surprisingly, an α_1-PDX resistant enzyme is also present in embryos, but not oocytes, that acts redundantly to cleave the S1 optimal, but not the S2 minimal, site. The best candidate for the α_1-PDX insensitive enzyme is PC7, which leads to several potential mechanisms for tissue-specific usage of the S2 site. One possibility is that BMP4 could be constitutively cleaved at the S1 site by PC7, which is ubiquitously expressed, resulting in a short-range signaling molecule, while BMP4 expresssed in tissues where Furin and/or PC6 are present could be cleaved at both the S1 and S2 sites, resulting in a long-range signal. Further studies defining the tissues in which the S2 site is cleaved and correlating those results with expression patterns of each of the PCs will be necessary to test this hypothesis.

In addition, if PC7 is the α_1-PDX insensitive enzyme, the data presented here would suggest that its activity is developmentally regulated, since it is present/active in embryos but not oocytes. Initial characterization of polyadenylation and proteolytic activation did not elucidate a mechanism for differential regulation, but several other possibilities exist and are discussed below.

II. FUTURE STUDIES TO ELUCIDATE WHETHER PC7 IS THE α_1-PDX INSENSITIVE ENZYME THAT CLEAVES BMP4

The data presented in Chapter 3 suggest that if PC7 is the α_1-PDX insensitive enzyme that redundantly cleaves BMP4 at the S1 site in embryos, it may be developmentally regulated. It would be interesting to tease apart at what point this regulation occurs. First, though, it would be important to directly test whether PC7 is active in embryos but not oocytes and can account for the activity we detect. This could be done by immunoprecipitating epitope-tagged Furin and PC7 from oocytes and embryos and testing the ability of these proteins to cleave BMP4 *in vitro*. Alternatively, the host transfer technique could be used to deplete *Pc7* from oocytes, inject embryos derived from these oocytes with RNAs encoding BMP4 and α_1-PDX, and then test whether the S1 site of BMP4 is cleaved. If either of these techniques rule out PC7 as the enzyme of interest, multiple alternative explanations could be explored, as described below. If the experiments support the involvement of PC7, experiments could be undertaken to determine how this enzyme is regulted.

II.A. Alternatives to PC7 as the α_1-PDX insensitive enzyme

If the α_1-PDX insensitive enzyme is not PC7, there are multiple alternative explanations. We originally hypothesized that differences in cleavage kinetics between and optimal and a minimal site might account for the α_1-PDX resistance of S1 cleavage, the logic being that if Furin and PC6 cleave an optimal site more efficiently than a minimal site, it might be more difficult to block that cleavage. If this were the case, however, we would expect to see a dose dependent inhibition of S2, and then S1 cleavage in oocytes, but we do not. Even at the lowest doses of α_1-PDX that produce detectable

inhibition, cleavage of both sites is blocked in oocytes. Conversely, even at the highest doses of α_1-PDX in embryos, which most certainly surpass levels of endogenous Furin and PC6, cleavage of the S1 site persists. Since α_1-PDX acts as an irreversible inhibitor with an SI of 2 for Furin and 8 for PC6, it seems unlikely that we would be unable to completely inhibit the endogenous covertases that are targeted by this serpin (Jean et al., 1998).

We cannot absolutely rule out PACE4 as the α_1-PDX resistant enzyme, but it is an unlikely candidate. Although PACE4 is less sensitive to inhibition by α_1-PDX than are Furin or PC6, several reports have shown that it can be inhibited when overexpressed, and it is capable of cleaving both optimal and minimal sites of BMP4 (Cui et al., 1998; Jean et al., 1998; Tsuji et al., 1999a; Tsuji et al., 2002). *In vivo* developmental studies, reviewed in the introduction, do not support a role for PACE4 in cleaving BMP4. Instead, biochemical and genetic studies suggest that Nodal, but not BMP4, is an important substrate for PACE4. Even in a mouse missing both PACE4 and Furin, BMP4 protein is still cleaved, suggesting that another PC is able to compensate (Beck et al., 2002).

Alternatively, a non-PC enzyme could potentially cleave the optimal site of BMP4. HIV-1 gp160 is a known target of PCs and is cleaved following an optimal (-R-E-K-R-) motif (Hallenberger et al., 1992). There is some evidence, though, that it can be cleaved at this same site by alternate, Ca^{2+}-independent, serine proteases – Viral Envelope glycoprotein Maturase (VEM) and VEM-Like Protease (VLP) (Bendjennat et al., 2001; Kido et al., 1993). VEM and VLP have yet to be cloned, though, so there is still much to be learned about these potential poly-basic site endoproteases.

II.B. Developmental regulation of PC7

If future studies confirm that PC7 does cleave the S1 site of BMP4 in embryos, but not oocytes, then it will be important to understand how its expression or activity is developmentally regulated. Northern analysis demonstrated that *Pc7* mRNA is already present in oocytes, indicating that it is maternally expressed and regulation must therefore be post-transcriptional. There are several post-trascriptional processes where this could occur, including mRNA processing (addition of the m^7G cap structure to the 5′ end of the nascent mRNA, removal of intronic sequences, and addition of the poly(A) tail), export from the nucleus, mRNA decay, translation, proteolytic activation, and protein stability (reviewed in Lackner and Bahler, 2008). An assay measuring the length of the *Pc7* poly(A) tail revealed no difference in oocytes vs. embryos, and Northern analysis demonstrated that maternal *Pc7* transcripts are stable up to and through mid blastula transition (when *de novo* transcription begins in the *Xenopus* embryo), indicating that regulation is likely at the level of protein synthesis, activation, or stability.

The most definitive test of whether PC7 expression is regulated at the level of protein synthesis is to generate antibodies that recognize endogenous PC7 and assay for its presence by immunostaining and/or Western blot. If PC7 protein is present in embryos but not oocytes, then we can further tease apart the step at which translational regulation occurs. If antibodies cannot be developed, several alternative assays for translation exist as discussed below.

Protein synthesis occurs in three main steps – initiation, elongation, and termination – each of which can be regulated via various mechanisms (reviewed in Lackner and Bahler, 2008). Translation initiation is thought to be the rate-limiting step in

most situations, and more than 25 proteins are important for proper initiation. It is at this step, therefore, that most regulation takes place, generally involving initiation factors, ribosomes, and/or interactions between RNA binding proteins (RBPs) and the mRNA transcript itself. Once translation has been initiated, the transcript becomes associated with multiple ribosomal complexes, referred to as a polysome. As these complexes are very large, sucrose gradient centrifugation can be used to separate mRNAs associated with polysomes vs. those that are not associated and therefore not being translated. In this way, one could determine whether *Pc7* is translated in oocytes, if the simpler alternative, to make antibodies that recognize PC7, is not successful. Alternatively, a technique called RIP (RBP immunoprecipitation) was developed relatively recently that examines interactions between a specific RBP and mRNAs. This involves immunoprecipitation of an mRNA binding protein followed by RNA purification and detection via Northern analysis or RT-PCR. If an antibody could be identified that recognizes an endogenous *Xenopus* ribosomal protein, or if a tagged protein could be introduced, this method might reveal the translational status of *Pc7*.

If PC7 protein is being synthesized, it could be regulated at the level of proteolytic activation. As described in detail in Chapter 1, PCs are generated as inactive precursor zymogens that undergo autocatalytic endoproteolytic processing in order to generate active enzyme (reviewed in Seidah et al., 2008). Most of the PCs undergo sequential cleavages in order to dissociate from their autoinhibitory prodomains. PC7, though, does not have any upstream sequences resembling a secondary cleavage motif. As for the other PCs, autoproteolytic cleavage of PC7 is required for exit from the ER, but it is not clear if the prodomain remains associated or how this intramolecular

inhibition is released (van de Loo et al., 1997). This could be a point of regulation that differs in oocytes and embryos, such that the mature PC7 detected in oocytes remains in the inhibited state. It could be informative to perform co-immunoprecipitation studies comparing the prodomain-mature enzyme association of wild-type PC7 with PC7 retained in the ER (via a KDEL retention motif), misdirected to the PC6B-associated post-TGN compartment (using the AC2 motif), or secreted (by removing its transmembrane domain and cytoplasmic tail). These and other experiments could provide insight into the mechanism of PC7 activation.

It is also possible that PC7 requires a chaperone for proper activation. Precedence for the necessity of a chaperone in PC activation is seen with PC2, which requires its co-activator 7B2 (Mbikay et al., 2001 and references therein). Without 7B2, PC2 can fold, exit the ER, receive complex carbohydrate modifications in the TGN, and become cleaved. However, the mature enzyme created under this condition is inactive (Muller et al., 1997). If PC2 and 7B2 are both present, 7B2 interacts with PC2 in the ER and traffics with it to the TGN where proteolysis results in active PC2 enzyme capable of cleaving substrates in trans. Mature PC2 proteins generated in the presence or absence of 7B2 appear the same when analyzed via reducing SDS-PAGE, but it was recently shown that 7B2 is necessary to maintain an activation-competent folding conformation of pro-PC2 and to prevent non-productive aggregation (Lee and Lindberg, 2008). The authors hypothesized that without 7B2, pro-PC2 partially unfolds and exposes the primary cleavage site for proteolysis by other PCs. Though this protein is cleaved at the correct site, it remains unfolded and is therefore inactive. If PC7 also requires a chaperone, which is absent in oocytes, then it is possible that the exogenously expressed mature PC7

protein generated in oocytes is inactive. The activation status might be detectable by using oocyte lysates to cleave a fluorogenic peptide (pyr-GRTKR-methylcoumarinamide), a standard assay used to detect PC activity *in vitro* or in cell culture. If the mature PC7 protein in oocytes is not active, experiments could be undertaken to identify a potential chaperone via co-immuniprecipitation followed by mass spectrometry or via a candidate approach.

7B2 is a member of the granin family, so association with other proteins from this family could be tested. Seven members have been identified so far – chromogranin A (CgA) and secretogranins (Sg) I-VI, 7B2 being SgV (reviewed in Taupenot et al., 2003). Granins are a group of acidic proteins broadly expressed in neuroendocrine cells that tends to aggregate at acidic pH in the presence of calcium, suggesting that they play an important role in the formation of dense core secretory granules within the regulated secretory pathway. More recently, though, researchers have begun to explore other roles for these proteins. For example, Holling et al showed that SgII, SgIII, and 7B2 are expressed maternally and during early embryogenesis in Xenopus (expression of other granins was not explored), and Stich and colleagues reported an upregulation of SgII in human mesenchymal stem cells in response to chemotactic stimulus (Holling et al., 2000; Stich et al., 2009). These and other studies suggest much broader roles and expression patterns for granin family members than was originally thought. Also, a 36-residue portion of 7B2 consisting of three motifs – a C-terminal proline-rich motif, two cysteines that form a disulfide bridge, and an N-terminal α-helix with two conserved hydrophobic residues – was shown to be necessary and sufficient for interaction with PC2, and this interaction occurs mainly with the catalytic domain, which is the most highly conserved

domain between PCs (Muller et al., 1999). A bioinformatics approach using this information might be able to identify candidate PC7 chaperones.

If analysis of fluorogenic peptide cleavage reveals that the exogenous mature PC7 in oocytes is active, it is still possible that endogenous protein levels are insufficient to cleave the S1 site of BMP4 appreciably due to mislocalization and/or degradation. PC7 has been shown to be palmitoylated at two cysteines within its cytoplasmic tail, a modification that has been shown to affect the localization and/or stabilization of proteins via various mechanisms (reviewed in Linder and Deschenes, 2007; van de Loo et al., 2000). To test whether differential palmitoylation is a means by which PC7 is developmentally regulated, its palmitoylation status in oocytes could be compared to that of embryos. In addition, palmitoylation of two other type I transmembrane proteins was demonstrated to be necessary for their retrieval from late endosomes via interaction with the retromer complex, thereby preventing lysosomal degradation (McCormick et al., 2008). Retromer components could be depleted (most feasibly in cell culture) to test the influence of this complex on the half-life of PC7.

Taken together, the studies described above would yield valuable insight into the general, as well as the potentially developmental, regulation of PC7 activity.

III. EVOLUTION OF PC7 AND DUAL CLEAVAGE OF BMP2/BMP4/DPP SUBSTRATES

The number and optimal vs. minimal arrangement of BMP2/BMP4/DPP cleavage sites have not been well conserved throughout evolution (Kunnapuu et al., 2009). Cnidaria have one optimal site, vertebrates and echinoderms have an S1 optimal and an S2 minimal, cephalocordates, urochordates, hemichordates, and some arthropods have

two optimal sites, and Diptera and Lepidoptera have one minimal site between two optimal sites. Cleavage in all of these cases has not been characterized, though, so it is not known if all of these sites are utilized *in vivo*.

PC7 is the vertebrate PC most similar to convertases in lower organisms, but its requirement for an optimal recognition sequence is not a conserved characteristic for the other proteins in this group (Figure 4-1). The recognition sequences for Nv_PC, Sp_PC, and Bf_PC (all predicted proteins with similarity to PCs) have not been explored, but Dm_Furin2 was shown to be capapable of cleaving the minimial site of DPP (Kunnapuu et al., 2009). It is therefore unlikely that the proposed role of PC7 as an optimal site protease required for dual cleavage of BMP4 is evolutionarily conserved before vertebrates.

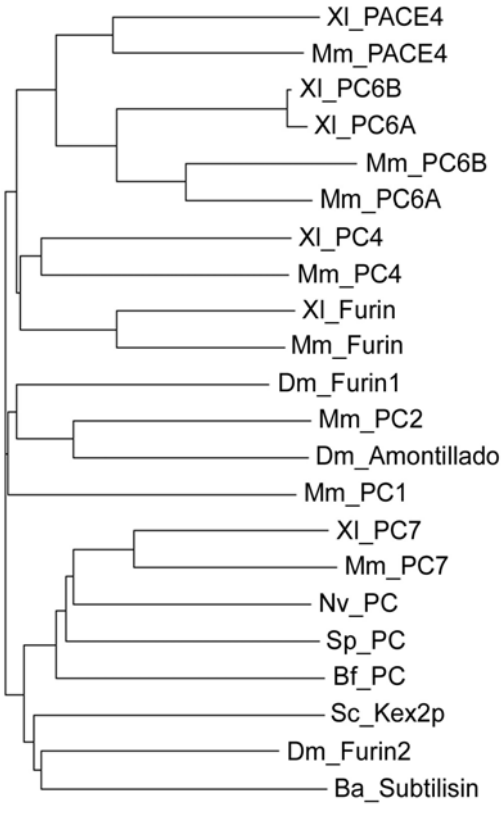

Figure 4-1. Phylogenetic tree of PCs. Tree was constructed based protein sequences using the T-Coffee alignment and the TREECON phylogenetic tree construction freeware programs (http://www.tcoffee.org/; Van de Peer and De Wachter, 1994). Sequences are from genbank accession numbers: Ba_Subtilisin, YP_001420645; Bf_PC, XM_002209274; Dm_Amontillado, NM_057970; Dm_Furin1, NM_080146; Dm_Furin2, NM_206763; Mm_Furin, NM_001081454; Mm_PACE4, NM_01104; Mm_PC1, NM_013628; Mm_PC2, NM_008792; Mm_PC4, NM_008793; Mm_PC6A, NM_001163144; Mm_PC6B, D17583; Mm_PC7, NM_008794; Nv_PC, XM_001638615; Sc_Kex2p, M24201; Sp_PC, XM_001196759; Xl_Furin, NM_001087807; Xl_PACE4, AY685228; Xl_PC4, BC170270; Xl_PC6A, AY901985; Xl_PC6B, AY901986; Xl_PC7, NP_001090019. Species are: Ba, *Bacillus amyloliquefaciens* FZB4; Bf, *Branchiostoma floridae* (Florida lancelet); Dm, *Drosophila melanogaster* (fruit fly); Mm, *Mus musculus* (house mouse); Nv, *Nematostella vectensis* (starlet sea anemone); Sc, *Saccharomyces cerevisiae* (baker's yeast); Sp, *Strongylocentrotus purpuratus* (purple sea urchin); Xl, *Xenopus laevis* (African clawed frog).

IV. POTENTIAL MECHANISMS TO REGULATE TISSUE-SPECIFIC CLEAVAGE OF BMP4

The studies reported here were intended to test potential models by which the S2 site of BMP4 is cleaved in a tissue-specific manner. As described in chapter 3, my results rule out a model in which tissue-specific expression of an S2 site-specific protease regulates this process, since Furin and PC6 were shown to function redundantly as the major endogenous convertases for both the S1 and the S2 site. My results are consistent with the possibility that the S1 site is constitutively cleaved in all tissues by a combination of Furin, PC6 and PC7, and that the S2 sites is cleaved in all tissues except for those that lack active PC6 and Furin. As described above, further studies are required to definitively prove that PC7 cleaves the S1 site of BMP4. Closer examination of the *Pc7* null mice, or combinatorial knockouts with potentially compensatory PCs, may define more clearly the role of PC7 in development in general and in BMP4 cleavage in particular. In addition, future studies will be required to directly analyze cleavage of the S1 and/or S2 site of BMP4 in various tissues, and correlate that information with detailed analysis of the expression patterns of each PC. Antibodies that recognize endogenous BMP4 are not available, so we generated a knock-in mouse in which wildtype BMP4 has epitope tags in the prodomain and mature domain. This mouse will be invaluable for future studies on this topic.

V. CONCLUSIONS

Regulation of BMP4 activity is critical for normal development, and one way this is achieved is through proteolytic activation of the proBMP4 precursor protein. In addition, proteolysis of the S2 site of BMP4 appears to be regulated in a tissue-specific fashion as a means of determining short- versus long-range activity of the ligand, but the mechanism by which S2 cleavage is regulated is unknown. The studies presented herein began to test the hypothesis that expression/activation of an S2-specific enzyme is a potential mechanism. We cloned and characterized the expression of PC homologues in *Xenopus* and identified the PCs responsible for BMP4 cleavage *in vivo*. We found that PC7 is ubiquitously expressed while Furin and PC6 are more selectively expressed, and all three enzymes cleave the optimal S1 site of BMP4 while only Furin and PC6 cleave the minimal S2 site. These observations lead to the hypothesis diagramed in Figure 4-2 and described in the legend, in which BMP4 is constitutively cleaved at the S1 site by PC7, and tissue-specific expression of an S2 site enzyme (i.e. Furin and/or PC6) results in S1 and S2 cleavage of BMP4.

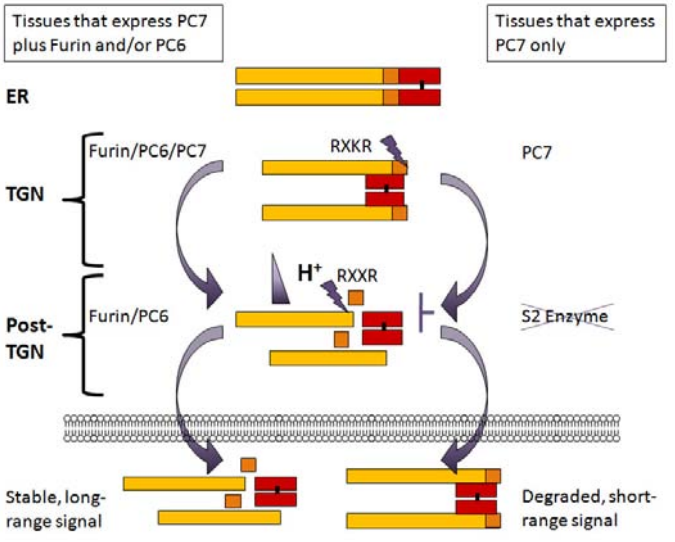

Figure 5-1. Model for tissue-specific cleavage at the S2 site of BMP4. Cleavage of the S2 site of BMP4 could be regulated by tissue-specific expression of the S2 site enzymes. In this scenario, PC7 cleaves the S1 site of BMP4 constitutively to generate the short-range signaling molecule, while coexpression of Furin or PC6 results in cleavage of BMP4 at both the S1 and S2 sites to generate the long-range signaling molecule.

Future studies will build on this information by characterizing the cleavage pattern of BMP4 in various tissues and correlating that with BMP4 trafficking and regulation of PC expression and activity. Taken together, this information will further our understanding of the intricacies of BMP4 regulation that are essential for its normal activity.

In addition, the techniques developed here could be employed for cleavage studies of other TGFβ family members. Several proteins from this family have more than one potential PC cleavage site, but in most cases it is not known if the upstream site is utilized, how its usage might be regulated, or how differential cleavage might affect protein activity. These studies would greatly enhance our knowledge of a family of proteins that are vital for life.

Appendix

Detailed Methods

I. RNA EXTRACTION FROM *XENOPUS* OOCYTES/EMBRYOS

General notes: Gloves should always be worn when working with RNA. Tubes and tips should be autoclaved, and samples should be kept on ice.

1. Homogenize embryos by pipeting up and down in 0.75-1 ml of homogenization buffer (w/ proteinase K) per 20 embryos (400 μl for 10 whole embryos/100 μl for 20 animal caps). Incubate 1 hr @ 37°C.
2. Add ½ volume phenol and ½ volume sevag (chloroform:isoamyl alcohol, 24:1). Vortex for ≥ 15 sec, and spin in microfuge 5 min @ 4°C. Transfer aqueous layer to a clean tube, avoiding material near the aqueous-organic interface. Repeat extraction once.
3. Add ammonium acetate to 0.4 M ($^{1}/_{25}$ volume 10 M). Add two volumes 100% EtOH. Leave @ -20°C for 15 min to overnight.
4. Spin in microfuge 10 min @ 4°C. Rinse pellet with 70% EtOH and air dry briefly (overdrying will make pellet difficult to resuspend).
5. Dissolve in DEPC treated water equal to at least 25% of the volume of buffer used in step 1 (100 μl/25 μl). Add an equal volume of 8 M LiCl. Leave @ -20°C overnight.
6. Spin in microfuge 20 min @ 4°C. Wash pellet with ice-cold 100% EtOH and air dry briefly. Resuspend in DEPC treated water (14 μl/7 μl).

II. NORTHERN ANALYSIS

Template preparation

1. Cut 20 μg template DNA overnight with the appropriate enzyme in a reaction volume of 100 μl.
2. Run 5 μl of the rection on an agarose gel to verify that cutting is complete.
3. Extract once with phenol:sevag, 1:1 (as described in I.2), once with an equal volume sevag.
4. Add ammonium acetate to 0.4 M ($^1/_{25}$ volume 10 M) and two volumes 100% EtOH. Leave @ -20°C ≥ 15 min, spin in microfuge 10 min @ 4°C. Rinse pellet with 70% EtOH, vacuum dry, and resuspend in 36 μl DEPC treated water (~0.5 μg/μl).

Northern probe synthesis

5. Add the following components, in the order shown, to a sterile microcentrifuge tube at room temperature (RT; DNA template might precipitate if mixed on ice), and incubate 1 hr @ 37°C:

   0.8 μl DEPC treated dH_2O
   2 μl 10x transcription buffer
   2 μl 100 mM DTT
   0.8 μl RNasin
   4 μl 2.5 mM ATP, GTP, UTP (mix equal volumes 10 mM ATP, GTP, UTP, and DEPC treated dH_2O, store @ -20°C)
   2.4 μl 100 μM CTP
   2 μl 0.5 μg/μl linearized template
   5 μl 10 μCi/μl α-^{32}P CTP (50 μCi total)
   1 μl RNA polymerase

6. Add 1 μl RQ1 DNase, and incubate 15 min @ 37°C. Meanwhile, drain a Sephadex G-50 column by spinning in the IEC centrifuge, 2 min at setting 4.
7. Add 30 μl DEPC treated water, apply solution to the center of the column, and spin 4 min at setting 4. Monitor the radioactivity remaining on the column and that in the eluate using a Geiger counter (typically at least 50% of the counts are in the eluate).
8. Count 1 μl and calculate cpm.

Sample preparation and Northern blot

9. Mix agarose, dH_2O, and MOPS buffer in a flask and microwave until the agarose has dissolved. Cool by swirling flask under tap water, then add formaldehyde in fume hood. Pour gel in hood and cover with plastic wrap or buffer once it has set.

50 ml 1% gel:	150 ml 1% gel:
36 ml dH_2O	108.75 ml dH_2O
5 ml 10x MOPS buffer	15 ml 10x MOPS buffer
0.5 g agarose	1.5 g agarose
8.75 ml 37% formaldehyde	26.25 ml 37% formaldehyde

10. Add 23 μl sample buffer to 6.7 μl RNA (typically 10-20 μg of total RNA or 1-5 μg of poly(A)$^+$ RNA dissolved in DEPC treated dH_2O), heat 5 min @ 60°C, immediately transfer to ice for 2 min. Add 1 μl dye (w/ EtBr) and load gel.
11. Run gel ~80 V, using 1x MOPS for running buffer, until the lower dye has run ½ to $^2/_3$ the legth of the gel.
12. Soak gel 30 min in 20x SSC, and set up transfer (Figure A-1). Blot overnight onto nylon membrane using 10x SSC as the transfer buffer.

13. The next morning, mark wells using a VWR marker. Rinse membrane 10 min in 2x SSC, air dry, and UV-crosslink using a Stratalinker. The filter can now be stored @ RT between filter paper until hybiridization.

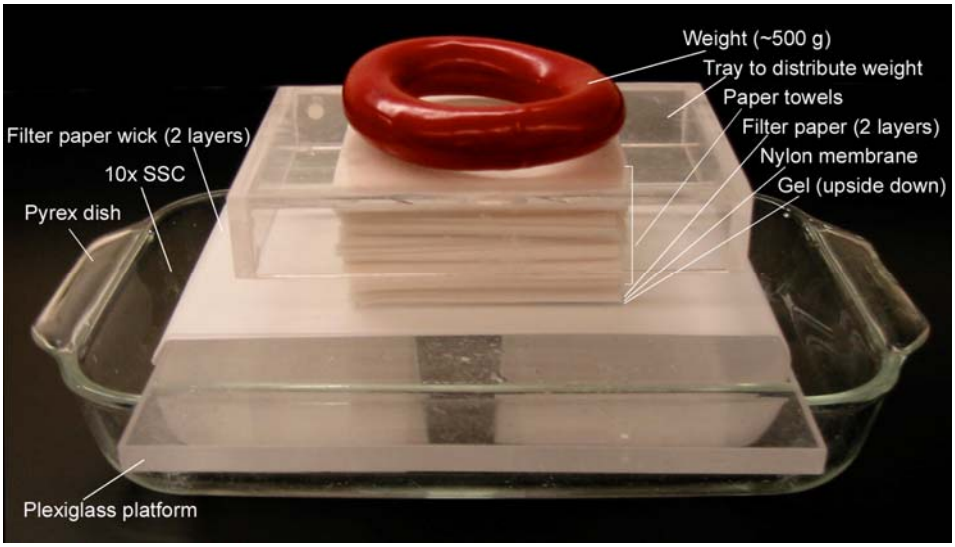

Figure A-1. Northern transfer setup. Assemble Pyrex dish with plexiglass platform and filter paper wick as shown. Wet wick with 10x SSC. Layer gel (face down), nylon membrane (pre-wet with dH_2O then 10x SSC), two pieces filter paper (pre-wet with 10x SSC), and paper towels. Center tray and weight on top, fill reservoir with 10x SSC, and cover entire setup with plastic wrap to minimize evaporation.

Northern blot hybridization

14. Using forceps, transfer the membrane to a hybridization tube, rinse with 2x SSC, drain, and add 10 ml hybridization solution. Incubate in hybridization oven 2-4 hr @ 65°C.
15. Add 1-5 x 10^6 cpm of probe per ml of hybridization solution (usually 2 x 10^7 cpm in 10 ml). Incubate O/N @ 65°C.
16. The next morning, drain the probe into a screw-cap tube and store @ -20°C for later use. Rinse membrane w/ ~10 ml rinse solution at RT, count 10 µl, and calculate radioactive waste disposal. Repeat rinse.

17. Wash the membrane in ~50 ml wash solution two to four times for 15-30 min each @ 65°C until the poured off solution is at background as monitored with a Geiger counter.
18. Wrap membrane in plastic wrap and expose to film or phosphoscreen.

III. RIBONUCLEASE PROTECTION ASSAY

Template preparation

1. Cut 20 μg template DNA, check, and clean up (as described in II.1-4). Use a restriction enzyme that leaves a 5′ overhang and yields an antisense probe of 200-400 nucleotides.

Probe synthesis

2. Add the following components, in the order shown, to a sterile 0.5 ml microcentrifuge tube @ RT, and incubate 1 hr @ 37°C:

   1 μl 10x transcription buffer
   1 μl 100 mM DTT
   0.4 μl RNasin
   2 μl 2.5 mM ATP, GTP, UTP (mix equal volumes 10 mM ATP, GTP, UTP, and DEPC treated dH_2O, store @ -20°C)
   1.2 μl 100 μM CTP
   1 μl 0.5 μg/μl linearized template
   2.5 μl 10 μCi/μl α-^{32}P CTP (25 μCi total)
   1 μl RNA polymerase

3. Add 1 μl RQ1 DNase, and incubate 15 min @ 37°C. Meanwhile, drain a Sephadex G-50 column by spinning in the IEC centrifuge, 2 min at setting 4.

4. Apply solution to the center of the column, and spin 4 min at setting 4. Monitor the radioactivity remaining on the column and that in the eluate using a Geiger counter (typically at least 50% of the counts are in the eluate).
5. Add 100 µl DEPC treated dH_2O to the eluate, mix, and count 1 µl. Dilute the probe with DEPC treated dH_2O to achieve ~$5x10^4$ cpm/µl.

Sample preparation and analysis

6. Ethanol precipitate 10-50 µg of total RNA (as described in I.3-6). Always include one sample of 10 µg yeast tRNA per probe as a negative control. Resuspend samples completely in 3 µl DEPC treated dH_2O.
7. Add 28 µl of the following mix to each RNA sample:

Per sample:	15 samples:
24 µl deionized formamide	372 µl deionized formamide
3 µl 10x RPA salts	46.5 µl 10x RPA salts
1 µl probe ($5x10^4$ cpm)	15.5 µl probe ($5x10^4$ cpm)

8. Mix and centrifuge briefly. Heat 5 min @ 65°C, then O/N @ 45°C in the circulating water bath.
9. Add 300 µl of the following mix to each sample and vortex. Incubate 30 min @ 37°C:

Up to 15 samples:

50 µl 1 M Tris, pH 7.5
50 µl 0.5 M EDTA, pH 8.0
300 µl 5 M NaCl
20 µl RNase A (10 mg/ml; 40 µg/ml final)
7-10 µl (10 µg) RNase T1 (2 µg/ml final)
4.57 ml dH_2O

10. Add 10 μl 20% SDS and 4 μl 25 mg/ml Proteinase K to each sample and incubate 15 min @ 37°C. In the meantime, pour a 20 cm 5% Urea/Acrylamide gel:

    25 g Urea (get into solution using stir plate)
    4.2 ml 30% Acrylamide/bis solution
    10 ml 5x TBE
    dH_2O to 25 ml
    200 μl 10% Ammonium persulfate and 10 μl TEMED (immediately before pouring)

11. Add 150 μl each phenol and sevag, vortex, spin 5 min. Remove ONLY 320 μl of each supernatant to a new tube which contains 10 μg of yeast tRNA. Add 600 μl of 100% EtOH (do NOT add salt). Incubate ≥ 15 min @ -80°C. In the meantime, rinse gel wells and prerun for 30 min @ 22 milliamps.
12. Spin samples 10 min, rinse pellets with 70% EtOH, and vacuum dry. Resuspend pellets in 5 μl RPA sample buffer. Also dilute a portion of each probe to 500 cpm/μl in RPA sample buffer. Heat 5 min @ 95-100°C, place on ice.
13. Load samples, including one lane with 500-2000 cpm of probe. Run gel at 22-25 milliamps until bromophenol blue is at the bottom.

IV. ^{35}S INJECTIONS INTO *XENOPUS* OOCYTES

Day1: Surgical Removal of Oocytes

1. Obtain a frog that has not been surgerized or that has completely healed (cut is closed, sutures are gone, ~1 month between surgeries)
2. Place her in a beaker with 500 ml 0.2% tricane (inside an ice bucket w/ a weighted lid so she can't get out) for 20-30 min or until she does not respond when you pinch her foot

3. Once asleep, place her belly up on plastic side of bench paper and cover her head and legs with paper towels soaked in tricane
4. Cut a small slit in the skin then the muscle (10-15 mm)
5. Pull out several lobes of ovary (~5 ml for 1000 oocytes) and transfer to a 35 mm Tissue Culture (TC) dish containing DS.
6. Suture muscle then skin (~3 each) using square knot
7. Move frog to "Frog House" with salt water and cover her with wet paper towels to keep her moist – container should be propped so she can recover with her nostrils out of water
8. Using forceps, tear ovary tissue into smaller pieces and rinse with DS
9. Transfer oocytes to 50 ml tube containing 20 ml DS, add 200 µl liberase
10. Incubate 90 min @ RT on the nutator
    a. under treatment results in oocytes still covered with follicle cell layer; over treatment results in squishy oocytes
11. Clean tools with soap and water and rinse with EtOH; filter tricane to be reused
12. Wash liberased oocytes 2-3x with DS, then 2-3x with MBSH
13. Transfer to 35 mm TC dishes in MBSH and sort out mature, healthy oocytes
14. Incubate O/N @ 18°C in MBSH

<u>Day 2: Oocyte injections</u>

15. Make solution of capped RNA and ^{35}S-met,cys (frozen stock is 10x ^{35}S, use 20% total volume)
16. In MBSH, inject oocytes with a maximum volume of ~50 nl (use designated radioactive tray) – aim for the border of the vegetal and animal poles

17. Transfer injected oocytes to multi-well TC dish containing 800 µl MBSH, incubate O/N @ 18°C

Day 3: Protein Prep and Immunoprecipitation

18. Pipette off media and transfer to 1.5 ml MC IP tube, wash oocytes with 200 µl MBSH and add to tube containing media
19. Transfer oocytes to 1.5 ml MC tube (6-20 oocytes/tube), remove excess liquid
    - Samples can be frozen with liquid nitrogen and stored @ -80°C
20. Media:
    - Add 110 µl 10x media buffer (10% triton, 1 M NaCl) to 1 ml media

    Lysates:
    - For 6-10 oocytes, resuspend in 30 µl (60µl for 12-20 oocytes) HB + 1x protease inhibitor cocktail
    - Add 100 µl (200 µl) SDS solution
    - Incubate 30 min @ 37°C
    - Add 500 µl (1000 µl) TxSWB
    - Incubate 45 min on ice
    - Spin 10 min @ 4°C, transfer supernatant to fresh MC tube
    - Samples can be stored @ -80°C
21. Add antibody (60 µl supernatant or ~2 µg purified) to samples – can continue or incubate 2 hr-O/N on ice
22. Add 20 µl protein A beads and incubate O/N @ 4°C on rocker

Day 4: IP washes and electrophoresis

23. Spin down beads (30 sec at top speed in cold room), remove and store supernatants in -80°C freezer (they can be re-IP'd)
24. Wash beads 3x with 750 µl TxSWB w/ PMSF (shake vigorously, spin, aspirate wash)
25. Wash beads 2x with 0.1 M Tris/ 0.1 M NaCl

If deglycosylating, skip step 4 and follow "PNGase Treatment" instructions

26. Add 16 µl loading buffer (w/ β-ME if reducing), boil 5 min, ice
27. Run products on acrylamide gel (For big gels, 200 V ~3 hr or 50 V O/N; for small gels ≤ 150 V)
28. Fix gel 10-15 min, place on filter paper, dry ~2 hr, expose

PNGase/EndoH Treatment (see product insert for more details)

29. Resuspend beads in 20 µl 1x denaturation buffer (comes as 10x)
30. Incubate 10min @ 100°C (non-reducing 10x = 5% SDS)
31. Add 2.5 µl 10x G7 buffer and 2.5 µl 10% NP-40 (PNGase) / add 2.5 µl 10x G5 buffer (EndoH)
32. Spin down, add 0.5 µl PNGase/EndoH, incubate 1 hr (or more) @ 37°C
33. Add 6 µl 4x loading dye w/ β-ME (without for non-reducing), boil 5 min, load on gel

V. ANTISENSE-MEDIATED KNOCK-DOWN

1. Surgically remove and liberase treat oocytes (section IV.1-14).
2. The next day, inject oocytes with 5-10 ng phosphorothioate modified oligonucleotides. Incubate ~72 hrs @ 18°C to allow protein turnover (duration depends on half-life of targeted protein).

3. 24 hrs after injection, harvest a subset (10-20 oocytes) for RNA extraction and Northern analysis (sections I-II) to verify knock-down of the target mRNA.
4. If necessary, inject a second time and analyze results via IP (section IV.15-33) or Western analysis (section VI).

VI. WESTERN ANALYSIS OF PROTEINS FROM *XENOPUS* BLASTOCOEL FLUID AND EMBRYOS

Embryo injection

1. Dilute capped RNA in nuclease free water:
    a. BMP4 (for 5 ng inject 9.2 nl of 543 ng/μl)
2. Inject into one cell in the animal pole of 2- to 8-cell embryos
3. Culture until St. 9 in 5% Ficoll / 0.1x MBS
4. The next morning, transfer embryos to 0.1x MBS

Blastocoel fluid extraction

5. Eject oil from needle ~1/2 way, insert needle into animal pole of embryo (straight, shallow), and press "fill". Watch the needle to make sure clear fluid is entering, and stop pressing fill when white stuff (cells) enter the needle. Press "eject" to get rid of any white stuff that gets in - you don't want cells in the fluid, and they'll clog the tip.
6. Repeat this until you have blastocoel fluid from 10 embryos. You can expect ~1 μl-2.5 μl total.
7. Eject the fluid onto a piece of parafilm, and use a micropipette to transfer it to a microcentrifuge tube containing 20 μl 1x denaturation buffer on ice, proceed with deglycosylation (below).

Preparation of embryo lysates

8. Transfer the 10 depleted embryos to a separate tube on ice; remove excess MBS
9. To embryos, add 100 µl lysis buffer (10 µl/embryo) and homogenize using a micropipette
10. Spin 10 min (top speed) in a microcentrifuge @ 4°C
11. Transfer 80 µl (4/5) to a fresh tube, avoiding the yolk, and spin another 10 min
12. Transfer 64 µl (4/5) to a fresh tube

Deglycosylation

13. For each sample, add 13 µl embryo lysate (2 embryo equivalents) to 5 µl H_20 and 2 µl 10x denaturation buffer on ice
14. Incubate lysates and blastocoel fluid 10 min @ 100°C
15. Add 2.5 µl 10x G7 buffer and 2.5 µl 10% NP-40
16. Spin down, add 0.5µl PNGase, incubate 1 hr (or more) @ 37°C

SDS PAGE and Western blot

17. Add 6 µl 4x loading dye w/ β-ME to each sample, boil 5 min, load on gel (use 5 µl ladder)
18. Run acrylamide gel ~100V 1-2 hrs
19. Transfer
    - Wet PVDF membrane with MeOH, poor off, wet with transfer buffer
    - Assemble cassette in transfer buffer: white side, 3 mm sponge, blotting paper, membrane, gel, blotting paper, 6mm sponge, black side
    - Run transfer 0.2 amps 2-5 hrs or .07 amps O/N
20. Dry the blot 1 hr @ RT or 15-30 min @ 37°C

21. Wet the blot in MeOH then rinse with 1x PBS
22. Block the membrane with 5% non-fat dry milk in TBST for 1 h @ RT or O/N in the cold room
23. Remove the blocking solution and add primary antibody diluted in TBT (5-7 ml for small box, 12.5 ml for large box). Incubate 2 h @ RT or O/N in the cold room
    - Use HA (3F10, α-rat) at 1:2000
24. Remove the primary antibody (can be saved in freezer) and wash the blot 3x with TBST for 10 min ea
25. Incubate the blot for 1h @ RT with secondary antibody HRP conjugate diluted in TBT
    - Use α-rat HRP at 1:5,000
26. Wash the blot 3x with TBST for 10 min ea
27. Carry out ECL
    - Blot dry membrane
    - Mix 1:1 ECL (3 ml for small membrane)
    - Lay plastic film out flat, lay down membrane, layer ECL
    - Incubate 5 min (don't let it dry out)
    - Blot dry membrane
    - Cover in plastic (no bubbles)
    - Expose 30 sec-30 min (ECL gone after that)

VII. LINKAGE-MEDIATED POLY(A) TAIL ASSAY (LM-PAT)

cDNA synthesis

1. In two microcentrifuge tubes (one will be a no RT control), mix 250 ng total RNA and 20 ng Poly(dT)$_{12\text{-}18}$ primer with DEPC treated dH_2O in a volume of 7 µl. Heat 10 min @ 65°C, transfer to 42°C.
2. In the meantime, mix the following per reaction and pre-warm @ 42°C:

   4 µl 5x AMV-RT buffer
   1 µl 400 U/µl RNasin
   2 µl 0.1M DTT
   1 µl 10mM ea dNTP mix
   1 µl 10mM ATP
   1 µl 40 U/µl T4 DNA ligase
   3 µl DEPC dH_2O
3. Combine mix with primed RNA and incubate 30 min @ 42°C.
4. While at 42°C, add 200 ng Oligo(dT)-linker primer [5′-GAGAGAACTAGTCTCGAG(T)$_{18}$], vortex, spin, and incubate 2 hrs @ 14°C.
5. Transfer to 42°C for 2 min, add 2 µl AMV-RT (NOT to the no RT control), vortex, incubate 1 hr @ 42°C.
6. Heat inactivate RT and ligase for 20 min @ 65°C, PCR.

RT-PCR

7. Design two target-specific primers, a reverse primer that anneals just 5′ of the poly-A tail within the 3′ UTR and a forward primer that anneals ~200-300bp upstream of the reverse primer (referred to as Primer F/R). For each target there should be two sets of primers: Primer F + Primer R (no poly-A size control) and Primer F + Linker [5′-GAGAGAACTAGTCTCGAGT] (amplifies control fragment plus entire length of poly-A tail). There should also be two template controls per primer set: no template (dH_2O) and no-RT control.
8. In a PCR tube, mix the following per reaction:

   8.4 µl dH_2O
   0.4 µl 10mM dNTPs
   2 µl 10 pmol/µl Primer F
   2 µl 10 pmol/µl Primer R or Linker
   4 µl 5x Buffer
   2 µl 25mM $MgCl_2$
   1 µl Template
   0.2 µl 5U/ µl Taq DNA polymerase
9. Perform PCR, adjusting cycle number and annealing temperature as needed. A good place to start is as follows: 94°C for 5 min, followed by 30 cycles at 94°C for 30 sec; 60°C for 30 sec; and 72°C for 1 min, followed by incubation at 72°C for 7 min.

Southern probe synthesis

10. Prepare template by PCR amplification of cDNA using Primer F and Primer R (as described in section VII.8-9) followed by agarose gel electrophoresis (estimate concentration by band intensity) and purification (assume ~80% recovery) using the BIO 101 Systems GENECLEAN II Kit (Cat. #1001-400). Elute to 25 ng/µl.

11. Boil template DNA 10 min to denature and place on ice.
12. Add the following components from the Roche Random Primed DNA Labeling Kit (Cat. No. 11 004 760 001), in the order shown, to a sterile microcentrifuge tube @ RT and incubate 1 hr @ 37°C:

    25 ng DNA in 9 μl total volume, denatured
    3 μl 0.5 mM ea. AGT mix (1:1:1 ratio from tubes 2, 4, and 5)
    2 μl reaction mix (tube 6)
    5 μl 10 μCi/μl α-^{32}P CTP (50 μCi total)
    1 μl Klenow enzyme (tube 7)

13. Add 30 μl dH_2O, and incubate apply to the center of a drained Sephadex G-50 column (spun in the IEC centrifuge, 2 min at setting 4), spin 4 min at setting 4.
14. Monitor the radioactivity remaining on the column and that in the eluate using a Geiger counter (typically at least 50% of the counts are in the eluate), and count 1 μl.

<u>Southern blot preparation and hybridization</u>

15. Pour agarose gel just as you would for any DNA sample (probe binds to ladder: 400, 500, and 1600bp)
16. Load PCR products (all for Primer F + Linker, $^{1}/_{10}^{th}$ for Primer F + Primer R) with EtBr in the loading dye and run until desired length has been reached.
17. Photograph gel with ruler for later comparison (you may not see a band for Primer F + Linker samples). Place gel in dish with about 2-3 gel volumes of 0.25M HCl and rock 30 min @ RT. Loading dye should change color.
18. Pour off HCl and rinse w/ DI water. Add 2-3 gel volumes of denaturation solution and rock for another 20 min. Loading dye should change color again.

19. Pour off denaturation solution and rinse with dH_2O. Replace with 2-3 gel volumes of neutralization solution and rock for 20 min. Pour off and replace with fresh neutralization solution and rock for another 20 min.
20. Soak gel briefly in 20x SSC and soak nylon membrane briefly in dH_2O then 20x SSC. Set up standard transfer apparatus just as you would a Northern (Figure A-1), but use 20x SSC as the transfer buffer. Transfer O/N.
21. The next morning, mark wells using a VWR marker. Rinse membrane 10 min in 2x SSC, air dry, and UV-crosslink using a Stratalinker. The filter can now be stored @ RT between filter paper until hybiridization
22. Soak membrane in 6x SSC and place in a hybridization tube DNA side facing in. Add 10 ml hybridization solution and pre-hyb for 2-5 hrs @ 42°C.
23. Boil DNA probe ($1\text{-}5x10^7$ cpm) for 5-10 min, ice, and add probe to hybridization tube. Incubate in hyb oven O/N @ 42°C.
24. The next morning, drain the probe into a screw-cap tube and store @ -20°C for later use. Rinse membrane w/ ~10 ml rinse solution at RT, count 10 µl, and calculate radioactive waste disposal. Repeat rinse.
25. Wash the membrane in ~50 ml wash solution two to four times for 15-30 min each @ 42°C until the poured off solution is at background as monitored with a Geiger counter.
26. Wrap membrane in plastic wrap and expose to film or phosphoscreen.

VIII. SOLUTIONS

RNA Homogenization Buffer:	50 ml:
50 mM NaCl	0.5 ml 5 M NaCl
50 mM Tris-HCl, pH 7.5	2.5 ml 1 M Tris-HCl
5 mM EDTA, pH 8.0	0.5 ml 0.5 M EDTA
0.5% SDS	1.25 ml 20% SDS
	45.25 ml DEPC treated dH_2O

Add 8 μl 25 mg/ml proteinase K per ml of buffer immediately before each use.

RNA Sample Buffer:	1 ml:
	642 μl deionized formamide
	229 μl 37% formaldehyde
	128 μl 10x MOPS

RNA Loading Dye:	1 ml:
	40 μl 10% Bromophenol blue
	40 μl 10% Xylene cyanol
	10 μl 37% Formaldehyde
	500 μl 100% Glycerol
	210 μl 10x DEPC treated dH_2O
	200 μl 10 mg/ml EtBr (optional)

Northern Hybridization Solution:	50 ml:
50% Formamide	5 ml Formamide
50 mM Phosphate buffer, pH 6.8	2.5 ml 1 M Phosphate buffer
0.8 M NaCl	8 ml 5 M NaCl
1 mM EDTA, pH 8.0	100 μl 0.5 M EDTA
2.5x Denhardt's solution	1.25ml 100x Denhardt's solution
400 μg/ml Sonicated herring sperm DNA	(add fresh)
	2.23 ml DEPC treated dH_2O

Before use, boil sperm DNA 5 min, place on ice, add 440 μl per 10 ml buffer

Rinse Solution:	500 ml:
2x SSC	50 ml 20x SSC
0.5% SDS	12.5 ml 20% SDS
	437.5 ml dH_2O

Wash Solution:	1 L:
0.2x SSC	10 ml 20x SSC
0.5% SDS	25 ml 20% SDS
	965 ml dH_2O

10x RPA Salts:	50 ml:
400 mM PIPES, pH 7.4	40 ml 0.5 M PIPES
4 M NaCl	11.7 g NaCl
10 mM EDTA, pH8.0	1 ml 0.5 M EDTA
	DEPC treated dH_2O to 50 ml

RPA Sample Buffer:	1 ml:
88% Formamide	880 µl deionized formamide
10 mM EDTA, pH8.0	20 µl 0.5 M EDTA
1 mg/ml Xylene cyanol	10 µl 10% Xylene cyanol
1 mg/ml Bromophenol blue	10 µl 10% Bromophenol blue
	80 µl DEPC treated dH_2O

DS (filter sterilize):	1 L 20x Partial:
82.5 mM NaCl	96.43 g NaCl
2.0 mM KCl	2.98 g KCl
1.0 mM $MgCl_2$	203.31 g $MgCl_2 \cdot 6H_2O$
5.0 mM HEPES-Hemi Na, pH 7.5	

For 1L: add 50 ml 20x & 1.25 g HEPES, sterilize w/ 0.2 µM filter, store in cold room

Liberase (Blendzyme 3, Roche Cat. No. 1 814 184, 70 mg):

Add 10 ml sterile dH_2O, reconstitute 30 min on ice, aliquot 200 µl/tube, store @ -20°C.

MBSH (filter sterilize):	1 L 20x Partial:
88.0 mM NaCl	102.85 g NaCl
1.0 mM KCl	1.49 g KCl
0.33 mM $Ca(NO_3)_2 \cdot 4H_2O$	1.56 g $Ca(NO_3)_2 \cdot 4H_2O$
0.41 mM $CaCl_2 \cdot 2H_2O$	
0.82 mM $MgSO_4$	
2.4 mM $NaHCO_3$	
10.0 mM HEPES-Hemi Na, pH 7.5-7.55	
250 mg/L Amikacin	

For 1 L: add 50 ml 20x, 0.82 ml 1 M $MgSO_4$, 4.8 ml 0.5 M $NaHCO_3$, 2.49 g HEPES, sterilize w/ 0.2 μM filter, add 250 mg Amikacin, store in cold room

HB Buffer (filter sterilize):	50 ml:
0.25 M Sucrose	4.3 g Sucrose
50 mM Tris-HCl, pH 7.5	2.5 ml 1 M Tris
5 mM KOAc, pH 7.5	250 μl 1 M KOAc, pH 7.5
5 mM MgOAc, pH 7.5	250 μl 1 M MgOAc
	dH_2O to 50 ml

SDS Solution:	50 ml:
1% SDS	2.5 ml 20% SDS
0.1M Tris-HCL, pH 8.9	5.0 ml 1M Tris
	42.5 ml dH_2O

TxSWB:	500 ml:
1% Triton	25 ml 20% Triton X-100
0.1 M NaCl	10 ml 5 M NaCl
0.1 M Tris, pH 8.0	50 ml 1 M Tris
10 mM EDTA	10 ml 500 mM EDTA
	405 ml dH_2O
<u>fresh</u> 0.1 mM PMSF (isopropanol)	5 μl 20 0mM PMSF in 10 ml

7x Protease Inhibitors:

One tablet in 1.5 ml TxSWB buffer, store @ -20°C

Fixer:	500 ml:
15% Methanol	75.0 ml Methanol
7.5% Acetic Acid	37.5 ml Acetic Acid
	387.5 ml dH_2O

4x Loading Dye:	10 ml:
200mM Tris-Hcl, pH 6.8	2 ml 1M Tris
8% SDS	4 ml 20% SDS
0.4% Bromphenol Blue	0.04 g BPB
40% Glycerol	4 ml Glycerol

For reducing, add $1/20^{th}$ volume β-ME (14.4 M) before use

Lysis Buffer:	50 ml:
	2.5 ml 1M Tris pH 7.5
	1.5 ml 5M NaCl
	100 µl 0.5M EDTA
	500 µl Triton X-100
	500 µl 10% SDS
	1.25 ml IGEPAL (NP-40)

TBST:	500 ml:
10 mM Tris-Cl, pH7.2-7.5	5 ml 1M Tris
0.9% NaCl	4.5 g NaCl
0.1% Tween 20	5 ml 10% Tween

Blocking Solution:

TBST w/ 5% non-fat dried milk	1g = 1 ml

TBT:	100 ml:
TBST w/ 0.2% BSA	0.2 g BSA

1:2000 = 1 µl Ab in 2 ml TBT

Southern Hybridization Solution:	50 ml:
50% Formamide	5 ml Formamide
6x SSC	2.5 ml 1 M Phosphate buffer
0.8 M NaCl	8 ml 5 M NaCl
1 mM EDTA, pH 8.0	100 µl 0.5 M EDTA
5x Denhardt's solution	1.25ml 100x Denhardt's solution
400 µg/ml Sonicated herring sperm DNA	(add fresh)
	2.23 ml DEPC treated dH_2O

Before use, boil sperm DNA 5 min, place on ice, add 440 µl per 10 ml buffer

Denaturation Solution:	2 L:
	40 g NaOH
	175.3 g NaCl
	dH_2O to 2 L

Neutralization Solution:	2 L:
	121.1 g Tris
	175.3 g NaCl
	dH_2O to 2 L

pH to 7.0 with concentrated HCl

References

Ahmad, M. E., Dada, R., Dada, T., Kucheria, K., 2003. 14q(22) deletion in a familial case of anophthalmia with polydactyly. Am J Med Genet A. 120A**,** 117-22.

Akamatsu, T., Daikoku, S., Nagamune, H., Yoshida, S., Mori, K., Tsuji, A., Matsuda, Y., 1997. Developmental expression of a novel Kexin family protease, PACE4E, in the rat olfactory system. Histochem Cell Biol. 108**,** 95-103.

Alliston, T., Ko, T. C., Cao, Y., Liang, Y. Y., Feng, X. H., Chang, C., Derynck, R., 2005. Repression of bone morphogenetic protein and activin-inducible transcription by Evi-1. J Biol Chem. 280**,** 24227-37.

Anderson, E. D., Molloy, S. S., Jean, F., Fei, H., Shimamura, S., Thomas, G., 2002. The ordered and compartment-specfific autoproteolytic removal of the furin intramolecular chaperone is required for enzyme activation. J Biol Chem. 277**,** 12879-90.

Anderson, E. D., Thomas, L., Hayflick, J. S., Thomas, G., 1993. Inhibition of HIV-1 gp160-dependent membrane fusion by a furin-directed alpha 1-antitrypsin variant. J Biol Chem. 268**,** 24887-91.

Anderson, E. D., VanSlyke, J. K., Thulin, C. D., Jean, F., Thomas, G., 1997. Activation of the furin endoprotease is a multiple-step process: requirements for acidification and internal propeptide cleavage. EMBO J. 16**,** 1508-18.

Aono, A., Hazama, M., Notoya, K., Taketomi, S., Yamasaki, H., Tsukuda, R., Sasaki, S., Fujisawa, Y., 1995. Potent ectopic bone-inducing activity of bone morphogenetic protein-4/7 heterodimer. Biochem Biophys Res Commun. 210**,** 670-7.

Apletalina, E., Appel, J., Lamango, N. S., Houghten, R. A., Lindberg, I., 1998. Identification of inhibitors of prohormone convertases 1 and 2 using a peptide combinatorial library. J Biol Chem. 273**,** 26589-95.

Armes, N. A., Smith, J. C., 1997. The ALK-2 and ALK-4 activin receptors transduce distinct mesoderm-inducing signals during early Xenopus development but do not co-operate to establish thresholds. Development. 124**,** 3797-804.

Arora, K., Levine, M. S., O'Connor, M. B., 1994. The screw gene encodes a ubiquitously expressed member of the TGF-beta family required for specification of dorsal cell fates in the Drosophila embryo. Genes Dev. 8**,** 2588-601.

Ashe, H. L., Levine, M., 1999. Local inhibition and long-range enhancement of Dpp signal transduction by Sog. Nature. 398**,** 427-31.

Bae, S. J., Sturtevant, J. M., 1995. Thermodynamics of the thermal unfolding of eglin c in the presence and absence of guanidinium chloride. Biophys Chem. 55**,** 247-52.

Baker, J. C., Harland, R. M., 1996. A novel mesoderm inducer, Madr2, functions in the activin signal transduction pathway. Genes Dev. 10**,** 1880-9.

Bakrania, P., Efthymiou, M., Klein, J. C., Salt, A., Bunyan, D. J., Wyatt, A., Ponting, C. P., Martin, A., Williams, S., Lindley, V., Gilmore, J., Restori, M., Robson, A. G.,

Neveu, M. M., Holder, G. E., Collin, J. R., Robinson, D. O., Farndon, P., Johansen-Berg, H., Gerrelli, D., Ragge, N. K., 2008. Mutations in BMP4 cause eye, brain, and digit developmental anomalies: overlap between the BMP4 and hedgehog signaling pathways. Am J Hum Genet. 82**,** 304-19.

Balemans, W., Van Hul, W., 2002. Extracellular regulation of BMP signaling in vertebrates: a cocktail of modulators. Dev Biol. 250**,** 231-50.

Basak, A., 2005. Inhibitors of proprotein convertases. J Mol Med. 83**,** 844-55.

Basak, A., Toure, B. B., Lazure, C., Mbikay, M., Chretien, M., Seidah, N. G., 1999. Enzymic characterization in vitro of recombinant proprotein convertase PC4. Biochem J. 343 Pt 1**,** 29-37.

Basak, S., Chretien, M., Mbikay, M., Basak, A., 2004. In vitro elucidation of substrate specificity and bioassay of proprotein convertase 4 using intramolecularly quenched fluorogenic peptides. Biochem J. 380**,** 505-14.

Beck, S., Le Good, J. A., Guzman, M., Ben Haim, N., Roy, K., Beermann, F., Constam, D. B., 2002. Extraembryonic proteases regulate Nodal signalling during gastrulation. Nat Cell Biol. 4**,** 981-5.

Bendjennat, M., Bahbouhi, B., Bahraoui, E., 2001. Purification and characterization of a Ca2+-independent endoprotease activity from peripheral blood lymphocytes: involvement in HIV-1 gp160 maturation. Biochemistry. 40**,** 4800-10.

Benjannet, S., Rondeau, N., Day, R., Chretien, M., Seidah, N. G., 1991. PC1 and PC2 are proprotein convertases capable of cleaving proopiomelanocortin at distinct pairs of basic residues. Proc Natl Acad Sci U S A. 88**,** 3564-8.

Bennett, C. P., Betts, D. R., Seller, M. J., 1991. Deletion 14q (q22q23) associated with anophthalmia, absent pituitary, and other abnormalities. J Med Genet. 28**,** 280-1.

Bhattacharjya, S., Xu, P., Zhong, M., Chretien, M., Seidah, N. G., Ni, F., 2000. Inhibitory activity and structural characterization of a C-terminal peptide fragment derived from the prosegment of the proprotein convertase PC7. Biochemistry. 39**,** 2868-77.

Billings, P. C., Fiori, J. L., Bentwood, J. L., O'Connell, M. P., Jiao, X., Nussbaum, B., Caron, R. J., Shore, E. M., Kaplan, F. S., 2008. Dysregulated BMP signaling and enhanced osteogenic differentiation of connective tissue progenitor cells from patients with fibrodysplasia ossificans progressiva (FOP). J Bone Miner Res. 23**,** 305-13.

Birsoy, B., Berg, L., Williams, P. H., Smith, J. C., Wylie, C. C., Christian, J. L., Heasman, J., 2005. XPACE4 is a localized pro-protein convertase required for mesoderm induction and the cleavage of specific TGFbeta proteins in Xenopus development. Development. 132**,** 591-602.

Bosshart, H., Humphrey, J., Deignan, E., Davidson, J., Drazba, J., Yuan, L., Oorschot, V., Peters, P. J., Bonifacino, J. S., 1994. The cytoplasmic domain mediates

localization of furin to the trans-Golgi network en route to the endosomal/lysosomal system. J Cell Biol. 126**,** 1157-72.

Boudreault, A., Gauthier, D., Lazure, C., 1998. Proprotein convertase PC1/3-related peptides are potent slow tight-binding inhibitors of murine PC1/3 and Hfurin. J Biol Chem. 273**,** 31574-80.

Brennan, S. O., Nakayama, K., 1994. Cleavage of proalbumin peptides by furin reveals unexpected restrictions at the P2 and P'1 sites. FEBS Lett. 347**,** 80-4.

Bresnahan, P. A., Leduc, R., Thomas, L., Thorner, J., Gibson, H. L., Brake, A. J., Barr, P. J., Thomas, G., 1990. Human fur gene encodes a yeast KEX2-like endoprotease that cleaves pro-beta-NGF in vivo. J Cell Biol. 111**,** 2851-9.

Brugger, S. M., Merrill, A. E., Torres-Vazquez, J., Wu, N., Ting, M. C., Cho, J. Y., Dobias, S. L., Yi, S. E., Lyons, K., Bell, J. R., Arora, K., Warrior, R., Maxson, R., 2004. A phylogenetically conserved cis-regulatory module in the Msx2 promoter is sufficient for BMP-dependent transcription in murine and Drosophila embryos. Development. 131**,** 5153-65.

Brunet, L. J., McMahon, J. A., McMahon, A. P., Harland, R. M., 1998. Noggin, cartilage morphogenesis, and joint formation in the mammalian skeleton. Science. 280**,** 1455-7.

Bruning, M., Lummer, M., Bentele, C., Smolenaars, M. M., Rodenburg, K. W., Ragg, H., 2007. The Spn4 gene from Drosophila melanogaster is a multipurpose defence

tool directed against proteases from three different peptidase families. Biochem J. 401**,** 325-31.

Bruzzaniti, A., Goodge, K., Jay, P., Taviaux, S. A., Lam, M. H., Berta, P., Martin, T. J., Moseley, J. M., Gillespie, M. T., 1996. PC8 [corrected], a new member of the convertase family. Biochem J. 314 (Pt 3)**,** 727-31.

Cameron, A., Appel, J., Houghten, R. A., Lindberg, I., 2000a. Polyarginines are potent furin inhibitors. J Biol Chem. 275**,** 36741-9.

Cameron, A., Fortenberry, Y., Lindberg, I., 2000b. The SAAS granin exhibits structural and functional homology to 7B2 and contains a highly potent hexapeptide inhibitor of PC1. FEBS Lett. 473**,** 135-8.

Candia, A. F., Watabe, T., Hawley, S. H., Onichtchouk, D., Zhang, Y., Derynck, R., Niehrs, C., Cho, K. W., 1997. Cellular interpretation of multiple TGF-beta signals: intracellular antagonism between activin/BVg1 and BMP-2/4 signaling mediated by Smads. Development. 124**,** 4467-80.

Chang, W., Lin, Z., Kulessa, H., Hebert, J., Hogan, B. L., Wu, D. K., 2008. Bmp4 is essential for the formation of the vestibular apparatus that detects angular head movements. PLoS Genet. 4**,** e1000050.

Chapman, R. E., Munro, S., 1994. Retrieval of TGN proteins from the cell surface requires endosomal acidification. EMBO J. 13**,** 2305-12.

Chen, H. B., Shen, J., Ip, Y. T., Xu, L., 2006. Identification of phosphatases for Smad in the BMP/DPP pathway. Genes Dev. 20**,** 648-53.

Chen, Y., Bhushan, A., Vale, W., 1997. Smad8 mediates the signaling of the ALK-2 [corrected] receptor serine kinase. Proc Natl Acad Sci U S A. 94**,** 12938-43.

Christian, J. L., McMahon, J. A., McMahon, A. P., Moon, R. T., 1991. Xwnt-8, a Xenopus Wnt-1/int-1-related gene responsive to mesoderm- inducing growth factors, may play a role in ventral mesodermal patterning during embryogenesis. Development. 111**,** 1045-55.

Christian, J. L., Moon, R. T., 1993. Interactions between Xwnt-8 and Spemann organizer signaling pathways generate dorsoventral pattern in the embryonic mesoderm of Xenopus. Genes Dev. 7**,** 13-28.

Clark, H. F., Gurney, A. L., Abaya, E., Baker, K., Baldwin, D., Brush, J., Chen, J., Chow, B., Chui, C., Crowley, C., Currell, B., Deuel, B., Dowd, P., Eaton, D., Foster, J., Grimaldi, C., Gu, Q., Hass, P. E., Heldens, S., Huang, A., Kim, H. S., Klimowski, L., Jin, Y., Johnson, S., Lee, J., Lewis, L., Liao, D., Mark, M., Robbie, E., Sanchez, C., Schoenfeld, J., Seshagiri, S., Simmons, L., Singh, J., Smith, V., Stinson, J., Vagts, A., Vandlen, R., Watanabe, C., Wieand, D., Woods, K., Xie, M. H., Yansura, D., Yi, S., Yu, G., Yuan, J., Zhang, M., Zhang, Z., Goddard, A., Wood, W. I., Godowski, P., Gray, A., 2003. The secreted protein discovery initiative (SPDI), a large-scale effort to identify novel human secreted and transmembrane proteins: a bioinformatics assessment. Genome Res. 13**,** 2265-70.

Conlon, F. L., Barth, K. S., Robertson, E. J., 1991. A novel retrovirally induced embryonic lethal mutation in the mouse: assessment of the developmental fate of embryonic stem cells homozygous for the 413.d proviral integration. Development. 111**,** 969-81.

Conlon, F. L., Lyons, K. M., Takaesu, N., Barth, K. S., Kispert, A., Herrmann, B., Robertson, E. J., 1994. A primary requirement for nodal in the formation and maintenance of the primitive streak in the mouse. Development. 120**,** 1919-28.

Constam, D. B., Calfon, M., Robertson, E. J., 1996. SPC4, SPC6, and the novel protease SPC7 are coexpressed with bone morphogenetic proteins at distinct sites during embryogenesis. J Cell Biol. 134**,** 181-91.

Constam, D. B., Robertson, E. J., 1999. Regulation of bone morphogenetic protein activity by pro domains and proprotein convertases. J Cell Biol. 144**,** 139-49.

Constam, D. B., Robertson, E. J., 2000a. SPC4/PACE4 regulates a TGFbeta signaling network during axis formation. Genes Dev. 14**,** 1146-55.

Constam, D. B., Robertson, E. J., 2000b. Tissue-specific requirements for the proprotein convertase furin/SPC1 during embryonic turning and heart looping. Development. 127**,** 245-54.

Creemers, J. W., Groot Kormelink, P. J., Roebroek, A. J., Nakayama, K., Van de Ven, W. J., 1993a. Proprotein processing activity and cleavage site selectivity of the Kex2-like endoprotease PACE4. FEBS Lett. 336**,** 65-9.

Creemers, J. W., Siezen, R. J., Roebroek, A. J., Ayoubi, T. A., Huylebroeck, D., Van de Ven, W. J., 1993b. Modulation of furin-mediated proprotein processing activity by site-directed mutagenesis. J Biol Chem. 268**,** 21826-34.

Crump, C. M., Xiang, Y., Thomas, L., Gu, F., Austin, C., Tooze, S. A., Thomas, G., 2001. PACS-1 binding to adaptors is required for acidic cluster motif-mediated protein traffic. EMBO J. 20**,** 2191-201.

Cui, Y., Brown, J. D., Moon, R. T., Christian, J. L., 1995. Xwnt-8b: a maternally expressed Xenopus Wnt gene with a potential role in establishing the dorsoventral axis. Development. 121**,** 2177-86.

Cui, Y., Hackenmiller, R., Berg, L., Jean, F., Nakayama, T., Thomas, G., Christian, J. L., 2001. The activity and signaling range of mature BMP-4 is regulated by sequential cleavage at two sites within the prodomain of the precursor. Genes Dev. 15**,** 2797-802.

Cui, Y., Jean, F., Thomas, G., Christian, J. L., 1998. BMP-4 is proteolytically activated by furin and/or PC6 during vertebrate embryonic development. EMBO J. 17**,** 4735-43.

Dahlen, J. R., Jean, F., Thomas, G., Foster, D. C., Kisiel, W., 1998. Inhibition of soluble recombinant furin by human proteinase inhibitor 8. J Biol Chem. 273**,** 1851-4.

Dale, L., Howes, G., Price, B. M., Smith, J. C., 1992. Bone morphogenetic protein 4: a ventralizing factor in early Xenopus development. Development. 115**,** 573-85.

Dale, L., Jones, C. M., 1999. BMP signalling in early Xenopus development. Bioessays. 21**,** 751-60.

De Bie, I., Marcinkiewicz, M., Malide, D., Lazure, C., Nakayama, K., Bendayan, M., Seidah, N. G., 1996. The isoforms of proprotein convertase PC5 are sorted to different subcellular compartments. J Cell Biol. 135**,** 1261-75.

De Bie, I., Savaria, D., Roebroek, A. J., Day, R., Lazure, C., Van de Ven, W. J., Seidah, N. G., 1995. Processing specificity and biosynthesis of the Drosophila melanogaster convertases dfurin1, dfurin1-CRR, dfurin1-X, and dfurin2. J Biol Chem. 270**,** 1020-8.

De Robertis, E. M., 2008. Evo-devo: variations on ancestral themes. Cell. 132**,** 185-95.

Decroly, E., Wouters, S., Di Bello, C., Lazure, C., Ruysschaert, J. M., Seidah, N. G., 1996. Identification of the paired basic convertases implicated in HIV gp160 processing based on in vitro assays and expression in CD4(+) cell lines. J Biol Chem. 271**,** 30442-50.

Degnin, C., Jean, F., Thomas, G., Christian, J. L., 2004. Cleavages within the prodomain direct intracellular trafficking and degradation of mature bone morphogenetic protein-4. Mol Biol Cell. 15**,** 5012-20.

Denault, J., Bissonnette, L., Longpre, J., Charest, G., Lavigne, P., Leduc, R., 2002. Ectodomain shedding of furin: kinetics and role of the cysteine-rich region. FEBS Lett. 527**,** 309-14.

Denault, J. B., D'Orleans-Juste, P., Masaki, T., Leduc, R., 1995. Inhibition of convertase-related processing of proendothelin-1. J Cardiovasc Pharmacol. 26 Suppl 3**,** S47-50.

Deng, Z., Morse, J. H., Slager, S. L., Cuervo, N., Moore, K. J., Venetos, G., Kalachikov, S., Cayanis, E., Fischer, S. G., Barst, R. J., Hodge, S. E., Knowles, J. A., 2000. Familial primary pulmonary hypertension (gene PPH1) is caused by mutations in the bone morphogenetic protein receptor-II gene. Am J Hum Genet. 67**,** 737-44.

Dennler, S., Itoh, S., Vivien, D., ten Dijke, P., Huet, S., Gauthier, J. M., 1998. Direct binding of Smad3 and Smad4 to critical TGF beta-inducible elements in the promoter of human plasminogen activator inhibitor-type 1 gene. EMBO J. 17**,** 3091-100.

Dosch, R., Gawantka, V., Delius, H., Blumenstock, C., Niehrs, C., 1997. Bmp-4 acts as a morphogen in dorsoventral mesoderm patterning in Xenopus. Development. 124**,** 2325-34.

Dufour, E. K., Denault, J. B., Bissonnette, L., Hopkins, P. C., Lavigne, P., Leduc, R., 2001. The contribution of arginine residues within the P6-P1 region of alpha 1-antitrypsin to its reaction with furin. J Biol Chem. 276**,** 38971-9.

Dunn, N. R., Winnier, G. E., Hargett, L. K., Schrick, J. J., Fogo, A. B., Hogan, B. L., 1997. Haploinsufficient phenotypes in Bmp4 heterozygous null mice and modification by mutations in Gli3 and Alx4. Dev Biol. 188**,** 235-47.

Ebisawa, T., Fukuchi, M., Murakami, G., Chiba, T., Tanaka, K., Imamura, T., Miyazono, K., 2001. Smurf1 interacts with transforming growth factor-beta type I receptor through Smad7 and induces receptor degradation. J Biol Chem. 276**,** 12477-80.

Eblaghie, M. C., Reedy, M., Oliver, T., Mishina, Y., Hogan, B. L., 2006. Evidence that autocrine signaling through Bmpr1a regulates the proliferation, survival and morphogenetic behavior of distal lung epithelial cells. Dev Biol. 291**,** 67-82.

Elliott, J., Maltby, E. L., Reynolds, B., 1993. A case of deletion 14(q22.1-->q22.3) associated with anophthalmia and pituitary abnormalities. J Med Genet. 30**,** 251-2.

Esquela, A. F., Lee, S. J., 2003. Regulation of metanephric kidney development by growth/differentiation factor 11. Dev Biol. 257**,** 356-70.

Essalmani, R., Hamelin, J., Marcinkiewicz, J., Chamberland, A., Mbikay, M., Chretien, M., Seidah, N. G., Prat, A., 2006. Deletion of the gene encoding proprotein convertase 5/6 causes early embryonic lethality in the mouse. Mol Cell Biol. 26**,** 354-61.

Essalmani, R., Zaid, A., Marcinkiewicz, J., Chamberland, A., Pasquato, A., Seidah, N. G., Prat, A., 2008. In vivo functions of the proprotein convertase PC5/6 during mouse development: Gdf11 is a likely substrate. Proc Natl Acad Sci U S A. 105**,** 5750-5.

Fainsod, A., Deissler, K., Yelin, R., Marom, K., Epstein, M., Pillemer, G., Steinbeisser, H., Blum, M., 1997. The dorsalizing and neural inducing gene follistatin is an antagonist of BMP-4. Mech Dev. 63**,** 39-50.

Fainsod, A., Steinbeisser, H., De Robertis, E. M., 1994. On the function of BMP-4 in patterning the marginal zone of the Xenopus embryo. EMBO J. 13**,** 5015-25.

Feliciangeli, S. F., Thomas, L., Scott, G. K., Subbian, E., Hung, C. H., Molloy, S. S., Jean, F., Shinde, U., Thomas, G., 2006. Identification of a pH sensor in the furin propeptide that regulates enzyme activation. J Biol Chem. 281**,** 16108-16.

Ferguson, E. L., Anderson, K. V., 1992. Decapentaplegic acts as a morphogen to organize dorsal-ventral pattern in the Drosophila embryo. Cell. 71**,** 451-61.

Frohman, M. A., 1993. Rapid amplification of complementary DNA ends for generation of full-length complementary DNAs: thermal RACE. Methods Enzymol. 218**,** 340-56.

Fuentealba, L. C., Eivers, E., Ikeda, A., Hurtado, C., Kuroda, H., Pera, E. M., De Robertis, E. M., 2007. Integrating patterning signals: Wnt/GSK3 regulates the duration of the BMP/Smad1 signal. Cell. 131**,** 980-93.

Fugere, M., Appel, J., Houghten, R. A., Lindberg, I., Day, R., 2007. Short polybasic peptide sequences are potent inhibitors of PC5/6 and PC7: Use of positional scanning-synthetic peptide combinatorial libraries as a tool for the optimization of inhibitory sequences. Mol Pharmacol. 71**,** 323-32.

Fugere, M., Day, R., 2005. Cutting back on pro-protein convertases: the latest approaches to pharmacological inhibition. Trends Pharmacol Sci. 26**,** 294-301.

Fugere, M., Limperis, P. C., Beaulieu-Audy, V., Gagnon, F., Lavigne, P., Klarskov, K., Leduc, R., Day, R., 2002. Inhibitory potency and specificity of subtilase-like pro-protein convertase (SPC) prodomains. J Biol Chem. 277**,** 7648-56.

Fuller, R. S., Brake, A. J., Thorner, J., 1989. Intracellular targeting and structural conservation of a prohormone-processing endoprotease. Science. 246**,** 482-6.

Furuta, Y., Piston, D. W., Hogan, B. L., 1997. Bone morphogenetic proteins (BMPs) as regulators of dorsal forebrain development. Development. 124**,** 2203-12.

Futter, C. E., Connolly, C. N., Cutler, D. F., Hopkins, C. R., 1995. Newly synthesized transferrin receptors can be detected in the endosome before they appear on the cell surface. J Biol Chem. 270**,** 10999-1003.

Garten, W., Hallenberger, S., Ortmann, D., Schafer, W., Vey, M., Angliker, H., Shaw, E., Klenk, H. D., 1994. Processing of viral glycoproteins by the subtilisin-like endoprotease furin and its inhibition by specific peptidylchloroalkylketones. Biochimie. 76**,** 217-25.

Garten, W., Stieneke, A., Shaw, E., Wikstrom, P., Klenk, H. D., 1989. Inhibition of proteolytic activation of influenza virus hemagglutinin by specific peptidyl chloroalkyl ketones. Virology. 172**,** 25-31.

Gluschankof, P., Fuller, R. S., 1994. A C-terminal domain conserved in precursor processing proteases is required for intramolecular N-terminal maturation of pro-Kex2 protease. EMBO J. 13**,** 2280-8.

Goldman, D. C., Donley, N., Christian, J. L., 2009. Genetic interaction between Bmp2 and Bmp4 reveals shared functions during multiple aspects of mouse organogenesis. Mech Dev. 126**,** 117-27.

Goldman, D. C., Hackenmiller, R., Nakayama, T., Sopory, S., Wong, C., Kulessa, H., Christian, J. L., 2006. Mutation of an upstream cleavage site in the BMP4 prodomain leads to tissue-specific loss of activity. Development. 133**,** 1933-42.

Gong, Y., Krakow, D., Marcelino, J., Wilkin, D., Chitayat, D., Babul-Hirji, R., Hudgins, L., Cremers, C. W., Cremers, F. P., Brunner, H. G., Reinker, K., Rimoin, D. L., Cohn, D. H., Goodman, F. R., Reardon, W., Patton, M., Francomano, C. A., Warman, M. L., 1999. Heterozygous mutations in the gene encoding noggin affect human joint morphogenesis. Nat Genet. 21**,** 302-4.

Goodge, K. A., Thomas, R. J., Martin, T. J., Gillespie, M. T., 1998. Gene organization and alternative splicing of human prohormone convertase PC8. Biochem J. 336 (Pt 2)**,** 353-9.

Graff, J. M., Bansal, A., Melton, D. A., 1996. Xenopus Mad proteins transduce distinct subsets of signals for the TGF beta superfamily. Cell. 85**,** 479-87.

Graff, J. M., Thies, R. S., Song, J. J., Celeste, A. J., Melton, D. A., 1994. Studies with a Xenopus BMP receptor suggest that ventral mesoderm-inducing signals override dorsal signals in vivo. Cell. 79**,** 169-79.

Griffiths, G., Pfeiffer, S., Simons, K., Matlin, K., 1985. Exit of newly synthesized membrane proteins from the trans cisterna of the Golgi complex to the plasma membrane. J Cell Biol. 101**,** 949-64.

Groppe, J., Greenwald, J., Wiater, E., Rodriguez-Leon, J., Economides, A. N., Kwiatkowski, W., Affolter, M., Vale, W. W., Belmonte, J. C., Choe, S., 2002. Structural basis of BMP signalling inhibition by the cystine knot protein Noggin. Nature. 420**,** 636-42.

Gyamera-Acheampong, C., Tantibhedhyangkul, J., Weerachatyanukul, W., Tadros, H., Xu, H., van de Loo, J. W., Pelletier, R. M., Tanphaichitr, N., Mbikay, M., 2006. Sperm from mice genetically deficient for the PCSK4 proteinase exhibit accelerated capacitation, precocious acrosome reaction, reduced binding to egg zona pellucida, and impaired fertilizing ability. Biol Reprod. 74**,** 666-73.

Hallenberger, S., Bosch, V., Angliker, H., Shaw, E., Klenk, H. D., Garten, W., 1992. Inhibition of furin-mediated cleavage activation of HIV-1 glycoprotein gp160. Nature. 360**,** 358-61.

Harland, R. M., 1991. In situ hybridization: an improved whole-mount method for Xenopus embryos. Methods Cell Biol. 36**,** 685-95.

Hata, A., Lagna, G., Massague, J., Hemmati-Brivanlou, A., 1998. Smad6 inhibits BMP/Smad1 signaling by specifically competing with the Smad4 tumor suppressor. Genes Dev. 12**,** 186-97.

Hata, A., Lo, R. S., Wotton, D., Lagna, G., Massague, J., 1997. Mutations increasing autoinhibition inactivate tumour suppressors Smad2 and Smad4. Nature. 388**,** 82-7.

Hayashi, H., Abdollah, S., Qiu, Y., Cai, J., Xu, Y. Y., Grinnell, B. W., Richardson, M. A., Topper, J. N., Gimbrone, M. A., Jr., Wrana, J. L., Falb, D., 1997. The MAD-related protein Smad7 associates with the TGFbeta receptor and functions as an antagonist of TGFbeta signaling. Cell. 89**,** 1165-73.

Hayashi, S., Okamoto, N., Makita, Y., Hata, A., Imoto, I., Inazawa, J., 2008. Heterozygous deletion at 14q22.1-q22.3 including the BMP4 gene in a patient with psychomotor retardation, congenital corneal opacity and feet polysyndactyly. Am J Med Genet A. 146A**,** 2905-10.

Hemmati-Brivanlou, A., Kelly, O. G., Melton, D. A., 1994. Follistatin, an antagonist of activin, is expressed in the Spemann organizer and displays direct neuralizing activity. Cell. 77**,** 283-95.

Henrich, S., Cameron, A., Bourenkov, G. P., Kiefersauer, R., Huber, R., Lindberg, I., Bode, W., Than, M. E., 2003. The crystal structure of the proprotein processing proteinase furin explains its stringent specificity. Nat Struct Biol. 10**,** 520-6.

Hirschberg, K., Miller, C. M., Ellenberg, J., Presley, J. F., Siggia, E. D., Phair, R. D., Lippincott-Schwartz, J., 1998. Kinetic analysis of secretory protein traffic and characterization of golgi to plasma membrane transport intermediates in living cells. J Cell Biol. 143**,** 1485-503.

Hogan, B. L., 1996. Bone morphogenetic proteins: multifunctional regulators of vertebrate development. Genes Dev. 10**,** 1580-94.

Holley, S. A., Jackson, P. D., Sasai, Y., Lu, B., De Robertis, E. M., Hoffmann, F. M., Ferguson, E. L., 1995. A conserved system for dorsal-ventral patterning in insects and vertebrates involving sog and chordin. Nature. 376**,** 249-53.

Holling, T. M., van Herp, F., Durston, A. J., Martens, G. J., 2000. Differential onset of expression of mRNAs encoding proopiomelanocortin, prohormone convertases 1 and 2, and granin family members during Xenopus laevis development. Brain Res Mol Brain Res. 75**,** 70-5.

Hoodless, P. A., Haerry, T., Abdollah, S., Stapleton, M., O'Connor, M. B., Attisano, L., Wrana, J. L., 1996. MADR1, a MAD-related protein that functions in BMP2 signaling pathways. Cell. 85**,** 489-500.

Horton, R. M., Cai, Z. L., Ho, S. N., Pease, L. R., 1990. Gene splicing by overlap extension: tailor-made genes using the polymerase chain reaction. Biotechniques. 8**,** 528-35.

Howe, J. R., Bair, J. L., Sayed, M. G., Anderson, M. E., Mitros, F. A., Petersen, G. M., Velculescu, V. E., Traverso, G., Vogelstein, B., 2001. Germline mutations of the

gene encoding bone morphogenetic protein receptor 1A in juvenile polyposis. Nat Genet. 28**,** 184-7.

Howe, J. R., Roth, S., Ringold, J. C., Summers, R. W., Jarvinen, H. J., Sistonen, P., Tomlinson, I. P., Houlston, R. S., Bevan, S., Mitros, F. A., Stone, E. M., Aaltonen, L. A., 1998. Mutations in the SMAD4/DPC4 gene in juvenile polyposis. Science. 280**,** 1086-8.

Hsu, D. R., Economides, A. N., Wang, X., Eimon, P. M., Harland, R. M., 1998. The Xenopus dorsalizing factor Gremlin identifies a novel family of secreted proteins that antagonize BMP activities. Mol Cell. 1**,** 673-83.

Huntington, J. A., Read, R. J., Carrell, R. W., 2000. Structure of a serpin-protease complex shows inhibition by deformation. Nature. 407**,** 923-6.

Iemura, S., Yamamoto, T. S., Takagi, C., Uchiyama, H., Natsume, T., Shimasaki, S., Sugino, H., Ueno, N., 1998. Direct binding of follistatin to a complex of bone-morphogenetic protein and its receptor inhibits ventral and epidermal cell fates in early Xenopus embryo. Proc Natl Acad Sci U S A. 95**,** 9337-42.

Imamura, T., Takase, M., Nishihara, A., Oeda, E., Hanai, J., Kawabata, M., Miyazono, K., 1997. Smad6 inhibits signalling by the TGF-beta superfamily. Nature. 389**,** 622-6.

Inman, G. J., Nicolas, F. J., Hill, C. S., 2002. Nucleocytoplasmic shuttling of Smads 2, 3, and 4 permits sensing of TGF-beta receptor activity. Mol Cell. 10**,** 283-94.

Inomata, H., Haraguchi, T., Sasai, Y., 2008. Robust stability of the embryonic axial pattern requires a secreted scaffold for chordin degradation. Cell. 134**,** 854-65.

Ishida, W., Hamamoto, T., Kusanagi, K., Yagi, K., Kawabata, M., Takehara, K., Sampath, T. K., Kato, M., Miyazono, K., 2000. Smad6 is a Smad1/5-induced smad inhibitor. Characterization of bone morphogenetic protein-responsive element in the mouse Smad6 promoter. J Biol Chem. 275**,** 6075-9.

Jarvinen, H., Franssila, K. O., 1984. Familial juvenile polyposis coli; increased risk of colorectal cancer. Gut. 25**,** 792-800.

Jean, F., Stella, K., Thomas, L., Liu, G., Xiang, Y., Reason, A. J., Thomas, G., 1998. alpha1-Antitrypsin Portland, a bioengineered serpin highly selective for furin: application as an antipathogenic agent. Proc Natl Acad Sci U S A. 95**,** 7293-8.

Jean, F., Thomas, L., Molloy, S. S., Liu, G., Jarvis, M. A., Nelson, J. A., Thomas, G., 2000. A protein-based therapeutic for human cytomegalovirus infection. Proc Natl Acad Sci U S A. 97**,** 2864-9.

Jiao, K., Kulessa, H., Tompkins, K., Zhou, Y., Batts, L., Baldwin, H. S., Hogan, B. L., 2003. An essential role of Bmp4 in the atrioventricular septation of the mouse heart. Genes Dev. 17**,** 2362-7.

Johansson, B. M., Wiles, M. V., 1995. Evidence for involvement of activin A and bone morphogenetic protein 4 in mammalian mesoderm and hematopoietic development. Mol Cell Biol. 15**,** 141-51.

Jones, B. G., Thomas, L., Molloy, S. S., Thulin, C. D., Fry, M. D., Walsh, K. A., Thomas, G., 1995. Intracellular trafficking of furin is modulated by the phosphorylation state of a casein kinase II site in its cytoplasmic tail. EMBO J. 14**,** 5869-83.

Jones, C. M., Dale, L., Hogan, B. L., Wright, C. V., Smith, J. C., 1996. Bone morphogenetic protein-4 (BMP-4) acts during gastrula stages to cause ventralization of Xenopus embryos. Development. 122**,** 1545-54.

Jones, C. M., Lyons, K. M., Hogan, B. L., 1991. Involvement of Bone Morphogenetic Protein-4 (BMP-4) and Vgr-1 in morphogenesis and neurogenesis in the mouse. Development. 111**,** 531-42.

Julius, D., Brake, A., Blair, L., Kunisawa, R., Thorner, J., 1984. Isolation of the putative structural gene for the lysine-arginine-cleaving endopeptidase required for processing of yeast prepro-alpha-factor. Cell. 37**,** 1075-89.

Kacprzak, M. M., Peinado, J. R., Than, M. E., Appel, J., Henrich, S., Lipkind, G., Houghten, R. A., Bode, W., Lindberg, I., 2004. Inhibition of furin by polyarginine-containing peptides: nanomolar inhibition by nona-D-arginine. J Biol Chem. 279**,** 36788-94.

Kavsak, P., Rasmussen, R. K., Causing, C. G., Bonni, S., Zhu, H., Thomsen, G. H., Wrana, J. L., 2000. Smad7 binds to Smurf2 to form an E3 ubiquitin ligase that targets the TGF beta receptor for degradation. Mol Cell. 6**,** 1365-75.

Kido, H., Kamoshita, K., Fukutomi, A., Katunuma, N., 1993. Processing protease for gp160 human immunodeficiency virus type I envelope glycoprotein precursor in human T4+ lymphocytes. Purification and characterization. J Biol Chem. 268**,** 13406-13.

Kiefer, M. C., Tucker, J. E., Joh, R., Landsberg, K. E., Saltman, D., Barr, P. J., 1991. Identification of a second human subtilisin-like protease gene in the fes/fps region of chromosome 15. DNA Cell Biol. 10**,** 757-69.

Kim, J., Johnson, K., Chen, H. J., Carroll, S., Laughon, A., 1997. Drosophila Mad binds to DNA and directly mediates activation of vestigial by Decapentaplegic. Nature. 388**,** 304-8.

Knockaert, M., Sapkota, G., Alarcon, C., Massague, J., Brivanlou, A. H., 2006. Unique players in the BMP pathway: small C-terminal domain phosphatases dephosphorylate Smad1 to attenuate BMP signaling. Proc Natl Acad Sci U S A. 103**,** 11940-5.

Koenig, B. B., Cook, J. S., Wolsing, D. H., Ting, J., Tiesman, J. P., Correa, P. E., Olson, C. A., Pecquet, A. L., Ventura, F., Grant, R. A., et al., 1994. Characterization and cloning of a receptor for BMP-2 and BMP-4 from NIH 3T3 cells. Mol Cell Biol. 14**,** 5961-74.

Komiyama, T., Fuller, R. S., 2000. Engineered eglin c variants inhibit yeast and human proprotein processing proteases, Kex2 and furin. Biochemistry. 39**,** 15156-65.

Komiyama, T., Swanson, J. A., Fuller, R. S., 2005. Protection from anthrax toxin-mediated killing of macrophages by the combined effects of furin inhibitors and chloroquine. Antimicrob Agents Chemother. 49**,** 3875-82.

Komiyama, T., VanderLugt, B., Fugere, M., Day, R., Kaufman, R. J., Fuller, R. S., 2003. Optimization of protease-inhibitor interactions by randomizing adventitious contacts. Proc Natl Acad Sci U S A. 100**,** 8205-10.

Korner, J., Chun, J., O'Bryan, L., Axel, R., 1991. Prohormone processing in Xenopus oocytes: characterization of cleavage signals and cleavage enzymes. Proc Natl Acad Sci U S A. 88**,** 11393-7.

Kraut, J., 1977. Serine proteases: structure and mechanism of catalysis. Annu Rev Biochem. 46**,** 331-58.

Kretzschmar, M., Doody, J., Massague, J., 1997a. Opposing BMP and EGF signalling pathways converge on the TGF-beta family mediator Smad1. Nature. 389**,** 618-22.

Kretzschmar, M., Liu, F., Hata, A., Doody, J., Massague, J., 1997b. The TGF-beta family mediator Smad1 is phosphorylated directly and activated functionally by the BMP receptor kinase. Genes Dev. 11**,** 984-95.

Kreutter, K., Steinmetz, A. C., Liang, T. C., Prorok, M., Abeles, R. H., Ringe, D., 1994. Three-dimensional structure of chymotrypsin inactivated with (2S)-N-acetyl-L-alanyl-L-phenylalanyl alpha-chloroethane: implications for the mechanism of inactivation of serine proteases by chloroketones. Biochemistry. 33**,** 13792-800.

Kruger, O., Ladewig, J., Koster, K., Ragg, H., 2002. Widespread occurrence of serpin genes with multiple reactive centre-containing exon cassettes in insects and nematodes. Gene. 293**,** 97-105.

Krysan, D. J., Rockwell, N. C., Fuller, R. S., 1999. Quantitative characterization of furin specificity. Energetics of substrate discrimination using an internally consistent set of hexapeptidyl methylcoumarinamides. J Biol Chem. 274**,** 23229-34.

Kunnapuu, J., Bjorkgren, I., Shimmi, O., 2009. The Drosophila DPP signal is produced by cleavage of its proprotein at evolutionary diversified furin-recognition sites. Proc Natl Acad Sci U S A. 106**,** 8501-6.

Lackner, D. H., Bahler, J., 2008. Translational control of gene expression from transcripts to transcriptomes. Int Rev Cell Mol Biol. 271**,** 199-251.

Lagna, G., Hata, A., Hemmati-Brivanlou, A., Massague, J., 1996. Partnership between DPC4 and SMAD proteins in TGF-beta signalling pathways. Nature. 383**,** 832-6.

Lane, K. B., Machado, R. D., Pauciulo, M. W., Thomson, J. R., Phillips, J. A., 3rd, Loyd, J. E., Nichols, W. C., Trembath, R. C., 2000. Heterozygous germline mutations in BMPR2, encoding a TGF-beta receptor, cause familial primary pulmonary hypertension. The International PPH Consortium. Nat Genet. 26**,** 81-4.

Lawson, K. A., Dunn, N. R., Roelen, B. A., Zeinstra, L. M., Davis, A. M., Wright, C. V., Korving, J. P., Hogan, B. L., 1999. Bmp4 is required for the generation of primordial germ cells in the mouse embryo. Genes Dev. 13**,** 424-36.

Leblond, J., Laprise, M. H., Gaudreau, S., Grondin, F., Kisiel, W., Dubois, C. M., 2006. The serpin proteinase inhibitor 8: an endogenous furin inhibitor released from human platelets. Thromb Haemost. 95**,** 243-52.

Leduc, R., Molloy, S. S., Thorne, B. A., Thomas, G., 1992. Activation of human furin precursor processing endoprotease occurs by an intramolecular autoproteolytic cleavage. J Biol Chem. 267**,** 14304-8.

Lee, H. X., Ambrosio, A. L., Reversade, B., De Robertis, E. M., 2006. Embryonic dorsal-ventral signaling: secreted frizzled-related proteins as inhibitors of tolloid proteinases. Cell. 124**,** 147-59.

Lee, S. N., Lindberg, I., 2008. 7B2 prevents unfolding and aggregation of prohormone convertase 2. Endocrinology. 149**,** 4116-27.

Lehmann, K., Seemann, P., Boergermann, J., Morin, G., Reif, S., Knaus, P., Mundlos, S., 2006. A novel R486Q mutation in BMPR1B resulting in either a brachydactyly type C/symphalangism-like phenotype or brachydactyly type A2. Eur J Hum Genet. 14**,** 1248-54.

Lehmann, K., Seemann, P., Silan, F., Goecke, T. O., Irgang, S., Kjaer, K. W., Kjaergaard, S., Mahoney, M. J., Morlot, S., Reissner, C., Kerr, B., Wilkie, A. O., Mundlos, S., 2007. A new subtype of brachydactyly type B caused by point mutations in the bone morphogenetic protein antagonist NOGGIN. Am J Hum Genet. 81**,** 388-96.

Lehmann, K., Seemann, P., Stricker, S., Sammar, M., Meyer, B., Suring, K., Majewski, F., Tinschert, S., Grzeschik, K. H., Muller, D., Knaus, P., Nurnberg, P., Mundlos,

S., 2003. Mutations in bone morphogenetic protein receptor 1B cause brachydactyly type A2. Proc Natl Acad Sci U S A. 100**,** 12277-82.

Lemyre, E., Lemieux, N., Decarie, J. C., Lambert, M., 1998. Del(14)(q22.1q23.2) in a patient with anophthalmia and pituitary hypoplasia. Am J Med Genet. 77**,** 162-5.

Lennon, G., Auffray, C., Polymeropoulos, M., Soares, M. B., 1996. The I.M.A.G.E. Consortium: an integrated molecular analysis of genomes and their expression. Genomics. 33**,** 151-2.

Lindberg, I., van den Hurk, W. H., Bui, C., Batie, C. J., 1995. Enzymatic characterization of immunopurified prohormone convertase 2: potent inhibition by a 7B2 peptide fragment. Biochemistry. 34**,** 5486-93.

Linder, M. E., Deschenes, R. J., 2007. Palmitoylation: policing protein stability and traffic. Nat Rev Mol Cell Biol. 8**,** 74-84.

Lipkind, G. M., Zhou, A., Steiner, D. F., 1998. A model for the structure of the P domains in the subtilisin-like prohormone convertases. Proc Natl Acad Sci U S A. 95**,** 7310-5.

Liu, F., Hata, A., Baker, J. C., Doody, J., Carcamo, J., Harland, R. M., Massague, J., 1996. A human Mad protein acting as a BMP-regulated transcriptional activator. Nature. 381**,** 620-3.

Liu, F., Ventura, F., Doody, J., Massague, J., 1995. Human type II receptor for bone morphogenic proteins (BMPs): extension of the two-kinase receptor model to the BMPs. Mol Cell Biol. 15**,** 3479-86.

Liu, G., Thomas, L., Warren, R. A., Enns, C. A., Cunningham, C. C., Hartwig, J. H., Thomas, G., 1997. Cytoskeletal protein ABP-280 directs the intracellular trafficking of furin and modulates proprotein processing in the endocytic pathway. J Cell Biol. 139**,** 1719-33.

Liu, W., Selever, J., Wang, D., Lu, M. F., Moses, K. A., Schwartz, R. J., Martin, J. F., 2004. Bmp4 signaling is required for outflow-tract septation and branchial-arch artery remodeling. Proc Natl Acad Sci U S A. 101**,** 4489-94.

Lo, R. S., Massague, J., 1999. Ubiquitin-dependent degradation of TGF-beta-activated smad2. Nat Cell Biol. 1**,** 472-8.

Lowe, L. A., Yamada, S., Kuehn, M. R., 2001. Genetic dissection of nodal function in patterning the mouse embryo. Development. 128**,** 1831-43.

Macias-Silva, M., Abdollah, S., Hoodless, P. A., Pirone, R., Attisano, L., Wrana, J. L., 1996. MADR2 is a substrate of the TGFbeta receptor and its phosphorylation is required for nuclear accumulation and signaling. Cell. 87**,** 1215-24.

Mains, R. E., Berard, C. A., Denault, J. B., Zhou, A., Johnson, R. C., Leduc, R., 1997. PACE4: a subtilisin-like endoprotease with unique properties. Biochem J. 321 (Pt 3)**,** 587-93.

Marques, G., Musacchio, M., Shimell, M. J., Wunnenberg-Stapleton, K., Cho, K. W., O'Connor, M. B., 1997. Production of a DPP activity gradient in the early Drosophila embryo through the opposing actions of the SOG and TLD proteins. Cell. 91**,** 417-26.

Massague, J., 1998. TGF-beta signal transduction. Annu Rev Biochem. 67**,** 753-91.

Massague, J., Seoane, J., Wotton, D., 2005. Smad transcription factors. Genes Dev. 19**,** 2783-810.

Mathews, L. S., Vale, W. W., 1993. Characterization of type II activin receptors. Binding, processing, and phosphorylation. J Biol Chem. 268**,** 19013-8.

Mbikay, M., Raffin-Sanson, M. L., Tadros, H., Sirois, F., Seidah, N. G., Chretien, M., 1994. Structure of the gene for the testis-specific proprotein convertase 4 and of its alternate messenger RNA isoforms. Genomics. 20**,** 231-7.

Mbikay, M., Seidah, N. G., Chretien, M., 2001. Neuroendocrine secretory protein 7B2: structure, expression and functions. Biochem J. 357**,** 329-42.

McCormick, P. J., Dumaresq-Doiron, K., Pluviose, A. S., Pichette, V., Tosato, G., Lefrancois, S., 2008. Palmitoylation controls recycling in lysosomal sorting and trafficking. Traffic. 9**,** 1984-97.

McMahon, J. A., Takada, S., Zimmerman, L. B., Fan, C. M., Harland, R. M., McMahon, A. P., 1998. Noggin-mediated antagonism of BMP signaling is required for growth and patterning of the neural tube and somite. Genes Dev. 12**,** 1438-52.

McPherron, A. C., Lawler, A. M., Lee, S. J., 1999. Regulation of anterior/posterior patterning of the axial skeleton by growth/differentiation factor 11. Nat Genet. 22**,** 260-4.

Meerabux, J., Yaspo, M. L., Roebroek, A. J., Van de Ven, W. J., Lister, T. A., Young, B. D., 1996. A new member of the proprotein convertase gene family (LPC) is located at a chromosome translocation breakpoint in lymphomas. Cancer Res. 56**,** 448-51.

Mesnard, D., Guzman-Ayala, M., Constam, D. B., 2006. Nodal specifies embryonic visceral endoderm and sustains pluripotent cells in the epiblast before overt axial patterning. Development. 133**,** 2497-505.

Molloy, S. S., Anderson, E. D., Jean, F., Thomas, G., 1999. Bi-cycling the furin pathway: from TGN localization to pathogen activation and embryogenesis. Trends Cell Biol. 9**,** 28-35.

Molloy, S. S., Bresnahan, P. A., Leppla, S. H., Klimpel, K. R., Thomas, G., 1992. Human furin is a calcium-dependent serine endoprotease that recognizes the sequence Arg-X-X-Arg and efficiently cleaves anthrax toxin protective antigen. J Biol Chem. 267**,** 16396-402.

Molloy, S. S., Thomas, L., Kamibayashi, C., Mumby, M. C., Thomas, G., 1998. Regulation of endosome sorting by a specific PP2A isoform. J Cell Biol. 142**,** 1399-411.

Molloy, S. S., Thomas, L., VanSlyke, J. K., Stenberg, P. E., Thomas, G., 1994. Intracellular trafficking and activation of the furin proprotein convertase: localization to the TGN and recycling from the cell surface. EMBO J. 13**,** 18-33.

Moon, R. T., Christian, J. L., 1989. Microinjection and expression of synthetic mRNAs in *Xenopus* embryos. Technique. 1**,** 76-89.

Mori, K., Kii, S., Tsuji, A., Nagahama, M., Imamaki, A., Hayashi, K., Akamatsu, T., Nagamune, H., Matsuda, Y., 1997. A novel human PACE4 isoform, PACE4E is an active processing protease containing a hydrophobic cluster at the carboxy terminus. J Biochem. 121**,** 941-8.

Muller, L., Zhu, P., Juliano, M. A., Juliano, L., Lindberg, I., 1999. A 36-residue peptide contains all of the information required for 7B2-mediated activation of prohormone convertase 2. J Biol Chem. 274**,** 21471-7.

Muller, L., Zhu, X., Lindberg, I., 1997. Mechanism of the facilitation of PC2 maturation by 7B2: involvement in ProPC2 transport and activation but not folding. J Cell Biol. 139**,** 625-38.

Munzer, J. S., Basak, A., Zhong, M., Mamarbachi, A., Hamelin, J., Savaria, D., Lazure, C., Hendy, G. N., Benjannet, S., Chretien, M., Seidah, N. G., 1997. In vitro characterization of the novel proprotein convertase PC7. J Biol Chem. 272**,** 19672-81.

Nagahama, M., Taniguchi, T., Hashimoto, E., Imamaki, A., Mori, K., Tsuji, A., Matsuda, Y., 1998. Biosynthetic processing and quaternary interactions of proprotein convertase SPC4 (PACE4). FEBS Lett. 434**,** 155-9.

Nakagawa, T., Hosaka, M., Torii, S., Watanabe, T., Murakami, K., Nakayama, K., 1993a. Identification and functional expression of a new member of the mammalian Kex2-like processing endoprotease family: its striking structural similarity to PACE4. J Biochem. 113**,** 132-5.

Nakagawa, T., Murakami, K., Nakayama, K., 1993b. Identification of an isoform with an extremely large Cys-rich region of PC6, a Kex2-like processing endoprotease. FEBS Lett. 327**,** 165-71.

Nakao, A., Afrakhte, M., Moren, A., Nakayama, T., Christian, J. L., Heuchel, R., Itoh, S., Kawabata, M., Heldin, N. E., Heldin, C. H., ten Dijke, P., 1997. Identification of Smad7, a TGFbeta-inducible antagonist of TGF-beta signalling. Nature. 389**,** 631-5.

Nakashima, M., Toyono, T., Akamine, A., Joyner, A., 1999. Expression of growth/differentiation factor 11, a new member of the BMP/TGFbeta superfamily during mouse embryogenesis. Mech Dev. 80**,** 185-9.

Nakayama, K., Kim, W. S., Torii, S., Hosaka, M., Nakagawa, T., Ikemizu, J., Baba, T., Murakami, K., 1992. Identification of the fourth member of the mammalian endoprotease family homologous to the yeast Kex2 protease. Its testis-specific expression. J Biol Chem. 267**,** 5897-900.

Nakayama, T., Snyder, M. A., Grewal, S. S., Tsuneizumi, K., Tabata, T., Christian, J. L., 1998. Smad8 acts downstream of BMP-4 to modulate its activity during vertebrate embryonic patterning. Development. 125**,** 857-867.

Nastos, A., Pogge von Strandmann, E., Weber, H., Ryffel, G. U., 1998. The embryonic expression of the tissue-specific transcription factor HNF1alpha in Xenopus: rapid activation by HNF4 and delayed induction by mesoderm inducers. Nucleic Acids Res. 26**,** 5602-8.

Nelsen, S., Berg, L., Wong, C., Christian, J. L., 2005. Proprotein convertase genes in Xenopus development. Dev Dyn. 233**,** 1038-44.

Neumann, C., Cohen, S., 1997. Morphogens and pattern formation. Bioessays. 19**,** 721-9.

Nie, G. Y., Li, Y., Minoura, H., Findlay, J. K., Salamonsen, L. A., 2003. Specific and transient up-regulation of proprotein convertase 6 at the site of embryo implantation and identification of a unique transcript in mouse uterus during early pregnancy. Biol Reprod. 68**,** 439-47.

Nieuwkoop, P. D., Faber, J., 1967. *Normal lable of* Xenopus laevis. North Holland Publising, Amsterdam, The Netherlands.

Nohno, T., Ishikawa, T., Saito, T., Hosokawa, K., Noji, S., Wolsing, D. H., Rosenbaum, J. S., 1995. Identification of a human type II receptor for bone morphogenetic protein-4 that forms differential heteromeric complexes with bone morphogenetic protein type I receptors. J Biol Chem. 270**,** 22522-6.

Nolen, L. D., Amor, D., Haywood, A., St Heaps, L., Willcock, C., Mihelec, M., Tam, P., Billson, F., Grigg, J., Peters, G., Jamieson, R. V., 2006. Deletion at 14q22-23 indicates a contiguous gene syndrome comprising anophthalmia, pituitary hypoplasia, and ear anomalies. Am J Med Genet A. 140**,** 1711-8.

Nour, N., Basak, A., Chretien, M., Seidah, N. G., 2003. Structure-function analysis of the prosegment of the proprotein convertase PC5A. J Biol Chem. 278**,** 2886-95.

Nour, N., Mayer, G., Mort, J. S., Salvas, A., Mbikay, M., Morrison, C. J., Overall, C. M., Seidah, N. G., 2005. The cysteine-rich domain of the secreted proprotein convertases PC5A and PACE4 functions as a cell surface anchor and interacts with tissue inhibitors of metalloproteinases. Mol Biol Cell. 16**,** 5215-26.

Oley, M., Letzel, M. C., Ragg, H., 2004. Inhibition of furin by serpin Spn4A from Drosophila melanogaster. FEBS Lett. 577**,** 165-9.

Onichtchouk, D., Chen, Y. G., Dosch, R., Gawantka, V., Delius, H., Massague, J., Niehrs, C., 1999. Silencing of TGF-beta signalling by the pseudoreceptor BAMBI. Nature. 401**,** 480-5.

Osada, S. I., Wright, C. V., 1999. Xenopus nodal-related signaling is essential for mesendodermal patterning during early embryogenesis. Development. 126**,** 3229-40.

Osterwalder, T., Kuhnen, A., Leiserson, W. M., Kim, Y. S., Keshishian, H., 2004. Drosophila serpin 4 functions as a neuroserpin-like inhibitor of subtilisin-like proprotein convertases. J Neurosci. 24**,** 5482-91.

Pearson, K. L., Hunter, T., Janknecht, R., 1999. Activation of Smad1-mediated transcription by p300/CBP. Biochim Biophys Acta. 1489**,** 354-64.

Pera, E. M., Ikeda, A., Eivers, E., De Robertis, E. M., 2003. Integration of IGF, FGF, and anti-BMP signals via Smad1 phosphorylation in neural induction. Genes Dev. 17**,** 3023-8.

Perlmutter, D. H., Pierce, J. A., 1989. The alpha 1-antitrypsin gene and emphysema. Am J Physiol. 257**,** L147-62.

Petsko, G. A., Ringe, D., Primers in Biology: Protein Structure and Function. Blackwell Science and Sinauer Associates, 2004.

Phadke, S. R., Sharma, A. K., Agarwal, S. S., 1994. Anophthalmia with cleft palate and micrognathia: a new syndrome? J Med Genet. 31**,** 960-1.

Piccolo, S., Agius, E., Lu, B., Goodman, S., Dale, L., De Robertis, E. M., 1997. Cleavage of Chordin by Xolloid metalloprotease suggests a role for proteolytic processing in the regulation of Spemann organizer activity. Cell. 91**,** 407-16.

Piccolo, S., Sasai, Y., Lu, B., De Robertis, E. M., 1996. Dorsoventral patterning in Xenopus: inhibition of ventral signals by direct binding of chordin to BMP-4. Cell. 86**,** 589-98.

Plaimauer, B., Mohr, G., Wernhart, W., Himmelspach, M., Dorner, F., Schlokat, U., 2001. 'Shed' furin: mapping of the cleavage determinants and identification of its C-terminus. Biochem J. 354**,** 689-95.

Posakony, L. G., Raftery, L. A., Gelbart, W. M., 1990. Wing formation in Drosophila melanogaster requires decapentaplegic gene function along the anterior-posterior compartment boundary. Mech Dev. 33**,** 69-82.

Pouponnot, C., Jayaraman, L., Massague, J., 1998. Physical and functional interaction of SMADs and p300/CBP. J Biol Chem. 273**,** 22865-8.

Radford, H. E., Meijer, H. A., de Moor, C. H., 2008. Translational control by cytoplasmic polyadenylation in Xenopus oocytes. Biochim Biophys Acta. 1779**,** 217-29.

Rancourt, S. L., Rancourt, D. E., 1997. Murine subtilisin-like proteinase SPC6 is expressed during embryonic implantation, somitogenesis, and skeletal formation. Dev Genet. 21**,** 75-81.

Rehemtulla, A., Dorner, A. J., Kaufman, R. J., 1992. Regulation of PACE propeptide-processing activity: requirement for a post-endoplasmic reticulum compartment and autoproteolytic activation. Proc Natl Acad Sci U S A. 89**,** 8235-9.

Rehemtulla, A., Kaufman, R. J., 1992. Protein processing within the secretory pathway. Curr Opin Biotechnol. 3**,** 560-5.

Remacle, A. G., Shiryaev, S. A., Oh, E. S., Cieplak, P., Srinivasan, A., Wei, G., Liddington, R. C., Ratnikov, B. I., Parent, A., Desjardins, R., Day, R., Smith, J. W., Lebl, M., Strongin, A. Y., 2008. Substrate cleavage analysis of furin and related proprotein convertases. A comparative study. J Biol Chem. 283**,** 20897-906.

Reversade, B., Kuroda, H., Lee, H., Mays, A., De Robertis, E. M., 2005. Depletion of Bmp2, Bmp4, Bmp7 and Spemann organizer signals induces massive brain formation in Xenopus embryos. Development. 132**,** 3381-92.

Richer, M. J., Keays, C. A., Waterhouse, J., Minhas, J., Hashimoto, C., Jean, F., 2004. The Spn4 gene of Drosophila encodes a potent furin-directed secretory pathway serpin. Proc Natl Acad Sci U S A. 101**,** 10560-5.

Rockwell, N. C., Krysan, D. J., Komiyama, T., Fuller, R. S., 2002. Precursor processing by kex2/furin proteases. Chem Rev. 102**,** 4525-48.

Rodriguez-Boulan, E., Kreitzer, G., Musch, A., 2005. Organization of vesicular trafficking in epithelia. Nat Rev Mol Cell Biol. 6**,** 233-47.

Roebroek, A. J., Creemers, J. W., Pauli, I. G., Kurzik-Dumke, U., Rentrop, M., Gateff, E. A., Leunissen, J. A., Van de Ven, W. J., 1992. Cloning and functional expression of Dfurin2, a subtilisin-like proprotein processing enzyme of Drosophila melanogaster with multiple repeats of a cysteine motif. J Biol Chem. 267**,** 17208-15.

Roebroek, A. J., Schalken, J. A., Bussemakers, M. J., van Heerikhuizen, H., Onnekink, C., Debruyne, F. M., Bloemers, H. P., Van de Ven, W. J., 1986. Characterization of human c-fes/fps reveals a new transcription unit (fur) in the immediately upstream region of the proto-oncogene. Mol Biol Rep. 11**,** 117-25.

Roebroek, A. J., Umans, L., Pauli, I. G., Robertson, E. J., van Leuven, F., Van de Ven, W. J., Constam, D. B., 1998. Failure of ventral closure and axial rotation in embryos lacking the proprotein convertase Furin. Development. 125**,** 4863-76.

Rosenzweig, B. L., Imamura, T., Okadome, T., Cox, G. N., Yamashita, H., ten Dijke, P., Heldin, C. H., Miyazono, K., 1995. Cloning and characterization of a human type II receptor for bone morphogenetic proteins. Proc Natl Acad Sci U S A. 92**,** 7632-6.

Ross, S., Hill, C. S., 2008. How the Smads regulate transcription. Int J Biochem Cell Biol. 40**,** 383-408.

Rossi, J. M., Dunn, N. R., Hogan, B. L., Zaret, K. S., 2001. Distinct mesodermal signals, including BMPs from the septum transversum mesenchyme, are required in combination for hepatogenesis from the endoderm. Genes Dev. 15**,** 1998-2009.

Salles, F. J., Richards, W. G., Strickland, S., 1999. Assaying the polyadenylation state of mRNAs. Methods. 17**,** 38-45.

Sapkota, G., Alarcon, C., Spagnoli, F. M., Brivanlou, A. H., Massague, J., 2007. Balancing BMP signaling through integrated inputs into the Smad1 linker. Mol Cell. 25**,** 441-54.

Sarac, M. S., Cameron, A., Lindberg, I., 2002. The furin inhibitor hexa-D-arginine blocks the activation of Pseudomonas aeruginosa exotoxin A in vivo. Infect Immun. 70**,** 7136-9.

Sarac, M. S., Peinado, J. R., Leppla, S. H., Lindberg, I., 2004. Protection against anthrax toxemia by hexa-D-arginine in vitro and in vivo. Infect Immun. 72**,** 602-5.

Savage, C., Das, P., Finelli, A. L., Townsend, S. R., Sun, C. Y., Baird, S. E., Padgett, R. W., 1996. Caenorhabditis elegans genes sma-2, sma-3, and sma-4 define a conserved family of transforming growth factor beta pathway components. Proc Natl Acad Sci U S A. 93**,** 790-4.

Scamuffa, N., Calvo, F., Chretien, M., Seidah, N. G., Khatib, A. M., 2006. Proprotein convertases: lessons from knockouts. FASEB J. 20**,** 1954-63.

Schmierer, B., Hill, C. S., 2005. Kinetic analysis of Smad nucleocytoplasmic shuttling reveals a mechanism for transforming growth factor beta-dependent nuclear accumulation of Smads. Mol Cell Biol. 25**,** 9845-58.

Scott, G. K., Gu, F., Crump, C. M., Thomas, L., Wan, L., Xiang, Y., Thomas, G., 2003. The phosphorylation state of an autoregulatory domain controls PACS-1-directed protein traffic. EMBO J. 22**,** 6234-44.

Seemuller, U., Fritz, H., Eulitz, M., 1981. Eglin: Elastase-Cathepsin G Inhibitor from Leeches. Methods in Enzymology. 80**,** 804-816.

Seidah, N. G., Chretien, M., 1999. Proprotein and prohormone convertases: a family of subtilases generating diverse bioactive polypeptides. Brain Res. 848**,** 45-62.

Seidah, N. G., Day, R., Hamelin, J., Gaspar, A., Collard, M. W., Chretien, M., 1992. Testicular expression of PC4 in the rat: molecular diversity of a novel germ cell-specific Kex2/subtilisin-like proprotein convertase. Mol Endocrinol. 6**,** 1559-70.

Seidah, N. G., Gaspar, L., Mion, P., Marcinkiewicz, M., Mbikay, M., Chretien, M., 1990. cDNA sequence of two distinct pituitary proteins homologous to Kex2 and furin gene products: tissue-specific mRNAs encoding candidates for pro-hormone processing proteinases. DNA Cell Biol. 9**,** 789.

Seidah, N. G., Hamelin, J., Mamarbachi, M., Dong, W., Tardos, H., Mbikay, M., Chretien, M., Day, R., 1996. cDNA structure, tissue distribution, and chromosomal localization of rat PC7, a novel mammalian proprotein convertase closest to yeast kexin-like proteinases. Proc Natl Acad Sci U S A. 93**,** 3388-93.

Seidah, N. G., Marcinkiewicz, M., Benjannet, S., Gaspar, L., Beaubien, G., Mattei, M. G., Lazure, C., Mbikay, M., Chretien, M., 1991. Cloning and primary sequence of a mouse candidate prohormone convertase PC1 homologous to PC2, Furin, and Kex2: distinct chromosomal localization and messenger RNA distribution in brain and pituitary compared to PC2. Mol Endocrinol. 5**,** 111-22.

Seidah, N. G., Mayer, G., Zaid, A., Rousselet, E., Nassoury, N., Poirier, S., Essalmani, R., Prat, A., 2008. The activation and physiological functions of the proprotein convertases. Int J Biochem Cell Biol. 40**,** 1111-25.

Shennan, K. I., Smeekens, S. P., Steiner, D. F., Docherty, K., 1991. Characterization of PC2, a mammalian Kex2 homologue, following expression of the cDNA in microinjected Xenopus oocytes. FEBS Lett. 284**,** 277-80.

Shi, Y., Massague, J., 2003. Mechanisms of TGF-beta signaling from cell membrane to the nucleus. Cell. 113**,** 685-700.

Shore, E. M., Xu, M., Feldman, G. J., Fenstermacher, D. A., Cho, T. J., Choi, I. H., Connor, J. M., Delai, P., Glaser, D. L., LeMerrer, M., Morhart, R., Rogers, J. G., Smith, R., Triffitt, J. T., Urtizberea, J. A., Zasloff, M., Brown, M. A., Kaplan, F. S., 2006. A recurrent mutation in the BMP type I receptor ACVR1 causes inherited and sporadic fibrodysplasia ossificans progressiva. Nat Genet. 38**,** 525-7.

Sive, H. L., Grainger, R. M., Harland, R. M., 2000. Early Development of *Xenopus laevis*: a laboratory manual. Cold Spring Harbor Laboratory Press, Cold Spring Harbor.

Smeekens, S. P., Steiner, D. F., 1990. Identification of a human insulinoma cDNA encoding a novel mammalian protein structurally related to the yeast dibasic processing protease Kex2. J Biol Chem. 265**,** 2997-3000.

Smith, W. C., Harland, R. M., 1992. Expression cloning of noggin, a new dorsalizing factor localized to the Spemann organizer in Xenopus embryos. Cell. 70**,** 829-40.

Sopory, S., Nelsen, S. M., Degnin, C., Wong, C., Christian, J. L., 2006. Regulation of bone morphogenetic protein-4 activity by sequence elements within the prodomain. J Biol Chem. 281**,** 34021-31.

Spence, M. J., Sucic, J. F., Foley, B. T., Moehring, T. J., 1995. Analysis of mutations in alleles of the fur gene from an endoprotease-deficient Chinese hamster ovary cell strain. Somat Cell Mol Genet. 21**,** 1-18.

Spencer, F. A., Hoffmann, F. M., Gelbart, W. M., 1982. Decapentaplegic: a gene complex affecting morphogenesis in Drosophila melanogaster. Cell. 28**,** 451-61.

Sprecher, C. A., Morgenstern, K. A., Mathewes, S., Dahlen, J. R., Schrader, S. K., Foster, D. C., Kisiel, W., 1995. Molecular cloning, expression, and partial characterization of two novel members of the ovalbumin family of serine proteinase inhibitors. J Biol Chem. 270**,** 29854-61.

Steiner, D. F., 1998. The proprotein convertases. Curr Opin Chem Biol. 2**,** 31-9.

Steiner, D. F., Oyer, P. E., 1967. The Biosynthesis of Insulin and a Probable Precursor of Insulin by a Human Islet Cell Adenoma. Proc Natl Acad Sci U S A. 57**,** 473-480.

Stich, S., Haag, M., Haupl, T., Sezer, O., Notter, M., Kaps, C., Sittinger, M., Ringe, J., 2009. Gene expression profiling of human mesenchymal stem cells chemotactically induced with CXCL12. Cell Tissue Res.

Stieneke-Grober, A., Vey, M., Angliker, H., Shaw, E., Thomas, G., Roberts, C., Klenk, H. D., Garten, W., 1992. Influenza virus hemagglutinin with multibasic cleavage site is activated by furin, a subtilisin-like endoprotease. EMBO J. 11**,** 2407-14.

Strik, M. C., Bladergroen, B. A., Wouters, D., Kisiel, W., Hooijberg, J. H., Verlaan, A. R., Hordijk, P. L., Schneider, P., Hack, C. E., Kummer, J. A., 2002. Distribution of the human intracellular serpin protease inhibitor 8 in human tissues. J Histochem Cytochem. 50**,** 1443-54.

Sun, P. D., Davies, D. R., 1995. The cystine-knot growth-factor superfamily. Annu Rev Biophys Biomol Struct. 24**,** 269-91.

Suzuki, A., Chang, C., Yingling, J. M., Wang, X. F., Hemmati-Brivanlou, A., 1997. Smad5 induces ventral fates in Xenopus embryo. Dev Biol. 184**,** 402-5.

Suzuki, A., Thies, R. S., Yamaji, N., Song, J. J., Wozney, J. M., Murakami, K., Ueno, N., 1994. A truncated bone morphogenetic protein receptor affects dorsal-ventral patterning in the early Xenopus embryo. Proc Natl Acad Sci U S A. 91**,** 10255-9.

Szumska, D., Pieles, G., Essalmani, R., Bilski, M., Mesnard, D., Kaur, K., Franklyn, A., El Omari, K., Jefferis, J., Bentham, J., Taylor, J. M., Schneider, J. E., Arnold, S. J., Johnson, P., Tymowska-Lalanne, Z., Stammers, D., Clarke, K., Neubauer, S., Morris, A., Brown, S. D., Shaw-Smith, C., Cama, A., Capra, V., Ragoussis, J., Constam, D., Seidah, N. G., Prat, A., Bhattacharya, S., 2008. VACTERL/caudal regression/Currarino syndrome-like malformations in mice with mutation in the proprotein convertase Pcsk5. Genes Dev. 22**,** 1465-77.

Tadros, H., Chretien, M., Mbikay, M., 2001. The testicular germ-cell protease PC4 is also expressed in macrophage-like cells of the ovary. J Reprod Immunol. 49**,** 133-52.

Taupenot, L., Harper, K. L., O'Connor, D. T., 2003. The chromogranin-secretogranin family. N Engl J Med. 348**,** 1134-49.

Taylor, N. A., Van De Ven, W. J., Creemers, J. W., 2003. Curbing activation: proprotein convertases in homeostasis and pathology. Faseb J. 17**,** 1215-27.

ten Dijke, P., Yamashita, H., Sampath, T. K., Reddi, A. H., Estevez, M., Riddle, D. L., Ichijo, H., Heldin, C. H., Miyazono, K., 1994. Identification of type I receptors for osteogenic protein-1 and bone morphogenetic protein-4. J Biol Chem. 269**,** 16985-8.

Thomas, G., 2002. Furin at the cutting edge: from protein traffic to embryogenesis and disease. Nat Rev Mol Cell Biol. 3**,** 753-66.

Tian, Q., Nakayama, T., Dixon, M. P., Christian, J. L., 1999. Post-transcriptional regulation of Xwnt-8 expression is required for normal myogenesis during vertebrate embryonic development. Development. 126**,** 3371-80.

Torii, S., Yamagishi, T., Murakami, K., Nakayama, K., 1993. Localization of Kex2-like processing endoproteases, furin and PC4, within mouse testis by in situ hybridization. FEBS Lett. 316**,** 12-6.

Tsuji, A., Hashimoto, E., Ikoma, T., Taniguchi, T., Mori, K., Nagahama, M., Matsuda, Y., 1999a. Inactivation of proprotein convertase, PACE4, by alpha1-antitrypsin

Portland (alpha1-PDX), a blocker of proteolytic activation of bone morphogenetic protein during embryogenesis: evidence that PACE4 is able to form an SDS-stable acyl intermediate with alpha1-PDX. J Biochem. 126**,** 591-603.

Tsuji, A., Hine, C., Tamai, Y., Yonemoto, K., Mori, K., Yoshida, S., Bando, M., Sakai, E., Akamatsu, T., Matsuda, Y., 1997. Genomic organization and alternative splicing of human PACE4 (SPC4), kexin-like processing endoprotease. J Biochem. 122**,** 438-52.

Tsuji, A., Ikoma, T., Hashimoto, E., Matsuda, Y., 2002. Development of selectivity of alpha1-antitrypsin variant by mutagenesis in its reactive site loop against proprotein convertase. A crucial role of the P4 arginine in PACE4 inhibition. Protein Eng. 15**,** 123-30.

Tsuji, A., Sakurai, K., Kiyokage, E., Yamazaki, T., Koide, S., Toida, K., Ishimura, K., Matsuda, Y., 2003. Secretory proprotein convertases PACE4 and PC6A are heparin-binding proteins which are localized in the extracellular matrix. Potential role of PACE4 in the activation of proproteins in the extracellular matrix. Biochim Biophys Acta. 1645**,** 95-104.

Tsuji, A., Yoshida, S., Hasegawa, S., Bando, M., Yoshida, I., Koide, S., Mori, K., Matsuda, Y., 1999b. Human subtilisin-like proprotein convertase, PACE4 (SPC4) gene expression is highly regulated through E-box elements in HepG2 and GH4C1 cells. J Biochem. 126**,** 494-502.

Tsuneizumi, K., Nakayama, T., Kamoshida, Y., Kornberg, T. B., Christian, J. L., Tabata, T., 1997. Daughters against dpp modulates dpp organizing activity in Drosophila wing development. Nature. 389**,** 627-31.

van de Loo, J. W., Creemers, J. W., Bright, N. A., Young, B. D., Roebroek, A. J., Van de Ven, W. J., 1997. Biosynthesis, distinct post-translational modifications, and functional characterization of lymphoma proprotein convertase. J Biol Chem. 272**,** 27116-23.

van de Loo, J. W., Teuchert, M., Pauli, I., Plets, E., Van de Ven, W. J., Creemers, J. W., 2000. Dynamic palmitoylation of lymphoma proprotein convertase prolongs its half-life, but is not essential for trans-Golgi network localization. Biochem J. 352 Pt 3**,** 827-33.

Van de Peer, Y., De Wachter, R., 1994. TREECON for Windows: a software package for the construction and drawing of evolutionary trees for the Microsoft Windows environment. Comput Appl Biosci. 10**,** 569-70.

van den Ouweland, A. M., van Duijnhoven, H. L., Keizer, G. D., Dorssers, L. C., Van de Ven, W. J., 1990. Structural homology between the human fur gene product and the subtilisin-like protease encoded by yeast KEX2. Nucleic Acids Res. 18**,** 664.

Varlet, I., Collignon, J., Robertson, E. J., 1997. nodal expression in the primitive endoderm is required for specification of the anterior axis during mouse gastrulation. Development. 124**,** 1033-44.

Veale, A. M., McColl, I., Bussey, H. J., Morson, B. C., 1966. Juvenile polyposis coli. J Med Genet. 3**,** 5-16.

Vey, M., Schafer, W., Berghofer, S., Klenk, H. D., Garten, W., 1994. Maturation of the trans-Golgi network protease furin: compartmentalization of propeptide removal, substrate cleavage, and COOH-terminal truncation. J Cell Biol. 127**,** 1829-42.

Wan, L., Molloy, S. S., Thomas, L., Liu, G., Xiang, Y., Rybak, S. L., Thomas, G., 1998. PACS-1 defines a novel gene family of cytosolic sorting proteins required for trans-Golgi network localization. Cell. 94**,** 205-16.

Wang, W., Mariani, F. V., Harland, R. M., Luo, K., 2000. Ski represses bone morphogenic protein signaling in Xenopus and mammalian cells. Proc Natl Acad Sci U S A. 97**,** 14394-9.

Watanabe, M., Hirano, A., Stenglein, S., Nelson, J., Thomas, G., Wong, T. C., 1995. Engineered serine protease inhibitor prevents furin-catalyzed activation of the fusion glycoprotein and production of infectious measles virus. J Virol. 69**,** 3206-10.

Whitman, M., 1998. Smads and early developmental signaling by the TGFbeta superfamily. Genes Dev. 12**,** 2445-62.

Wickens, M., 1990. In the beginning is the end: regulation of poly(A) addition and removal during early development. Trends Biochem Sci. 15**,** 320-4.

Wilson, P. A., Hemmati-Brivanlou, A., 1995. Induction of epidermis and inhibition of neural fate by Bmp-4. Nature. 376**,** 331-3.

Winnier, G., Blessing, M., Labosky, P. A., Hogan, B. L., 1995. Bone morphogenetic protein-4 is required for mesoderm formation and patterning in the mouse. Genes Dev. 9**,** 2105-16.

Wouters, S., Leruth, M., Decroly, E., Vandenbranden, M., Creemers, J. W., van de Loo, J. W., Ruysschaert, J. M., Courtoy, P. J., 1998. Furin and proprotein convertase 7 (PC7)/lymphoma PC endogenously expressed in rat liver can be resolved into distinct post-Golgi compartments. Biochem J. 336 (Pt 2)**,** 311-6.

Wozney, J. M., Rosen, V., Celeste, A. J., Mitsock, L. M., Whitters, M. J., Kriz, R. W., Hewick, R. M., Wang, E. A., 1988. Novel regulators of bone formation: molecular clones and activities. Science. 242**,** 1528-34.

Wu, M. Y., Hill, C. S., 2009. Tgf-beta superfamily signaling in embryonic development and homeostasis. Dev Cell. 16**,** 329-43.

Xiang, Y., Molloy, S. S., Thomas, L., Thomas, G., 2000. The PC6B cytoplasmic domain contains two acidic clusters that direct sorting to distinct trans-Golgi network/endosomal compartments. Mol Biol Cell. 11**,** 1257-73.

Yao, L. C., Blitz, I. L., Peiffer, D. A., Phin, S., Wang, Y., Ogata, S., Cho, K. W., Arora, K., Warrior, R., 2006. Schnurri transcription factors from Drosophila and vertebrates can mediate Bmp signaling through a phylogenetically conserved mechanism. Development. 133**,** 4025-34.

Zawel, L., Dai, J. L., Buckhaults, P., Zhou, S., Kinzler, K. W., Vogelstein, B., Kern, S. E., 1998. Human Smad3 and Smad4 are sequence-specific transcription activators. Mol Cell. 1**,** 611-7.

Zhang, Y., Feng, X., We, R., Derynck, R., 1996. Receptor-associated Mad homologues synergize as effectors of the TGF-beta response. Nature. 383**,** 168-72.

Zheng, M., Streck, R. D., Scott, R. E., Seidah, N. G., Pintar, J. E., 1994. The developmental expression in rat of proteases furin, PC1, PC2, and carboxypeptidase E: implications for early maturation of proteolytic processing capacity. J Neurosci. 14**,** 4656-73.

Zhong, M., Benjannet, S., Lazure, C., Munzer, S., Seidah, N. G., 1996. Functional analysis of human PACE4-A and PACE4-C isoforms: identification of a new PACE4-CS isoform. FEBS Lett. 396**,** 31-6.

Zhong, M., Munzer, J. S., Basak, A., Benjannet, S., Mowla, S. J., Decroly, E., Chretien, M., Seidah, N. G., 1999. The prosegments of furin and PC7 as potent inhibitors of proprotein convertases. In vitro and ex vivo assessment of their efficacy and selectivity. J Biol Chem. 274**,** 33913-20.

Zhou, A., Martin, S., Lipkind, G., LaMendola, J., Steiner, D. F., 1998. Regulatory roles of the P domain of the subtilisin-like prohormone convertases. J Biol Chem. 273**,** 11107-14.

Zhou, Y., Lindberg, I., 1993. Purification and characterization of the prohormone convertase PC1(PC3). J Biol Chem. 268**,** 5615-23.

Zhu, H., Kavsak, P., Abdollah, S., Wrana, J. L., Thomsen, G. H., 1999. A SMAD ubiquitin ligase targets the BMP pathway and affects embryonic pattern formation. Nature. 400**,** 687-93.

Zimmerman, L. B., De Jesus-Escobar, J. M., Harland, R. M., 1996. The Spemann organizer signal noggin binds and inactivates bone morphogenetic protein 4. Cell. 86**,** 599-606.